Inhomogeneous plane waves in dissipative, isotropic and anisotropic media. Reflection/transmission coefficients.

Johana Brokešová, Vlastislav Červený

Department of Geophysics, Charles University, Ke Karlovu 3, 121 16 Praha 2, Czech Republic, E-mails: johana@seis.karlov.mff.cuni.cz, vcerveny@seis.karlov.mff.cuni.cz

Summary

To understand well the propagation of high-frequency seismic body waves in *dissipative*, 3-D laterally varying isotropic and anisotropic structures, containing curved structural interfaces, it is useful to study first the behavior of plane waves in relevant homogeneous media with planar interfaces. The ray methods represent, in fact, a local application of plane waves in more complex structures. For example, the reflection/transmission coefficients of plane waves at plane interfaces between two homogeneous halfspaces may be locally applied even to high-frequency seismic body waves incident at a curved interface between two inhomogeneous media. This is the reason why this contribution is devoted to plane waves in *dissipative* homogeneous media with planar interfaces.

Inhomogeneous, time-harmonic, plane waves, propagating in dissipative, isotropic and anisotropic media are investigated. The elastodynamic equation for the dissipative homogeneous media is solved in terms of eigenvalues and eigenvectors of the 3×3 Christoffel matrix $\hat{\mathbf{\Gamma}}$, with complex-valued elements $\Gamma_{ik} = a_{ijkl}p_jp_l$, where a_{ijkl} are complex-valued density normalized elastic moduli, and p_j the complex-valued components of the slowness vector $\mathbf{p}$. The eigenvalues of the Christoffel matrix can be used to determine the components of the slowness vector, and the eigenvectors to determine the (elliptical) polarization of individual inhomogeneous plane waves. Contrary to the traditionally used method based on Lame's elastic potentials, the used method can be applied quite generally, including anisotropic media. It can be also easily applied to the solution of the reflection/transmission problem at a plane interface between two dissipative halfspaces, or at a thin transition layer, simulated by a system of thin homogeneous parallel sublayers.

As p_i are complex-valued, $p_i = P_i + \mathrm{i}A_i$, the inhomogeneous plane waves are characterized by two planes: the plane of constant phases, $P_ix_i = const$, and plane of constant amplitudes, $A_ix_i = const$. The real-valued vector $\mathbf{P}$ is called the propagation vector, and the real-valued vector $\mathbf{A}$ the attenuation vector. The angle between them, called the attenuation angle and denoted by γ, may be an arbitrary acute angle different from 90^o in dissipative media. The plane wave with $\gamma = 0^o$ is called homogeneous. The reflection/transmission problem is solved here for an inhomogeneous incident plane wave, with an arbitrary attenuation angle γ, both for isotropic and anisotropic media. The homogeneous incident plane wave is included as a special case ($\gamma = 0^o$).

Seismic Waves in Complex 3-D Structures, Report No.7 (Department of Geophysics, Charles University, Prague 1998)

A computer routine COEF52 is described, designed to compute arbitrary frequency-dependent R/T coefficients on a plane interface between two dissipative isotropic halfspaces, with a constant-Q dispersion relations, assuming an incident plane wave with an arbitrary attenuation angle γ. Routine COEF52 is a generalization of routine COEF51, described by Brokešová and Červený (1997), where a special choice of the attenuation angle γ of the incident wave was used. The routine COEF52 may be also used to compute R/T coefficients from transition layers.

Results of extensive computations of "reference R/T coefficients" on a plane interface between two dissipative isotropic halfspaces are presented and discussed. In all cases, they are also compared with those for non-dissipative media. Under reference R/T coefficients, we understand the R/T coefficients for dissipative media, computed for the fixed frequency, equal to the reference frequency f_r, for which the complex-valued elastic moduli in the model are specified. The dependence of R/T coefficients on the attenuation angle γ of the incident wave is studied in detail. For the computations of R/T coefficients, see Section 6, and for the conclusions Section 7. In general, the differences between the moduli of the R/T coefficients for dissipative and non-dissipative models are usually small for realistic Q's and γ's. Exceptions are discussed in Section 6. The differences between the moduli are more distinct mainly in critical and post-critical regions of angles of incidence for the reflection coefficients S1S1 and P1P1, particularly for small Q's, large contrast of Q's across the interface, and for great $|\gamma|$'s (say, $|\gamma| > 50^o$). The differences between the phases of R/T coefficients for dissipative and non-dissipative media may be greater. In certain situations, for some γ's, the signs of the phases of R/T coefficients for dissipative and non-dissipative media may be roughly opposite, even for very high Q's.We speak of *anomalous phases*, see Section 6.2 for a detailed description.

1 Introduction

An inhomogeneous plane wave is characterized by two real planes: the plane of constant phases and the plane of constant amplitudes. Both these planes are mutually inclined. The angle between the normals to these planes (called the attenuation angle γ) may be an arbitrary acute angle different from 90^o in dissipative media. If the attenuation angle γ equals 0^o, the plane wave is called homogeneous. Homogeneous and inhomogeneous plane waves may propagate both in dissipative and non-dissipative media. In non-dissipative media, the attenuation angle of inhomogeneous waves always equals 90^o, see Červený (1997), Section 2.2.10. Contrary to non-dissipative media, the attenuation angle γ in dissipative media is always different from 90^o. If we formally considered an inhomogeneous plane wave with $\gamma = \pm 90^o$ in a dissipative medium, the phase velocity of this wave would be zero.

We discuss the propagation of inhomogeneous time-harmonic plane waves in dissipative, isotropic and anisotropic, media. The homogeneous wave with $\gamma = 0^o$ represents a special case. Contrary to non-dissipative media, the elastic moduli are complex-valued and frequency-dependent in dissipative media. It is also common to speak on linearly viscoelastic, or anelastic media.

A traditional approach to investigate the propagation of inhomogeneous plane waves in dissipative homogeneous isotropic media is based on Lame's elastic potentials. The displacement vector $\mathbf{u}$, satisfying the elastodynamic equation, is expressed in terms of scalar and vectorial Lame's elastic potentials, ϕ and $\boldsymbol{\psi}$. The elastodynamic equation for a homogeneous medium can be then decomposed into two standard wave equations: a scalar wave equation for ϕ and a vectorial wave equation for $\boldsymbol{\psi}$. These wave equations can be solved for inhomogeneous plane waves by classical methods. The scalar potential ϕ corresponds to a compressional (P) plane inhomogeneous wave, and the vectorial potential $\boldsymbol{\psi}$ to a shear (S) plane inhomogeneous wave. See Borcherdt (1973, 1977, 1982, 1988), Aki and Richards (1980), Krebes and Hron (1980a, b), Krebes (1983, 1984), Richards (1984), Borcherdt and Wennerberg (1985), Borcherdt, Glassmoyer and Wennerberg (1986), etc. Many other references can be found in these papers.

The methods based on Lame's elastic potentials have given many valuable results, but have also certain disadvantages. *First:* They cannot be used to investigate the plane waves propagating in dissipative anisotropic media, as the elastic potentials cannot be introduced there. *Second:* they do not offer a possibility to generate the results to weakly inhomogeneous media by asymptotic high-frequency methods (e.g., ray methods), as the Lame's elastic potentials cannot be introduced in inhomogeneous media. *Third:* The method based on elastic potentials have been applied to the reflection/transmission problem at a plane interface only for certain simple cases of special symmetries, particularly for the case of the normals to the interface, to the plane of constant phases and to the plane of constant amplitudes of the incident plane wave being coplanar. The solution of a general R/T situation in terms of potentials would be more cumbersome (even though possible) and has not yet been attempted.

In this contribution, a different, more systematic, approach is used to investigate the propagation of inhomogeneous plane waves in dissipative, isotropic and anisotropic, media. The method is not based on elastic Lame's potentials, but looks directly for the solution of the elastodynamic equation in terms of the displacement vector $\mathbf{u}$. Using a suitable ansatz solution for a plane inhomogeneous wave, the elastodynamic equation reduces to an eigenvalue problem for a 3×3 Christoffel matrix, which can be solved by similar methods as in non-dissipative media, see Červený (1997), Sections 2.2.4 – 2.2.6. In an anisotropic dissipative medium, the 3×3 Christoffel matrix $\hat{\boldsymbol{\Gamma}}$ has elements $\Gamma_{ik} = a_{ijkl}p_j p_l$, where a_{ijkl} are complex-valued density normalized elastic moduli, and p_i are Cartesian components of the complex-valued slowness vector $\mathbf{p}$. The eigenvalue problem yields three complex-valued eigenvalues $G_m(p_i)$, and three relevant complex-valued eigenvectors $\mathbf{g}^{(m)}, m = 1, 2, 3$. The elastodynamic equation yields constraint equations on the slowness vector components p_i, $G_m(p_i) = 1, m = 1, 2, 3$. The ansatz solution represents a plane wave only if p_i satisfy any of the constraint conditions $G_1(p_i) = 1, G_2(p_i) = 1$ or $G_3(p_i) = 1$. For this reason, the condition $G_m(p_i) = 1$ is called here the existence condition. As $m = 1, 2$ or 3, we have three different types of inhomogeneous plane waves which can propagate in dissipative anisotropic media: a quasi-compressional wave and two quasi-shear waves. The eigenvectors $\mathbf{g}^{(m)}$ then represent the relevant polarization vectors. As they are complex valued, with different directions of $\mathrm{Re}(\mathbf{g}^{(m)})$ and $\mathrm{Im}(\mathbf{g}^{(m)})$, the polarization of all inhomogeneous plane waves propagating in anisotropic dissipative media is elliptical. The elliptical polarization reduces to linear only under special conditions.

In isotropic media, the eigenvalue problem becomes degenerate, as two eigenvalues, say G_1 and G_2, corresponding to shear waves, are identical. A consequence is that the two corresponding eigenvectors, $\mathbf{g}^{(1)}$ and $\mathbf{g}^{(2)}$, cannot be completely determined; it is only possible to determine a complex plane in which they are situated. In fact, the complete system of all possible eigenvectors $\mathbf{g}^{(1)}$ and $\mathbf{g}^{(2)}$ is one-parametric. We denote the parameter specifying $\mathbf{g}^{(1)}$ and $\mathbf{g}^{(2)}$ by δ, with $-180^o < \delta \leq 180^o$. For any choice of δ, the relevant $\mathbf{g}^{(1)}$ and $\mathbf{g}^{(2)}$ represent the eigenvectors of the Christoffel matrix, and the ansatz solution represents an inhomogeneous plane shear wave. The parameter δ should be known from some other conditions imposed on the problem under consideration.

If we use the eigenvalue formulation, it is also simple to solve the boundary reflection/transmission problem for an inhomogeneous plane wave incident at a plane interface between two dissipative, isotropic or anisotropic, halfspaces, see Section 3. The equations derived in Section 3 remain valid for any inhomogeneous (or homogeneous) plane wave incident at a plane interface between two dissipative, isotropic or anisotropic, halfspaces. The appropriate equations are first derived for anisotropic dissipative media, see Section 3.1, and then they are specified for isotropic dissipative media, see Section 3.2.

In Section 4, all equations of Section 3 are used to discuss a special case of reflection/transmission on a plane between two isotropic halfspaces. In this special case, the normals to the interface, to the surface of constant phase and to the surface of constant amplitudes of the incident wave are coplanar. All equations in Section 4 are specified to a last detail. A great attention is devoted mainly to the correct determination of arguments of square roots involved in expressions for R/T coefficients. The criterion used in the determination of these arguments is based on critical angles.

All expressions given in Sections 2, 3 and 4 are quite exact, valid even for strongly dissipative media (low Q's). No low-loss approximation is used in their derivation.

A computer routine COEF52, designed to calculate R/T coefficients for an arbitrary inhomogeneous plane wave incident on a structural interface between two isotropic dissipative halfspaces, on a free surface and on an interface between two liquid halfspaces, is described in Section 5. The routine COEF52 is more general then the routine COEF51, described by Brokešová and Červený (1997), as it considers an arbitrary attenuation angle γ of the incident plane wave, see Section 5. The routine COEF52 can be even used to compute the R/T coefficients at a transition layer, simulated by a stack of thin parallel homogeneous dissipative layers. The routine COEF52, however, is limited to the special case discussed in Section 4: the normals to the interface and to the planes of constant phase and of constant amplitudes of the incident plane wave are coplanar.

Section 6 contains some results of extensive computations. Various types of R/T coefficients on a plane interface between two homogeneous dissipative halfspaces are computed and discussed. Only "reference R/T coefficients" are considered. Under "reference R/T coefficients", we understand the R/T coefficients computed for the reference frequency f_r, for which the elastic moduli in both halfspaces are specified, see Brokešová and Červený (1997). A great attention is devoted to the dependence of R/T coefficients on the attenuation angle γ of the incident wave. All R/T coefficients are compared with these for non-dissipative media. The discussion of results and some conclusions can be found in Section 7.

The theory and computer routines presented in this contribution can be generalized in several ways. It would be useful to consider a general *dissipative anisotropic stratified* *(one-dimensional) medium.* In such a case it would be suitable to apply general approach, proposed for isotropic stratified medium by Kennett (1983). See also Thomson, Clarke and Garmany (1986). The Kennett's approach was generalized even for an *anisotropic* stratified medium. See, e.g., a detailed treatment in Thomson (1998a) in this volume, and Chapman (1994). A very general Thomson's computer program **Rmatrix** for R/T coefficients at a stack of non-dissipative anisotropic layers is now available, see Thomson (1998b). Although the program Rmatrix is designed only for non-dissipative anisotropic media, it would be possible to generalize it even for dissipative anisotropic layers. This is open for further investigation.

2 Plane waves in dissipative media

In frequency domain, the elastodynamic equation in unbounded anisotropic homogeneous dissipative medium, with vanishing body forces, reads

$$a_{ijkl}u_{k,lj} + \omega^2 u_i = 0, \quad i = 1, 2, 3. \tag{1}$$

Here, ω is the circular frequency, u_i are Cartesian components of the displacement vector $\mathbf{u}$, and a_{ijkl} are density normalized elastic moduli. Whereas a_{ijkl} are real-valued and frequency-independent in non-dissipative elastic media, they are complex-valued and frequency-dependent in dissipative media,

$$a_{ijkl} = a^R_{ijkl} + \mathrm{i}a^I_{ijkl}. \tag{2}$$

The density normalized elastic moduli satisfy the symmetry relations

$$a_{ijkl} = a_{jikl} = a_{ijlk} = a_{klij}, \tag{3}$$

which reduce the number of independent elastic moduli from 81 to 21.

We shall describe a time-harmonic plane wave by the equation

$$u_k(\mathbf{x}, t) = U_k \exp[-\mathrm{i}\omega(t - p_i x_i)]. \tag{4}$$

Here, $\mathbf{U}$ with Cartesian components U_k is a complex-valued vectorial constant, and the vector $\mathbf{p}$ with Cartesian components p_i is the slowness vector. In general, p_i are complex-valued.

2.1 Plane waves in anisotropic dissipative media

Inserting (4) into (1) for a fixed frequency ω yields a system of three algebraic linear equations for U_i,

$$\Gamma_{ik}U_k - U_i = 0, \quad i = 1, 2, 3, \tag{5}$$

where

$$\Gamma_{ik} = a_{ijkl}p_j p_l. \tag{6}$$

Equations (5) — (6) are the same as for non-dissipative media, see Červený (1997), Section 2.2.4. The only difference is that a_{ijkl} and p_i are complex-valued. We shall call here the

3×3 matrix $\hat{\mathbf{\Gamma}}$ with components Γ_{ik} the *Christoffel matrix* and the equation (5) the *Christoffel equation.*

The Christoffel matrix $\hat{\mathbf{\Gamma}}$ has three complex-valued eigenvalues G_m and three relevant complex-valued eigenvectors $\mathbf{g}^{(m)}, m = 1, 2, 3$. They satisfy the relations

$$(\Gamma_{ik} - G_m \delta_{ik}) g_k^{(m)} = 0, \quad i = 1, 2, 3, \tag{7}$$

(no summation over m). We shall normalize the eigenvectors $\mathbf{g}^{(m)}$ in such a way to satisfy the relations

$$g_k^{(m)} g_k^{(m)*} = 1. \tag{8}$$

Here, $g_k^{(m)*}$ represents the complex conjugate of $g_k^{(m)}$.

Equation (7) represents a system of three homogeneous linear algebraic equations for $g_1^{(m)}, g_2^{(m)}, g_3^{(m)}$. The system has a non-trivial solution only if the determinant of the system vanishes,

$$\det(\Gamma_{ik} - G_m(p_i)\delta_{ik}) = 0. \tag{9}$$

This equation can be used to determine $G_m(p_i), m = 1, 2, 3$. After this, (7) with (8) can be used to determine $\mathbf{g}^{(m)}, m = 1, 2, 3$.

The Christoffel equation (5) can be expressed in the following form

$$(\Gamma_{ik} - \delta_{ik}) U_k = 0, \quad i = 1, 2, 3. \tag{10}$$

By comparison of (7) with (10), we can see that the Christoffel equation (10) is satisfied, if and only if, one of the three eigenvalues of the Christoffel matrix $\hat{\mathbf{\Gamma}}$ equals unity,

$$G_m(p_i) = 1. \tag{11}$$

Here m may be 1, 2 or 3. The corresponding eigenvector $\mathbf{g}^{(m)}$ then determines the direction of $\mathbf{U}$,

$$\mathbf{U} = A\mathbf{g}^{(m)}. \tag{12}$$

A is an arbitrary complex-valued scalar quantity.

We shall call equation (11) the *existence condition* of the m-th plane wave. Equation (4) represents a plane wave propagating in a homogeneous anisotropic dissipative medium only if p_i satisfy the existence condition (11), where G_m is an eigenvalue of the Christoffel matrix.

Consequently, we have obtained three different plane wave solutions in an anisotropic dissipative medium, representing one quasi-compressional (qP) and two quasi-shear waves (qS1 and qS2), The displacement vector of each of them is given by the relation

$$u_k(x_i, t) = A g_k^{(m)} \exp[-\mathrm{i}\omega(t - p_n x_n)]. \tag{13}$$

The Cartesian components p_n of the slowness vector $\mathbf{p}$ must satisfy the existence condition (11).

If $\mathrm{Re}(\mathbf{g}^{(m)}) \neq 0$ and $\mathrm{Im}(\mathbf{g}^{(m)}) \neq 0$, and if $\mathrm{Re}(\mathbf{g}^{(m)})$ is not parallel to $\mathrm{Im}(\mathbf{g}^{(m)})$, the plane wave (13) is elliptically polarized.

2.2 Plane waves in isotropic dissipative media

In an isotropic dissipative medium, the elements of the Christoffel matrix are given by the relation

$$\Gamma_{ik} = \frac{\lambda + \mu}{\rho} p_i p_i + \frac{\mu}{\rho} \delta_{ik} p_l p_l, \tag{14}$$

see Červený (1997), Eq. (2.2.43). Here λ and μ represent the Lame's elastic parameters. λ, μ and p_i are complex-valued. Similarly as in a non-dissipative medium, the three eigenvalues G_1, G_2, G_3 can be found analytically:

$$G_1(p_i) = G_2(p_i) = \beta^2 p_i p_i, \quad G_3(p_i) = \alpha^2 p_i p_i, \tag{15}$$

where

$$\alpha^2 = \frac{\lambda + 2\mu}{\rho}, \quad \beta^2 = \frac{\mu}{\rho}. \tag{16}$$

Both velocities α and β are complex-valued and frequency-dependent, as λ and μ are complex-valued and frequency-dependent. The eigenvalue G_3 corresponds to a plane P wave, and eigenvalues G_1, G_2 to a plane S wave. The eigenvectors $\mathbf{g}^{(1)}, \mathbf{g}^{(2)}, \mathbf{g}^{(3)}$ corresponding to eigenvalues G_1, G_2, G_3 satisfy the equation (7) with (14),

$$[(\alpha^2 - \beta^2) p_i p_k + \beta^2 \delta_{ik} p_l p_l - G_m \delta_{ik}] g_k^{(m)} = 0. \tag{17}$$

Equations (15) show that the eigenvalues G_1, G_2 corresponding to shear waves are identical, and the eigenvector problem (17) is degenerate. Consequently, $\mathbf{g}^{(1)}$ and $\mathbf{g}^{(2)}$ for S waves cannot be determined uniquely from (17). It is only possible to determine a complex plane in which $\mathbf{g}^{(1)}$ and $\mathbf{g}^{(2)}$ are situated. The strict position of $\mathbf{g}^{(1)}$ and $\mathbf{g}^{(2)}$ in the complex plane can be specified only by an additional input parameter. See paragraph 2d in this Section.

We shall now introduce notation for the slowness vector $\mathbf{p}$,

$$\mathbf{p} = \mathbf{P} + \mathrm{i}\mathbf{A}, \tag{18}$$

where $\mathbf{P}$ and $\mathbf{A}$ are real-valued vectors. We shall call the plane wave an *inhomogeneous plane wave* if

$$|\mathbf{P} \times \mathbf{A}| \neq 0. \tag{19}$$

and a *homogeneous plane wave* if

$$|\mathbf{P} \times \mathbf{A}| = 0. \tag{20}$$

For a more detailed discussion of inhomogeneous and homogeneous waves see Section 2.3. For inhomogeneous waves, we also introduce the real-valued *slowness vector plane* Σ^S, specified by real-valued vectors $\mathbf{P}$ and $\mathbf{A}$. The unit normal $\mathbf{n}^S$ to Σ^S is given by the relation

$$\mathbf{n}^S = (\mathbf{P} \times \mathbf{A})/|\mathbf{P} \times \mathbf{A}|. \tag{21}$$

Note that the notation (18) — (21) is applicable to all cases under consideration: to quasi-compressional and quasi-shear waves in anisotropic dissipative media and to P, S waves in isotropic dissipative media. Only the slowness vector $\mathbf{p}$ (and, consequently, $\mathbf{P}$ and $\mathbf{A}$ in (18)), is different in different cases. See Section 2.3.

1) Determination of the eigenvector $\mathbf{g}^{(3)}$ of P waves

We consider P waves, so that $G_3(p_i) = \alpha^2 p_i p_i = 1$, and insert this into (17). This yields

$$(\alpha^2 - \beta^2)(p_i p_k - \alpha^{-2}\delta_{ik})g_k^{(3)} = 0.$$

Multiplying this by $g_k^{(3)*}$ and taking into account the normalization condition (8) yields

$$(p_i g_i^{(3)*})(p_k g_k^{(3)}) = 1/\alpha^2. \tag{22}$$

It is not difficult to see that $g_i^{(3)}$ satisfy (22) if they are given by the relation

$$g_i^{(3)} = p_i/|\mathbf{p}|. \tag{23}$$

To prove it, we calculate the l.h.s. of (22) for $\mathbf{g}^{(3)}$ given by (23). We obtain

$$(p_i g_i^{(3)*})(p_k g_k^{(3)}) = \frac{p_i p_i^*}{|\mathbf{p}|} \cdot \frac{p_k p_k}{|\mathbf{p}|} = \frac{p_i p_i^*}{|\mathbf{p}|^2} \cdot p_k p_k = p_k p_k = \frac{1}{\alpha^2}.$$

Thus, (22) is satisfied for $g_i^{(3)}$ given by (23).

The same relation (23) remains valid even in non-dissipative medium.

2) Determination of the eigenvectors $\mathbf{g}^{(1)}$, $\mathbf{g}^{(2)}$ of S waves

We consider S waves, so that $G_1 = G_2 = \beta^2 p_i p_i = 1$, and insert this into (17). We obtain

$$(\alpha^2 - \beta^2) p_i p_k g_k^{(I)} = 0, \quad I = 1, 2.$$

As $\alpha^2 - \beta^2 \neq 0$, this yields

$$p_i (p_k g_k^{(I)}) = 0.$$

For non-trivial slowness vector $\mathbf{p}$, this equation yields

$$p_k g_k^{(I)} = 0. \tag{24}$$

Equation (24) is the same for both eigenvectors $\mathbf{g}^{(1)}$ and $\mathbf{g}^{(2)}$. It shows that $\mathbf{g}^{(1)}$ and $\mathbf{g}^{(2)}$ are situated in a complex plane perpendicular to the complex vector $\mathbf{p}$. We shall first find simple special solution of (24), and then generalize these solutions to obtain a complete set of $\mathbf{g}^{(1)}$ and $\mathbf{g}^{(2)}$. The special solutions will be found only for $\mathbf{g}^{(1)}$. The determination of $\mathbf{g}^{(2)}$ from $\mathbf{g}^{(1)}$ and $\mathbf{p}$ is discussed later.

2a) Type-II S plane waves

It is not difficult to show that (24) is satisfied by $\mathbf{g}^{(1)}$ given by the relation

$$\mathbf{g}^{(1)} = \mathbf{n}^S, \tag{25}$$

where $\mathbf{n}^S$ is perpendicular to Σ^S, specified by $\mathbf{P}$ and $\mathbf{A}$. Consequently, $\mathbf{n}^S \cdot \mathbf{P} = 0$ and $\mathbf{n}^S \cdot \mathbf{A} = 0$. It should be emphasized that $\mathbf{g}^{(1)}$ is real-valued in this case. This is quite exceptional, mostly we shall obtain complex-valued eigenvectors of S waves.

The plane S wave in a dissipative medium, with a polarization given by (25), is known in seismology as Type-II S wave. See Borcherdt (1977), Borcherdt and Wennerberg (1985), etc.

2b) Type-I S plane waves

Similarly as in previous case, we consider a trial solution of (24)

$$\mathbf{g}^{(1)} = (\mathbf{n}^S \times \mathbf{p})/|\mathbf{n}^S \times \mathbf{p}|. \tag{26}$$

We prove that (26) is a solution of (24), even for complex-valued $\mathbf{p}$. We obtain

$$\mathbf{p}\cdot\mathbf{g}^{(1)} \propto (\mathbf{P}+\mathrm{i}\mathbf{A})(\mathbf{n}^S\times(\mathbf{P}+\mathrm{i}\mathbf{A})) = \mathbf{P}\cdot(\mathbf{n}^S\times\mathbf{P}) - \mathbf{A}(\mathbf{n}^S\times\mathbf{A}) + \mathrm{i}[\mathbf{P}\cdot(\mathbf{n}^S\times\mathbf{A}) + \mathbf{A}(\mathbf{n}^S\times\mathbf{P})].$$

As $\mathbf{n}^S$ is perpendicular to $\mathbf{P}$ and to $\mathbf{A}$, the first two terms vanish. The third term also vanishes. This is simple to see if we consider a well-known vectorial identity $\mathbf{a}\cdot(\mathbf{b}\times\mathbf{c}) = -\mathbf{c}\cdot(\mathbf{b}\times\mathbf{a})$. Consequently, the expression $\mathbf{p}\cdot\mathbf{g}^{(1)}$ vanishes if $\mathbf{g}^{(1)}$ is given by (26) and $\mathbf{g}^{(1)}$ represents an eigenvector of a plane S wave. It should be noted that the vectors Re $(\mathbf{g}^{(1)})$ and Im $(\mathbf{g}^{(1)})$ are both situated *in the plane* Σ^S, along its intersection with planes perpendicular to $\mathbf{P}$ and $\mathbf{A}$.

Note that $\mathbf{g}^{(1)}$ given by (26) satisfies the normalization condition $g_k^{(1)} g_k^{(1)*} = 1$.

The plane S wave in a dissipative medium, with a polarization vector given by (26), is known in seismology as Type-I S wave. See Borcherdt (1977), Borcherdt and Wennerberg (1985), etc.

2c) One-parametric system of possible $\mathbf{g}^{(1)}$

Now we shall consider

$$\mathbf{g}^{(1)} = \mathbf{n}^S\cos\delta + \frac{\mathbf{n}^S\times\mathbf{p}}{|\mathbf{n}^S\times\mathbf{p}|}\sin\delta, \tag{27}$$

where δ is an arbitrary real-valued angle. It is obvious that $\mathbf{g}^{(1)}$ given by (27) satisfies (24), as both terms satisfy it.

Thus we have obtained a one-parametric system of eigenvectors $\mathbf{g}^{(1)}$, parametrized by the real-valued angle δ, $-\pi \le \delta \le \pi$. For any δ, the eigenvector $\mathbf{g}^{(1)}$ given by (27) is situated in a complex plane perpendicular to complex-valued slowness vector $\mathbf{p}$. For $\delta = 0^o$, $\mathbf{g}^{(1)}$ corresponds to the Type-II S plane wave, and for $\delta = 90^o$ to the Type-I S plane wave. Note that $\mathbf{g}^{(1)}$ given by (27) satisfies the normalization condition $g_k^{(1)} g_k^{(1)*} = 1$, for arbitrary δ.

2d) Complete one-parameteric systems of $\mathbf{g}^{(1)}$ and $\mathbf{g}^{(2)}$

Assuming $\mathbf{g}^{(1)}$ is given by (27), we wish to find expressions for $\mathbf{g}^{(2)}$, satisfying conditions $p_i g_i^{(2)} = 0, g_i^{(1)} g_i^{(2)} = 0$ and $g_i^{(2)} g_i^{(2)*} = 1$. It is obvious that $\mathbf{g}^{(2)}$ must be again given by (27), only the angle δ must be taken different. We shall consider $\frac{\pi}{2} + \delta$ instead of δ. Then we obtain for both $\mathbf{g}^{(1)}$ and $\mathbf{g}^{(2)}$

$$\begin{aligned} \mathbf{g}^{(1)} &= \mathbf{n}^S\cos\delta + \tfrac{\mathbf{n}^S\times\mathbf{p}}{|\mathbf{n}^S\times\mathbf{p}|}\sin\delta, \\ \mathbf{g}^{(2)} &= -\mathbf{n}^S\sin\delta + \tfrac{\mathbf{n}^S\times\mathbf{p}}{|\mathbf{n}^S\times\mathbf{p}|}\cos\delta. \end{aligned} \tag{28}$$

Thus, if we consider 3 vectors $\mathbf{g}^{(1)}$, $\mathbf{g}^{(2)}$, $\mathbf{p}^S = \mathbf{p}/|\mathbf{p}|$, where $\mathbf{p}^S$ is the normalized complex-valued slowness vector of plane S wave, they satisfy the relations

$$\begin{aligned} \mathbf{g}^{(1)} \cdot \mathbf{g}^{(2)} = 0, \quad \mathbf{g}^{(1)} \cdot \mathbf{p}^S = 0, \quad \mathbf{g}^{(2)} \cdot \mathbf{p}^S = 0, \\ \mathbf{g}^{(1)} \cdot \mathbf{g}^{(1)*} = 1, \quad \mathbf{g}^{(2)} \cdot \mathbf{g}^{(2)*} = 1, \quad \mathbf{p}^S \cdot \mathbf{p}^{S*} = 1. \end{aligned} \tag{29}$$

Relations (29) are satisfied for any selected angle δ. The angle δ should be taken from some other condition imposed on the problem under study. As we see, the eigenvectors $\mathbf{g}^{(\mathbf{1})}$, $\mathbf{g}^{(\mathbf{2})}$, cannot be determined uniquely; they depend on a free parameter δ (the degenerate case).

The degenerate behaviour of $\mathbf{g}^{(1)}$ and $\mathbf{g}^{(2)}$ is not a problem of inhomogeneous plane waves in dissipative media only. The same degenerate behaviour of $\mathbf{g}^{(1)}$ and $\mathbf{g}^{(2)}$ takes place even in non-dissipative media and for homogeneous plane waves in dissipative media. General relations (28) remain valid in all these cases.

2e) Final expressions for the displacement vectors of plane P and S waves

Using (4), (12) and expressions for $\mathbf{g}^{(1)}$, $\mathbf{g}^{(2)}$, $\mathbf{g}^{(3)}$ derived in this section, we obtain final expressions for plane P and S waves propagating in a homogeneous isotropic dissipative medium.

For P waves, we obtain

$$\mathbf{u}(x_i, t) = U^P \mathbf{g}^{(3)} \exp[-\mathrm{i}\omega(t - p_i x_i)], \tag{30}$$

where $\mathbf{g}^{(3)}$ is given by (23), p_i satisfy the existence condition $p_i p_i = 1/\alpha^2$, and U^P is an arbitrary complex-valued constant.

For S waves,

$$\mathbf{u}(x_i, t) = (U^{S1}\mathbf{g}^{(1)} + U^{S2}\mathbf{g}^{(2)}) \exp[-\mathrm{i}\omega(t - p_i x_i)]. \tag{31}$$

Here $\mathbf{g}^{(1)}$ and $\mathbf{g}^{(2)}$ are given by (28) (with δ chosen arbitrarily), p_i satisfy the existence condition $p_i p_i = 1/\beta^2$, and U^{S1}, U^{S2} are arbitrary complex-valued constants.

2.3 Homogeneous and inhomogeneous plane waves in isotropic dissipative media

In isotropic dissipative media, the velocities of P and S plane waves, α and β, are specified by (16). The Lame's elastic parameters λ and μ are, however, complex-valued. If we denote $\lambda = \lambda^R + \mathrm{i}\lambda^I$ and $\mu = \mu^R + \mathrm{i}\mu^I$, we obtain

$$\alpha^2 = \frac{\lambda^R + 2\mu^R}{\rho} + \mathrm{i}\frac{\lambda^I + 2\mu^I}{\rho}, \quad \beta^2 = \frac{\mu^R}{\rho} + \mathrm{i}\frac{\mu^I}{\rho.} \tag{32}$$

Instead of imaginary parts of λ and μ, it is common to use quality factors Q_P and Q_S as follows

$$Q_P^{-1} = -\frac{\lambda^I + 2\mu^I}{\lambda^R + 2\mu^R}, \quad Q_S^{-1} = -\frac{\mu^I}{\mu^R}. \tag{33}$$

Then (32) yields

$$\alpha^2 = V_P^2(1 - \frac{\mathrm{i}}{Q_P}), \quad \beta^2 = V_S^2(1 - \frac{\mathrm{i}}{Q_S}), \tag{34}$$

where

$$V_P = \sqrt{\frac{\lambda^R + 2\mu^R}{\rho}}, \quad V_S = \sqrt{\frac{\mu^R}{\rho}}. \tag{35}$$

We shall call V_P and V_S the real-valued velocities of plane P and S waves in dissipative isotropic media.

As the next treatment will be quite the same both for P and S waves, we shall use the same notation for both of them. We denote by V_C the complex-valued velocity. Then the existence condition (11) with (16) reads

$$p_i p_i = 1/V_C^2, \tag{36}$$

where

$$V_C^2 = V^2(1 - \frac{\mathrm{i}}{Q}). \tag{37}$$

For P waves, we have $V_C = \alpha, V = V_P$ and $Q = Q_P$. Similarly, for S waves, we have $V_C = \beta, V = V_S$ and $Q = Q_S$. Thus the following treatment is applicable to both P and S waves, only it is necessary to specify properly V_C, V and Q.

We shall now study the existence condition (36). We shall again use notation (18) for the complex-valued slowness vector

$$p_i = P_i + \mathrm{i}A_i, \tag{38}$$

where

$$P_i = PN_i^R, \quad A_i = AN_i^I. \tag{39}$$

Here $\mathbf{P}$ with Cartesian coordinates P_i is *propagation vector*, $\mathbf{A}$ with coordinates A_i is *attenuation vector*, and P, A are magnitudes of these vectors. N_i^R, N_i^I are components of real-valued unit vectors $\mathbf{N}^R$ and $\mathbf{N}^I$ specifying the directions of $\mathbf{P}$ and $\mathbf{A}$. It is common to call planes $P_i x_i = const$ the *planes of constant phase*, and the planes $A_i x_i = const$ the *planes of constant amplitudes*. Consequently, the vector $\mathbf{P}$ is perpendicular to the planes of constant phases, and the vector $\mathbf{A}$ to the planes of constant amplitudes. We also introduce the *attenuation angle* γ by the relation

$$\cos\gamma = N_i^R N_i^I. \tag{40}$$

Thus, γ is the angle between $\mathbf{P}$ and $\mathbf{A}$. We assume

$$-90^o \leq \gamma \leq 90^o. \tag{41}$$

One choice of γ plays an important role: $\gamma = 0$. Then $\mathbf{P}$ is parallel to $\mathbf{A}$ and the relevant plane wave is homogeneous (see Sec. 2.2). On the contrary, for $\gamma \neq 0$, we speak of inhomogeneous waves.

Using (38), the existence condition (36) reads

$$(P_i + \mathrm{i}A_i)(P_i + \mathrm{i}A_i) = s(1 + \frac{\mathrm{i}}{Q}), \tag{42}$$

where

$$s = \frac{1}{V^2(1+Q^{-2})}. \tag{43}$$

We now wish to determine P and A, for given V, Q and γ (i.e., for given s and Q in (42)). Equation (42) yields

$$P^2 - A^2 = s, \quad 2AP\cos\gamma = sQ^{-1}. \tag{44}$$

The two equations (44) have certain important consequences for inhomogeneous waves propagating in dissipative and non-dissipative media.

For *non-dissipative medium*, $Q^{-1} = 0$ and the second equation of (44) yields $2AP\cos\gamma = 0$. For $A \neq 0$ and $P \neq 0$, this is satisfied only for $\gamma = \pm\frac{1}{2}\pi$. Consequently, the inhomogeneous waves in non-dissipative media are possible, but the attenuation angle γ must equal $\pm\frac{1}{2}\pi$ in this case. Inhomogeneous waves with $\gamma \neq \pm\frac{1}{2}\pi$ cannot exist in non-dissipative media.

For *dissipative medium*, $Q^{-1} \neq 0$, and the second equation of (44) is not simplified. For $A \neq 0$ and $P \neq 0$, $\cos\gamma$ must be non-zero, otherwise the equation would not be satisfied. Consequently, the inhomogeneous waves in dissipative media are possible, but the attenuation angle γ must differ from $\pm\frac{1}{2}\pi$, $\gamma \neq \pm\frac{1}{2}\pi$. Inhomogeneous waves with $\gamma = \pm\frac{1}{2}\pi$ cannot exist in dissipative medium.

Consequently, the only type of inhomogeneous plane wave (with the attenuation angle $\pm 90^o$) which propagates in a non-dissipative medium, cannot propagate in a dissipative medium.

To solve (44) for P and A, we take a square of the second equation and insert $P^2 = s + A^2$, following from the first equation. We obtain

$$4(s + A^2)A^2\cos^2\gamma = s^2Q^{-2}. \tag{45}$$

This is a quadratic equation for A^2,

$$A^4 + sA^2 - s^2/(4Q^2\cos^2\gamma) = 0. \tag{46}$$

The solution for A^2 is as follows

$$A^2 = \tfrac{1}{2}s(-1 + \sqrt{1 + Q^{-2}\cos^{-2}\gamma}). \tag{47}$$

The second root would give negative value of A^2 and is not physically realisable. Considering $P^2 = s + A^2$, we further obtain

$$P^2 = \tfrac{1}{2}s(1 + \sqrt{1 + Q^{-2}\cos^{-2}\gamma}). \tag{48}$$

We denote

$$g = \sqrt{1 + Q^{-2}\cos^{-2}\gamma}. \tag{49}$$

Then the final solutions for P and A are as follows

$$P = \frac{1}{\sqrt{2}V\sqrt{1+Q^{-2}}}\sqrt{1+g}, \quad A = \frac{1}{\sqrt{2}V\sqrt{1+Q^{-2}}}\sqrt{-1+g}. \tag{50}$$

Both P and A are real-valued and positive for any V, Q and γ. The slowness vector (38) then reads

$$p_i = P_i + \mathrm{i}A_i = \frac{1}{\sqrt{2}V\sqrt{1+Q^{-2}}}(\sqrt{1+g}N_i^R + \mathrm{i}\sqrt{g-1}N_i^I). \tag{51}$$

Equation (51) is quite general and exact. No low-attenuation approximation is assumed.

Now we shall specify (50) — (51) for homogeneous plane waves ($\gamma = 0$). Then $g = \sqrt{1+Q^{-2}}$, and (50) reads

$$P = \frac{1}{\sqrt{2}V\sqrt{1+Q^{-2}}}\sqrt{1+\sqrt{1+Q^{-2}}}, \quad A = \frac{1}{\sqrt{2}V\sqrt{1+Q^{-2}}}\sqrt{-1+\sqrt{1+Q^{-2}}}. \tag{52}$$

Using the above relations, it is possible to introduce a real-valued *phase velocity vector* $\boldsymbol{\mathcal{C}}$ in the following way: It is perpendicular to the planes of constant phases, and its magnitude equals the velocity of propagation of the plane of a constant phase, along the normal. The Cartesian components of the phase velocity vector $\boldsymbol{\mathcal{C}}$ are given by the relation

$$\mathcal{C}_i = P_i/P^2 = \frac{\sqrt{2}V\sqrt{1+Q^{-2}}}{\sqrt{1+g}}N_i^R. \tag{53}$$

Consequently, the phase velocity $\mathcal{C} = |\boldsymbol{\mathcal{C}}|$ is given by the relation

$$\mathcal{C} = 1/P = \frac{\sqrt{2}V\sqrt{1+Q^{-2}}}{\sqrt{1+g}}. \tag{54}$$

Relations (53) and (54) are valid for any inhomogeneous plane waves propagating in dissipative homogeneous medium. For different attenuation angles γ, the phase velocity (54) is different. A particularly important role is played by the *phase velocity of a homogeneous wave*, for $\gamma = 0$. We denote it by $\mathcal{C}_H$. Using (54) and (49) for $\gamma = 0$, we obtain

$$\mathcal{C}_H = \sqrt{2}V\sqrt{1+Q^{-2}}/\sqrt{1+\sqrt{1+Q^{-2}}}. \tag{55}$$

Equations (54) and (55) immediately yield

$$\mathcal{C} \leq \mathcal{C}_H. \tag{56}$$

Thus, the phase velocity of an inhomogeneous wave $\mathcal{C}$ (for $\gamma \neq 0$) is always smaller than the phase velocity of the relevant homogeneous wave $\mathcal{C}_H$. It is interesting to note that, for fixed Q, $\mathcal{C} \to 0$ for $\gamma \to \pm 90^o$.

In seismological literature on plane waves in dissipative isotropic media, it is common to use the phase velocity $\mathcal{C}_H$ of a homogeneous plane wave as a medium parameter, instead of V.

The complex-valued velocity V_C can be expressed in terms of $\mathcal{C}_H$ using (37) and (55),

$$\begin{aligned} V_C^2 &= \mathcal{C}_H^2\frac{1+\sqrt{1+Q^{-2}}}{2(1+Q^{-2})}(1-\frac{\mathrm{i}}{Q}), \qquad & V_C^{-2} &= \mathcal{C}_H^{-2}\frac{2}{1+\sqrt{1+Q^{-2}}}(1+\frac{\mathrm{i}}{Q}), \\ V_C &= \mathcal{C}_H\frac{1+\sqrt{1+Q^{-2}}}{2\sqrt{1+Q^{-2}}}(1-\frac{\mathrm{i}}{2q}), \qquad & V_C^{-1} &= \frac{1}{\mathcal{C}_H}(1+\frac{\mathrm{i}}{2q}), \end{aligned} \tag{57}$$

where

$$q = \frac{1}{2}Q(1+\sqrt{1+Q^{-2}}). \qquad (58)$$

All equations are exact, no low-loss approximation was used. In low-loss approximation (high Q), $q \sim Q$.

Now we can express P and A given by (50) in terms of $\mathcal{C}_H$, instead of V. We obtain

$$P = \frac{1}{\mathcal{C}_H\sqrt{1+\sqrt{1+Q^{-2}}}}\sqrt{1+g}, \quad A = \frac{1}{\mathcal{C}_H\sqrt{1+\sqrt{1+Q^{-2}}}}\sqrt{g-1}, \qquad (59)$$

where g is given by (49). The slowness vector is then given by the relation

$$p_i = \frac{1}{\mathcal{C}_H\sqrt{1+\sqrt{1+Q^{-2}}}}(\sqrt{1+g}N_i^R + \mathrm{i}\sqrt{g-1}N_i^I). \qquad (60)$$

3 Reflection and transmission

In this section we shall discuss the reflection/transmission of plane waves at a plane interface between two homogeneous elastic (isotropic or anisotropic) dissipative media. We shall consider a plane interface $\Sigma(x_i) = 0$, passing through the origin of Cartesian coordinates x_i, with unit normal $\mathbf{n}$ oriented to either side of interface. We denote one of the two homogeneous halfspaces as halfspace 1, and the other as halfspace 2. We assume that the halfspaces are in welded contact across interface Σ. This means that the displacement components u_i and traction components T_i acting across surface Σ are the same on both sides of the interface Σ. We remind the readers that the traction components T_i can be expressed in terms of the spatial derivatives of the displacement components u_i as follows

$$T_i = c_{ijkl}n_j u_{k,l} = \rho a_{ijkl} n_j u_{k,l}, \qquad (61)$$

where ρ is the density, c_{ijkl} are the elastic moduli, a_{ijkl} are the density normalized elastic moduli, $a_{ijkl} = c_{ijkl}/\rho$. In dissipative anisotropic media, c_{ijkl} and a_{ijkl} are complex-valued. In isotropic media, the traction components are given by the relation

$$T_i = \lambda n_i u_{k,k} + \mu n_j(u_{i,j} + u_{j,i}) = \rho(\alpha^2 - 2\beta^2)n_i u_{k,k} + \rho\beta^2 n_j(u_{i,j} + u_{j,i}). \qquad (62)$$

Here λ, μ are Lame's elastic parameters, and α, β the velocities of P and S waves, given by (16). All these quantities are complex-valued in dissipative media.

Only time-harmonic plane waves, with a fixed circular frequency $\omega > 0$, will be considered here. It is easy to generalize the results to transient plane waves using the Fourier transform.

3.1 Anisotropic dissipative media

We denote the densities, elastic moduli and density-normalized elastic moduli in the halfspace 1 by $\rho^{(1)}, c_{ijkl}^{(1)}$ and $a_{ijkl}^{(1)}$, and in the halfspace 2 by $\rho^{(2)}, c_{ijkl}^{(2)}$ and $a_{ijkl}^{(2)}$. We assume that the plane wave is incident at interface Σ from halfspace 1 and that it is one of the three possible waves: a quasi-compressional (qP), or one of the two quasi-shear waves (qS1 or qS2). The slowness vector of the incident wave must satisfy the existence condition (11), and, consequently, Eq. (9) with $G_m = 1$. The displacement vector of the incident wave can be expressed as

$$u_i(\mathbf{x}, t) = Ag_i \exp[-\mathrm{i}\omega(t - p_i x_i)]. \tag{63}$$

All parameters of the incident wave, i.e. $\mathbf{p}$, $\mathbf{g}$ and A, are presumably known.

Six waves will, in general, be generated at interface Σ. Any of them can be described by a relation similar to (63),

$$u_i^k(\mathbf{x}, t) = A^k g_i^k \exp[-\mathrm{i}\omega(t - p_i^k x_i)], \tag{64}$$

with $k = 1, 2, \cdots, 6$ (no summation over k). The first three correspond to the first medium (reflected waves; $k = 1, 2, 3$), and the last three to the second medium (transmitted waves; $k = 4, 5, 6$). The unknown quantities of R/T waves ($\mathbf{p}^k, \mathbf{g}^k, A^k, k = 1, 2, \cdots, 6$) can be determined from the same known quantities of the incident wave ($\mathbf{p}, \mathbf{g}, A$), and from the boundary conditions of the welded contact at the interface Σ. Consequently, we also have to know $a_{ijkl}^{(1)}, a_{ijkl}^{(2)}, \rho_1$, and ρ_2, and the unit normal $\mathbf{n}$ to the interface Σ.

The boundary conditions imply that the arguments of the exponential functions of all waves must be the same along interface Σ, $-\mathrm{i}\omega(t - p_i x_i) = -\mathrm{i}\omega(t - p_i^k x_i), k = 1, 2, \cdots, 6$. This follows from the requirement that A^k are constants, independent of $\mathbf{x}$ and t, for time-harmonic plane waves in homogeneous media. The consequence is that the tangential components of the slowness vector must be equal for all waves along Σ,

$$\mathbf{p}_{tang}^k = \mathbf{p}_{tang}. \tag{65}$$

This can be expressed as follows

$$\mathbf{p}^k - \mathbf{n}(\mathbf{p}^k \cdot \mathbf{n}) = \mathbf{p} - \mathbf{n}(\mathbf{p} \cdot \mathbf{n}). \tag{66}$$

In principle, (66) represents a *Snell's law*, for a general interface between two anisotropic dissipative media. They are, however, not yet sufficient to determine the slowness vector $\mathbf{p}^k$ of generated waves; for this we also have to determine the normal components of $\mathbf{p}^k$.

A suitable procedure to determine the normal components of the complex-valued slowness vectors $\mathbf{p}^k$ is similar to that in non-dissipative media. We denote $\mathbf{a} = \mathbf{p}_{tang}$. As we see from (66), $\mathbf{a} = \mathbf{p} - \mathbf{n}(\mathbf{p} \cdot \mathbf{n}) = \mathbf{p}^k - \mathbf{n}(\mathbf{p}^k \cdot \mathbf{n})$. Thus, the complex-valued vector $\mathbf{a}$ is presumably known, as the incident wave is known. Consequently, the slowness vector $\mathbf{p}^k$ of any generated wave can be expressed as follows

$$\mathbf{p}^k = \mathbf{a} + \sigma^k \mathbf{n}, \tag{67}$$

where σ^k represents a complex-valued normal component of the slowness vector $\mathbf{p}^k$. The quantities σ^k can be determined from the existence conditions (11) for individual generated waves, or preferably from (9) (with $G_m = 1$), if analytical expressions for eigenvalues G_m are not known or are complicated.

To obtain required quantities for *reflected waves*, we insert $\mathbf{p} = \mathbf{a} + \sigma\mathbf{n}$ into (9) (with $G_m = 1$):

$$\det(a_{ijkl}^{(1)}(a_j + \sigma n_j)(a_l + \sigma n_l) - \delta_{ik}) = 0. \tag{68}$$

This is an algebraic equation of the sixth order for σ, so that it has six roots. In non-dissipative anisotropic media, the roots are real-valued, or appear in pairs of complex-conjugate quantities. In dissipative media, however, all roots are, in general, complex-valued. The determination of six roots of (68) is a standard numerical procedure, even if the roots are complex-valued. The final, but very important step consists in the selection of the three physical roots $\sigma^1, \sigma^2, \sigma^3$, corresponding to the three reflected waves $\mathbf{u}^1, \mathbf{u}^2, \mathbf{u}^3$ (see (64)), from six available roots of (68). For non-dissipative anisotropic media, this selection is discussed in detail in Červený (1997), Section 2.3.3, and is based on the energy consideration (direction of energy flux). For dissipative anisotropic media, the selection has not yet been discussed. As we are interested here mostly in isotropic media, we do not wish to increase this text inadmissibly and do not go here into details.

In the determination of three quantities $\sigma^4, \sigma^5, \sigma^6$ for the three *transmitted waves*, we proceed by the same way as for reflected waves. The required quantities $\sigma^4, \sigma^5, \sigma^6$ are roots of the equation

$$\det(a^{(2)}_{ijkl}(a_j + \sigma n_j)(a_l + \sigma n_l) - \delta_{ik}) = 0. \tag{69}$$

Again, (69) is an algebraic equation for σ of the sixth order, so that it has six roots. Similarly as for reflected waves, we have to select $\sigma^4, \sigma^5, \sigma^6$ from these six roots.

As soon as the complex-valued slowness vectors $\mathbf{p}^k$ are known for all six generated waves, we can determine even related eigenvectors $\mathbf{g}^k$ using (7), and can insert (64) into boundary conditions.

The boundary conditions require the displacement and traction components to be continuous across Σ. For the traction, we use (61). We then obtain the following system of six equations

$$\begin{array}{rcl} A^1 g^1_i + A^2 g^2_i + A^3 g^3_i + A^4 g^4_i + A^5 g^5_i + A^6 g^6_i & = & -A g_i, \\ A^1 X^1_i + A^2 X^2_i + A^3 X^3_i + A^4 X^4_i + A^5 X^5_i + A^6 X^6_i & = & -A X_i, \end{array} \tag{70}$$

$i = 1, 2, 3$. Here

$$\begin{array}{rcll} X^k_i & = & c^{(1)}_{ijnl} n_j g^k_n p^k_l, & k = 1, 2, 3, \\ X^k_i & = & c^{(2)}_{ijnl} n_j g^k_n p^k_l, & k = 4, 5, 6, \end{array} \tag{71}$$

with no summation over k. The right-hand sides of (70) correspond to the incident wave, and X_i are given by the same expressions as $X^k_i, k = 1, 2, 3$, according to the type of incident wave. In this case, g^k_n and p^k_l in the expression for X^k_i correspond to incident wave. The quantities $c^{(1)}_{ijnl}, c^{(2)}_{ijnl}, g^k_n, p^k_l$ in (71) are complex-valued, and n_j are real-valued.

System (70) represents the final system of six linear algebraic equations with six unknown amplitude factors A^k of the reflected/transmitted qP, qS1 and qS2 waves. All these amplitude factors are complex-valued.

Consequently, we obtain, for a given incident plane wave, six generated plane waves with displacement reflection/transmission coefficients

$$R^k = A^k / A. \tag{72}$$

The displacement vectors of the relevant waves read

$$u^k_i(\mathbf{x}, t) = A R^k g^k_i \exp[-\mathrm{i}\omega(t - p^k_i x_i)], \tag{73}$$

where p_i^k are given by (67), g_i^k are relevant eigenvectors, A is the amplitude factor of the incident wave, and R^k is the relevant R/T coefficient, see (72). There is no summation over k in (73).

As three different plane waves may incident from the halfspace 1, the number of R/T coefficients is, in general, eighteen (nine for reflected waves and nine for transmitted waves).

Note that the system of six equations (70) for $A^k, k = 1, 2 \cdots, 6$, can be decomposed into 2 independent systems only in exceptional cases of some planes of symmetry. Analytical solutions of (70) are very cumbersome. Mostly, the direct numerical solution of (70) is simplest and most straightforward. It is, however, not necessary to invert complete 6×6 system matrix; but only two 3×3 matrices.

3.2 Isotropic dissipative media

We denote the complex-valued velocities of the P and S waves and the density in halfspace 1 by $\alpha_1, \beta_1, \rho_1$, and in halfspace 2 by $\alpha_2, \beta_2, \rho_2$. Similarly, the complex-valued Lame's elastic parameters in halfspace 1 are λ_1, μ_1, and in halfspace 2 λ_2, μ_2. We assume that a plane wave is incident at the interface Σ from halfspace 1. The displacement vector of the incident P wave will be expressed as

$$u_k(\mathbf{x}, t) = A g_k^{(3)} \exp[-\mathrm{i}\omega(t - p_i x_i)], \tag{74}$$

where p_i satisfy the existence condition $p_i p_i = \alpha_1^{-2}$, and $\mathbf{g}^{(3)}$ is the eigenvector of P wave given by (23). For the incident S wave

$$u_k(\mathbf{x}, t) = (B g_k^{(1)} + C g_k^{(2)}) \exp[-\mathrm{i}\omega(t - p_i x_i)], \tag{75}$$

where p_i satisfy the existence condition $p_i p_i = \beta_1^{-2}$, and $\mathbf{g}^{(1)}, \mathbf{g}^{(2)}$ are eigenvectors of S wave given by (28), with an arbitrarily chosen δ.

To satisfy the six conditions of the welded contact at interface Σ, we introduce reflected P, S and transmitted P, S wave. We use the same notations as in (74) and (75). We denote the amplitude factors A, B, C corresponding to reflected waves by A^r, B^r and C^r, and the same factors for transmitted waves by A^t, B^t and C^t. In all expressions for R/T waves, we use $p_i, g_k^{(1)}, g_k^{(2)}, g_k^{(3)}$ corresponding to the R/T plane wave under consideration. The determination of these quantities will be described later.

1. Displacement R/T coefficients for dissipative isotropic media

The boundary conditions require the continuity of the displacement and traction vectors across interface Σ. The traction components in an isotropic dissipative solid can be expressed in terms of $\mathbf{u}$ using (62). Similarly as in anisotropic dissipative media, the boundary conditions imply that the tangential components of slowness vectors of all waves equal the tangential component of the slowness vector of the incident wave. This will be used later to determine the slowness vectors of all R/T plane waves. Now we shall write equations for $A^r, B^r, C^r, A^t, B^t, C^t$. Using (74), (75) and analogous expressions for R/T waves, and inserting them into boundary conditions, we obtain

$$\begin{array}{rcl} A^t g_i^{(3)t} + B^t g_i^{(1)t} + C^t g_i^{(2)t} - A^r g_i^{(3)r} - B^r g_i^{(1)r} - C^r g_i^{(2)r} & = & D_i, \\ A^t X_i^t + B^t Y_i^t + C^t Z_i^t - A^r X_i^r - B^r Y_i^r - C^r Z_i^r & = & E_i, \end{array} \tag{76}$$

where $i = 1, 2, 3$. The eigenvectors $\mathbf{g}^{(m)r}$ correspond to reflected waves, and eigenvectors $\mathbf{g}^{(m)t}$ to transmitted waves. The vector components X_i, Y_i and Z_i are given by relations

$$\begin{aligned} X_i &= \lambda n_i (g_k^{(3)} p_k) + 2\mu g_i^{(3)} (n_k p_l), \\ Y_i &= \mu n_j (g_i^{(1)} p_j + g_j^{(1)} p_i), \\ Z_i &= \mu n_j (g_i^{(2)} p_j + g_j^{(2)} p_i). \end{aligned} \tag{77}$$

Notation (77) is formally the same for reflected waves (X_i^r, Y_i^r, Z_i^r) and for transmitted waves (X_i^t, Y_i^t, Z_i^t), only all quantities $\lambda, \mu, g_i^{(m)}$ and p_i are properly specified for these waves. The r.h.s. expressions in (76), D_i and E_i, correspond to the incident wave. For P incident wave:

$$D_i = A g_i^{(3)}, \quad E_i = A X_i, \tag{78}$$

and for S incident wave:

$$D_i = B g_i^{(1)} + C g_i^{(2)}, \quad E_i = B Y_i + C Z_i. \tag{79}$$

Here X_i, Y_i and Z_i are again given by (77), with all quantities corresponding to the incident wave.

It should be again emphasized that $\lambda, \mu, p_k, g_k^{(m)r}, g_k^{(m)t}$ in (76) — (77) are complex-valued. For incident and reflected waves, we take $\lambda = \lambda_1$, $\mu = \mu_1$. Analogously, for transmitted waves, $\lambda = \lambda_2$, $\mu = \mu_2$.

System (76) represents the final system of six linear algebraic equations with six unknown amplitude factors A^r, B^r, C^r (corresponding to reflected waves) and A^t, B^t, C^t (corresponding to transmitted waves). A^r and A^t correspond to P waves, B^r, C^r and B^t, C^t to S waves.

We shall now introduce the displacement reflection/transmission coefficients, R_{mn}^r and R_{mn}^t. We shall formally consider the S1 and S2 components of the displacement of S waves as independent waves. In R_{mn}^r and R_{mn}^t, the index m specifies the type of the incident wave ($m = 1, 2, 3$) and n the type of the generated wave ($n = 1, 2, 3$). Index m, related to the incident wave, is defined as follows:

m=1 $\cdots$ S1 component of the incident wave (eigenvector $\mathbf{g}^{(1)}$),
m=2 $\cdots$ S2 component of the incident wave (eigenvector $\mathbf{g}^{(2)}$),
m=3 $\cdots$ P incident wave (eigenvector $\mathbf{g}^{(3)}$).

The definition of n is analogous, but it is related to the R/T waves. Thus, we obtain, for reflected waves

$$\begin{array}{lll} R_{11}^r = B^r/B, & R_{12}^r = C^r/B, & R_{13}^r = A^r/B, \\ R_{21}^r = B^r/C, & R_{22}^r = C^r/C, & R_{23}^r = A^r/C, \\ R_{31}^r = B^r/A, & R_{32}^r = C^r/A, & R_{33}^r = A^r/A. \end{array} \tag{80}$$

Definition of R_{mn}^t is analogous to (80), only the superscripts "r" are replaced by superscripts "t".

The R/T coefficients, as introduced here, represent the *R/T coefficients in displacements*. Traditionally, the *potential R/T coefficients* have been studied in dissipative isotropic media. Specific equations for potential R/T coefficients, however, were written only for very special cases, particularly for incident Type-II S waves and for incident P or Type-I S waves, with **P**, **A** and **n** coplanar. See Borcherdt (1977, 1982). We feel that it is considerably more suitable to work with displacement vectors than with potentials, particularly in general 3-D cases. Moreover, for anisotropic media, the potentials cannot be introduced at all. In our case, we are using a unique method both for anisotropic and isotropic dissipative media, applicable to any type of incident inhomogeneous plane wave. It is not required that **P**, **A** and **n** are coplanar.

2. Determination of complex-valued slowness vectors of generated waves

The solution of a system of six linear algebraic complex-valued equations (76) constitutes a standard numerical problem. Many standard numerical routines to solve it can be found in various subroutine packages. To solve the system, however, we must first find the slowness vectors **p** and eigenvectors **g** corresponding to individual R/T waves. We shall use an analogous procedure to that used for anisotropic media. The procedure, however, may be simplified, as analytical expressions for eigenvalues exist. For P waves, $G_3 = \alpha^2 p_i p_i$, and for S waves, $G_1 = G_2 = \beta^2 p_i p_i$. Thus, we can use the existence condition (11) instead of (9). The solution of (11) for σ is again analytical.

As the treatment is the same both for P and S waves, we shall again use the common notation of Section 2.3, with the existence condition $p_i p_i = 1/V_C^2$, see (36), where V_C is given by (37). Using the relation $\mathbf{p} = \mathbf{a} + \sigma\mathbf{n}$ and inserting it into existence condition $p_i p_i = 1/V_C^2$ yields

$$\sigma = \pm\mathcal{P}.\mathcal{V}.[1/V_C^2 - a^2]^{1/2}, \quad a = a_i a_i. \tag{81}$$

Here, $\mathcal{P}.\mathcal{V}.$ denotes the principal value of the complex square root, for which $-\pi/2 < \arg[1/V_C^2 - a^2]^{1/2} \leq \pi/2$. Note that the FORTRAN function CSQRT computes the principal value of the square root. Consequently, the computation of $\mathcal{P}.\mathcal{V}.[1/V_C^2 - a^2]^{1/2}$ is straightforward, but the choice of correct sign may be more complicated.

It should be noted that the sign in (81) also depends on the choice of the unit vector **n**, which may be oriented to either side of interface Σ. Moreover, the sign is, in general, different for reflected and transmitted waves. To make the problem of the choice of sign in (81) more transparent, we introduce the *orientation index* ε, which specifies the orientation of the unit vector **n** with respect to the propagation vector **P** of the incident wave

$$\varepsilon = \mathrm{sgn}(\mathbf{P}\cdot\mathbf{n}). \tag{82}$$

Thus, $\varepsilon = -1$ if the unit normal **n** is oriented into the first halfspace, and $\varepsilon = 1$ if it is oriented into the second halfspace.

Let us now consider an arbitrarily selected R/T wave, and denote all quantities related to this R/T wave by a tilde above the letter. Thus, the complex-valued slowness vector of this wave is denoted by $\tilde{\mathbf{p}}$, the real-valued propagation vector and attenuation vector by $\tilde{\mathbf{P}}$ and $\tilde{\mathbf{A}}$, so that $\tilde{\mathbf{p}} = \tilde{\mathbf{P}} + \mathrm{i}\tilde{\mathbf{A}}$. Then the slowness vector of the R/T wave under consideration may be expressed in the following form

$$\tilde{p}_i = a_i \pm \varepsilon[1/\tilde{V}_C^2 - a^2]^{1/2} n_i. \tag{83}$$

Here ε is given by (82), the upper sign corresponds to transmitted waves (P or S). $\tilde{V}_C$ is the complex-valued velocity of the selected generated wave.

For $a = 0$, we can use the following relation in (83)

$$\mathrm{Re}[1/\tilde{V}_C^2 - a^2]^{1/2} = \mathrm{Re}(1/\tilde{V}_C) > 0. \tag{84}$$

Thus, for the normal incidence ($a = 0$), we always have

$$[1/\tilde{V}_C^2 - a^2]^{1/2} = \mathcal{P}.\mathcal{V}.[1/\tilde{V}_C^2 - a^2]^{1/2}. \tag{85}$$

For $\mathrm{Re}(1/\tilde{V}_C^2 - a^2) < 0$, however, we have to consider two possible signs, see a detailed discussion bellow.

3. Criteria for determination of sign of $[1/\tilde{\mathbf{V}}_\mathbf{C}^2 - \mathbf{a}^2]^{1/2}$. Critical angles

Let us first briefly discuss the determination of the sign of $[1/\tilde{V}_C^2 - a^2]^{1/2}$ in *non-dissipative elastic isotropic media.* The situation is considerably simpler than in dissipative media, as $1/\tilde{V}_C^2 - a^2$ is always real-valued, positive or negative. For positive values we obtain

$$[1/\tilde{V}_C^2 - a^2]^{1/2} = \mathcal{P}.\mathcal{V}.[1/\tilde{V}_C^2 - a^2]^{1/2}, \quad \text{for} \quad 1/\tilde{V}_C^2 \geq a^2. \tag{86}$$

For $1/V_C^2 < a^2$, the square root is purely imaginary, and the R/T wave under consideration is inhomogeneous. The propagation vector $\tilde{\mathbf{P}}$ of this inhomogeneous wave is tangent to the interface and the attenuation vector $\tilde{\mathbf{A}}$ is perpendicular to it. The choice of sign of the purely imaginary square root specifies the direction of $\tilde{\mathbf{A}}$: towards the interface or away from it.

Thus, we have two possible inhomogeneous waves; one with amplitude *decreasing exponentially* and the second *increasing exponentially* with increasing distance from the interface Σ. Assuming an incident homogeneous wave, the boundary conditions and the properties of the incident wave are not sufficient to select one of these waves; both of them are fully admissible.

If we consider two infinite halfspaces, it is common to consider an independent requirement: we wish to select the inhomogeneous plane waves the amplitudes of which decrease exponentially with the increasing distance from Σ. In this case, the criterion would be as follows

$$[1/\tilde{V}_C^2 - a^2]^{1/2} = +\mathrm{i}\mathcal{P}.\mathcal{V}.[1/\tilde{V}_C^2 - a^2]^{1/2} \quad \text{for} \quad 1/\tilde{V}_C^2 < a^2. \tag{87}$$

This criterion can be simply verified if we insert (83) with (87) into $\exp[-i\omega(t - \tilde{p}_i x_i)]$. The amplitudes of all possible inhomogeneous R/T waves then decay exponentially with increasing distance from Σ. To see it clearly, we can introduce a Cartesian coordinate system x_i with $\mathbf{n}$ taken along x_3 axis.

For *dissipative elastic isotropic media*, the criterion is more involved. The direction of the attenuation vector $\tilde{\mathbf{A}}$ of any generated R/T wave is strictly determined by the incident wave and by boundary conditions. Thus, we do not have any possibility to choose the sign of the square root according to the direction of the attenuation vector $\tilde{\mathbf{A}}$. In dissipative media, the R/T plane waves with amplitude increasing with increasing distance from Σ are allowed. This fact has been known in seismological literature for a long time, see, e.g., Richards (1984), etc.

The criterion we shall use for dissipative media is based on the *analytic continuation* of the complex-valued square root in a complex plane. We start from the normal incidence (a=0), where the correct sign is given by (85), and require that the square root $[1/\tilde{V}_C^2 - a^2]^{1/2}$ changes smoothly if a is varying continuously. Technically, the actual form of the criterion will be based on *critical angles.*

We shall consider the propagation vectors $\mathbf{P}$ of the incident wave and $\tilde{\mathbf{P}}$ of the selected R/T wave, and express $\mathbf{P}$ in terms of the angle of incidence i. We define the *critical angle* of incidence i^* corresponding to the selected R/T wave as an angle of incidence for which the propagation vector $\tilde{\mathbf{P}}$ of the selected R/T wave is parallel to the interface Σ. Consequently,

$$\tilde{\mathbf{P}} \cdot \mathbf{n} = 0 \quad \text{for} \quad i = i^*. \tag{88}$$

Such a definition is common even in non-dissipative media. There are, however, some important differences. In non-dissipative media, all propagation vectors for angles of incidence $i > i^*$ are parallel to the interface Σ. In dissipative media, however the situation is different; the critical angles are *discrete.* If $\mathrm{Re}[1/\tilde{V}_C^2 - a^2]^{1/2}$ is positive for $i < i^*$, it is negative for $i > i^*$. Thus the positions of critical angles play an important role in the determination of correct signs of relevant square roots.

We shall now give an alternative definition of critical angles which is more useful for computation. The definition takes into account only the expression under the square root, not the square root itself. It is as follows

$$\mathrm{Im}[1/\tilde{V}_C^2 - a^2] = 0, \quad \mathrm{Re}[1/\tilde{V}_C^2 - a^2] < 0. \tag{89}$$

If we take the square root $[1/\tilde{V}_C^2 - a^2]^{1/2}$, where $1/\tilde{V}_C^2 - a^2$ satisfies conditions (89), we obtain purely imaginary $[1/\tilde{V}_C^2 - a^2]^{1/2}$. Consequently, the real part of $[1/\tilde{V}_C^2 - a^2]^{1/2}$ vanishes, $\tilde{\mathbf{P}} = \mathbf{a}$, and (88) is satisfied.

In isotropic media, even the second critical angle i^{**} may exist, $i^* < i^{**} < 90^o$. It again satisfies (89).

Thus, the *criterion to choose the sign* of $[1/\tilde{V}_C^2 - a^2]^{1/2}$ is as follows:
1) If no critical angle exists:

$$[1/\tilde{V}_C^2 - a^2]^{1/2} = \mathcal{P}.\mathcal{V}.[1/\tilde{V}_C^2 - a^2]^{1/2}. \tag{90}$$

2) If one critical angle i^* exists, $0^o < i^* < 90^o$:

$$\begin{aligned} [1/\tilde{V}_C^2 - a^2]^{1/2} &= \mathcal{P}.\mathcal{V}.[1/\tilde{V}_C^2 - a^2]^{1/2} \qquad \text{for} \qquad i < i^*, \\ [1/\tilde{V}_C^2 - a^2]^{1/2} &= -\mathcal{P}.\mathcal{V}.[1/\tilde{V}_C^2 - a^2]^{1/2} \qquad \text{for} \qquad i > i^*. \end{aligned} \tag{91}$$

3) If two critical angles, i^* and i^{**}, exist, $0^o < i^* < i^{**} < 90^o$:

$$\begin{aligned} [1/\tilde{V}_C^2 - a^2]^{1/2} &= \mathcal{P}.\mathcal{V}.[1/\tilde{V}_C^2 - a^2]^{1/2} \qquad \text{for} \qquad i < i^* \quad \text{or} \quad i > i^{**}, \\ [1/\tilde{V}_C^2 - a^2]^{1/2} &= -\mathcal{P}.\mathcal{V}.[1/\tilde{V}_C^2 - a^2]^{1/2} \qquad \text{for} \qquad i^* < i < i^{**}. \end{aligned} \tag{92}$$

This is the final solution of the problem. The criteria (90) — (92) are used in our computations and computer programs. Such criteria were first proposed by Krebes (1985) for special cases discussed in Section 4. In that section, we shall also give analytical expressions for critical angles.

As we can see from (89), an important role in the determination of discrete critical angles i^* and i^{**} is played by the sign of $\mathrm{Re}[1/\tilde{V}_C^2 - a^2]$. For normal incidence, $\mathrm{Re}[1/\tilde{V}_C^2 -$

$a^2] > 0$, see (84), but for $i > 0$, $\mathrm{Re}[1/\tilde{V}_C^2 - a^2]$ decreases with increasing angle of incidence. Often, it is positive for all angles of incidence i, $0^o \le i < 90^o$, but sometimes it changes sign at some angle of incidence i^R, from positive to negative. To simplify the following discussion, we shall introduce the following terminology:

We shall call the region of angles of incidence $i < i^R$, for which $\mathrm{Re}[1/\tilde{V}_C^2 - a^2] > 0$, the *sub-critical region* of angles of incidence. Similarly, we shall call the region of angles of incidence $i > i^R$, for which $\mathrm{Re}[1/\tilde{V}_C^2 - a^2] < 0$, the *post-critical region* of angles of incidence. The sub-critical and post-critical regions of angles of incidence are mutually separated by the angle i^R, which may be called the *boundary angle of critical regions*. Note that $i = i^R$ represents always a critical angle in the non-dissipative media. Moreover, in non-dissipative media, condition (88) is satisfied for the whole post-critical region, $i^R < i < 90^o$. In dissipative media, $i = i^R$ usually does not represent a critical angle. The discrete critical angles i^* and i^{**}, if they exist, are, however, always *situated in the post-critical region*.

4. Determination of parameters of R/T inhomogeneous plane waves

The complex-valued slowness vector $\tilde{\mathbf{p}}$ of a selected R/T wave is given by (83). Equation (83) yields the following relations for the Cartesian components $\tilde{P}_i$ of the propagation vector $\tilde{\mathbf{P}}$, and the Cartesian components $\tilde{A}_i$ of the attenuation vector $\tilde{\mathbf{A}}$:

$$\tilde{P}_i = \mathrm{Re}[a_i \pm \varepsilon(1/\tilde{V}_C^2 - a^2)^{1/2} n_i], \quad \tilde{A}_i = \mathrm{Im}[a_i \pm \varepsilon(1/\tilde{V}_C^2 - a^2)^{1/2} n_i]. \tag{93}$$

Here a_i are known complex-valued tangential components of the incident wave, $a^2 = a_i a_i$, V_C is the complex-valued velocity corresponding to the selected R/T wave, n_i are Cartesian components of the real-valued unit vector normal to the interface Σ, and ε is the orientation index defined by (82). The upper sign "+" corresponds to the transmitted waves, and the lower sign "$-$" to the reflected waves.

As soon as $\tilde{p}_i$ and $\tilde{A}_i$ are known, we can calculate the lengths $\tilde{P}$ and $\tilde{A}$ of the real-valued vectors $\tilde{\mathbf{P}}$ and $\tilde{\mathbf{A}}$

$$\tilde{P} = |\tilde{\mathbf{P}} \cdot \tilde{\mathbf{P}}|^{1/2}, \quad \tilde{A} = |\tilde{\mathbf{A}} \cdot \tilde{\mathbf{A}}|^{1/2}, \tag{94}$$

and the relevant unit vectors, specifying the directions of $\tilde{\mathbf{P}}$ and $\tilde{\mathbf{N}}$; see (39)

$$\tilde{N}_i^R = \tilde{P}_i/\tilde{P}, \quad \tilde{N}_i^I = \tilde{A}_i/\tilde{A}, \tag{95}$$

$\tilde{N}_i^R$ can be used, e.g., to determine the real-valued angle of reflection/transmission $\tilde{i}$, representing the angle between $\mathbf{n}$ and $\tilde{\mathbf{N}}^R$,

$$\cos\tilde{i} = \tilde{\mathbf{N}}^R \cdot \mathbf{n}. \tag{96}$$

We consider here angles of reflection/transmission $\tilde{i}$ in the following range: $0^o \le \tilde{i} \le 180^o$. This is useful, as $\tilde{i}$ may be grater than 90^o at post-critical regions.

The attenuation angle $\tilde{\gamma}$ is given by the relation (40),

$$cos\tilde{\gamma} = \tilde{N}_i^R \tilde{N}_i^I. \tag{97}$$

Finally, the real-valued phase velocity $\tilde{\mathcal{C}}$ of the selected R/T wave under consideration is given by (54),

$$\tilde{\mathcal{C}} = \mathrm{Re}(\tilde{V}_C)\sqrt{\frac{2(1+\tilde{Q}^{-2})}{1+\sqrt{1+\tilde{Q}^{-2}\cos^{-2}\tilde{\gamma}}}}, \tag{98}$$

where $\tilde{V}_C$ is the complex-valued velocity of the R/T wave, $\tilde{Q}$ is the quality factor of the R/T wave and $\cos\tilde{\gamma}$ is given by (97). Instead of $\mathrm{Re}(\tilde{V}_C) = \tilde{V}$, we can also use $\tilde{\mathcal{C}}_H$, the phase velocity of the relevant homogeneous R/T wave, see (55).

Using the above equations, we can also write a new relation for the complex-valued slowness vector of the selected R/T wave

$$\tilde{p}_i = \frac{1}{\tilde{\mathcal{C}}}(\tilde{N}_i^R + \mathrm{i}\tilde{b}\tilde{N}_i^I), \tag{99}$$

where

$$\tilde{b} = \sqrt{\frac{\tilde{g}-1}{\tilde{g}+1}} = \sqrt{\frac{\sqrt{1+\tilde{Q}^{-2}\cos^{-2}\tilde{\gamma}}-1}{\sqrt{1+\tilde{Q}^{-2}\cos^{-2}\tilde{\gamma}}+1}} = \frac{1}{\tilde{Q}\cos\tilde{\gamma}[\sqrt{1+\tilde{Q}^{-2}\cos^{-2}\tilde{\gamma}}+1]}. \tag{100}$$

5. Several remarks and conclusions

Here we shall make several remarks which may clarify certain results derived above, and make some conclusions useful in the following.

5a) Anomalous direction of the propagation vector of R/T waves

As shown above, the angle of reflection/transmission is greater than 90^o behind the critical angle. For example, the propagation vector of the transmitted wave is oriented back to the first halfspace, or the propagation vector of the reflected wave is oriented into the second halfspace. Such orientation is impossible in isotropic non-dissipative media. Analogous situation is, however, well-known in anisotropic non-dissipative media. See Červený (1997), Section 2.3.3.

5b) Energy flux

The next remark is devoted to energy flux. In anisotropic non-dissipative media, the selection of individual roots σ_i of (68), corresponding to reflected waves (or the selection of roots of (69), corresponding to transmitted waves) is based on the orientation of energy flux. Similar criteria, based on energy flux, were proposed even for elastic dissipative media, see Borcherdt (1977). However, it was claimed by Krebes (1985) that the criteria based on energy flux do not work properly in dissipative media. It will be very useful to verify again the results of Krebes, as simple criteria based on energy flux would simplify the selection of σ_i considerably.

5c) Energy balance on the interface

It is possible to study the energy flux across the interface in the whole R/T process, and to study the energy balance. In dissipative media, however, the situation is more complex than in non-dissipative media. In addition to energy fluxes of individual waves, it is also necessary to consider *interaction energy flux*, which vanishes in dissipative media. See Borcherdt (1977), Krebes (1984), etc. For simple cases studied by Krebes (1984), the energy balance on the interface was fulfilled.

5d) Moduli of R/T coefficients for post-critical angles of incidence

The conclusion following from the point 5c) is that the moduli of reflection coefficients of non-converted reflected wave at post-critical region may exceed unity. This is not possible in non-dissipative medium. The energy balance is preserved even in this case, as the interaction energy flux may be negative.

5e) Anomalous behaviour of phases of R/T coefficients

Consider now the R/T coefficients for post-critical angles of incidence in dissipative media, and take the limit $Q \to \infty$ in both halfspaces. We intuitively expect that we must obtain the same results as in non-dissipative media. This is, however, not always true. The reason is the criterion (87) used to select the sign of $[1/\tilde{V}_C^2 - a^2]^{1/2}$ in non-dissipative media. This criterion fixes the orientation of the attenuation vector $\tilde{\mathbf{A}}$ of the inhomogeneous transmitted wave at post-critical distances. Such a criterion cannot be used in dissipative media, where the orientation of the attenuation vector $\tilde{\mathbf{A}}$ is fully determined by the parameters of incident wave and by boundary conditions. Consequently, certain square roots may have opposite signs than required by (87) for $Q \to \infty$ in dissipative media. The choice of sign in (87) influences directly the signs of the phases of R/T coefficients. If we compute the R/T coefficients in dissipative media for $Q \to \infty$, we may obtain opposite signs of their phases in comparison with non-dissipative media. This fact is influenced mainly by ratios of Q's corresponding to incident and selected R/T wave. For a more detailed discussion and examples, see Section 4.2.

4 Decomposition of the system of equations for displacement R/T coefficients in isotropic media

In certain special cases, the system of six equations (76) for $A^r, B^r, C^r, A^t, B^t, C^t$ for isotropic dissipative media can be decomposed into two subsystems. The first subsystem consists of four equations and second of two equations. Whereas such decomposition is always possible in isotropic non-dissipative media, see Červený (1997), Section 2.3.2, the decomposition in non-dissipative media is possible only exceptionally.

The basic assumption we shall make is that the *slowness vector plane* Σ^S *of the incident wave, defined by Section 2.2, is perpendicular to the interface* Σ. A consequence is that the propagation vector $\mathbf{P}$ of the incident wave, the attenuation vector $\mathbf{A}$ of the incident wave, and the normal $\mathbf{n}$ to the interface are *coplanar*. Similarly as in non-dissipative media, we shall call the plane defined by the propagation vector $\mathbf{P}$ of the incident wave and by the normal $\mathbf{n}$ to the interface the *plane of incidence*. Thus, the plane Σ^S represents the plane of incidence in this case.

We shall further assume that the eigenvectors of incident S wave are given by the relations

$$\mathbf{g}^{(1)} = -\frac{\mathbf{n}^S \times \mathbf{p}}{|\mathbf{n}^S \times \mathbf{p}|}, \quad \mathbf{g}^{(2)} = \mathbf{n}^S. \tag{101}$$

This is a special case of the general relations (28), with $\delta = -\frac{1}{2}\pi$. Note that $\mathbf{g}^{(2)}$ is real-valued, perpendicular to Σ^S, and $\mathbf{g}^{(1)}$ is complex-valued, situated in Σ^S.

In this particular case, it is useful (but not necessary) to introduce a local Cartesian coordinate system, the x_2-axis of which coincides with $\mathbf{n}^S$, and the x_3-axis is normal to interface. Traditionally, the x_3-axis is considered to be vertical, and the x_1-, x_2-axes to be horizontal. Consequently, it is usual in seismology to call the S2 component of the S wave (linearly polarized along $\mathbf{g}^{(2)} = \mathbf{n}^S$) the SH component (S-horizontal), or even *SH wave*. Similarly, the S1 component (elliptically polarized in the plane of incidence Σ^S) is called the SV component (S-vertical), or even *SV wave*. Alternatively, in the terminology of viscoelastic media, SH component corresponds to the Type-II S wave, and SV component to the Type-I S wave.

It follows from (83) that the complex-valued slowness vectors $\tilde{\mathbf{p}}$ of all generated waves will be again situated in the plane of incidence Σ^S. Consequently, even the real-valued vectors $\tilde{\mathbf{P}}$ and $\tilde{\mathbf{A}}$ of all generated waves are situated in the plane of incidence Σ^S. Further, even the complex valued eigenvectors $\tilde{\mathbf{g}}^{(3)}$ of the generated plane P waves are confined to the plane of incidence Σ^S, see (23). The polarization vectors $\tilde{\mathbf{g}}^{(1)}$ and $\tilde{\mathbf{g}}^{(2)}$ of generated S waves may be again specified by (28), as the angle δ in (28) may be chosen arbitrarily. We take $\delta = -\frac{1}{2}\pi$ in (28) and obtain equations (101) (where $\mathbf{p}$ should be replaced by $\tilde{\mathbf{p}}$). Then $\tilde{\mathbf{g}}^{(1)}$ is complex-valued and is situated in the plane of incidence and $\tilde{\mathbf{g}}^{(2)}$ is real-valued and is perpendicular to it.

Consequently, the system of six equations (76) can be considerably simplified. If we again use superscript "r" for reflected waves and "t" for transmitted waves (instead of a tilde above the letter), we obtain

$$\begin{array}{ccccccccccccccc}
n_1 & = & n_2 & = & 0, n_3 & = & 1, & & p_2 & = & p_2^r & = & p_2^t & = & 0, \\
P_2 & = & P_2^r & = & P_2^t & = & 0, & & A_2 & = & A_2^r & = & A_2^t & = & 0, \\
g_2^{(3)} & = & g_2^{(3)r} & = & g_2^{(3)t} & = & 0, & & g_2^{(1)} & = & g_2^{(1)r} & = & g_2^{(1)t} & = & 0, \\
g_1^{(2)} & = & g_1^{(2)r} & = & g_1^{(2)t} & = & 0, & & g_3^{(2)} & = & g_3^{(2)r} & = & g_3^{(2)t} & = & 0, \\
g_2^{(2)} & = & g_2^{(2)r} & = & g_2^{(2)t} & = & 1. & & & & & & & &
\end{array} \tag{102}$$

All the components in (102) correspond to the local Cartesian coordinate system introduced above.

Then the system (76) can be decomposed into two subsystems. The first contains only four linear equations for A^r, B^r, A^t, B^t:

$$\begin{array}{rcl}
A^t g_1^{(3)t} + B^t g_1^{(1)t} - A^r g_1^{(3)r} - B^r g_1^{(1)r} & = & D_1, \\
A^t g_3^{(3)t} + B^t g_3^{(1)t} - A^r g_3^{(3)r} - B^r g_3^{(1)r} & = & D_3, \\
A^t X_1^t + B^t Y_1^t - A^r X_1^r - B^r Y_1^r & = & E_1, \\
A^t X_3^t + B^t Y_3^t - A^r X_3^r - B^r Y_3^r & = & E_3.
\end{array} \tag{103}$$

Here X_i and Y_i are again given by (77), but may be simplified using (102). Note that D_1, D_3, E_1 and E_3 are given by (78) for the incident P wave, and by (79) for the incident S wave. In (103), the terms with C, C^r and C^t vanish due to (102). The second subsystem consists only of two linear equations for C^r and C^t

$$\begin{array}{rcl}
C^t - C^r & = & C, \\
C^t Z_2^t - C^r Z_2^r & = & C Z_2,
\end{array} \tag{104}$$

where Z_2 is again given by (77).

Systems (103) and (104) have certain important consequences. Let us consider three possible incident waves:
a)*Incident P wave* ($A \neq 0, B = C = 0$). Then $D_2 = E_2 = 0$, and only P and SV reflected and transmitted waves are generated.
b)*Incident SV wave* ($B \neq 0, A = C = 0$). Then $D_2 = E_2 = 0$, and only P and SV reflected and transmitted waves are generated.
c)*Incident SH wave* ($C \neq 0, A = B = 0$). Then $D_1 = D_3 = E_1 = E_3 = 0$, and only SH, reflected and transmitted, waves are generated.

Thus the SH waves are fully separated from P and SV waves in the process of reflection and transmission of plane waves at a plane interface in this case. For this reason, system (103) is also called the P-SV system, and system (104) the SH system.

There is, however, a basic difference between the decomposition of general system of six equations (76) into two subsystems (103) and (104) in dissipative and non-dissipative media. In non-dissipative media, such a decomposition is possible *always*. Even if the real-valued polarization vectors of incident S waves, $\mathbf{g}^{(1)}$ and $\mathbf{g}^{(2)}$, are not polarized in the plane of incidence and perpendicularly to it, we can rotate them into these positions. See Červený (1997), Section 5.3.5, sub 3. In dissipative media, such a decomposition is possible only if the vectors $\mathbf{P}$ and $\mathbf{A}$ of the incident wave are coplanar with $\mathbf{n}$ (the unit normal to the interface). For generally oriented $\mathbf{A}$, the decomposition is impossible, and any rotation cannot help. The computation of R/T coefficients must be then performed using the system of six equation (76).

As we can see from (103) and (80), the P-SV system (103) yields only four reflection coefficients $R^r_{11}, R^r_{13}, R^r_{31}$ and R^r_{33}, and the system (104) yields only one reflection coefficient R^r_{22}. The remaining four reflection coefficients $R^r_{12}, R^r_{21}, R^r_{23} = R^r_{32}$ vanish. Consequently, the number of non-vanishing coefficients is only five, not nine. For transmission coefficients, the situation is analogous.

To determine the tangential component p_1 of the complex-valued slowness vector of the incidence wave, we can use (60). If we again denote the angle of incidence i, we can write

$$N_1^R = \sin i, \quad N_1^I = \sin(i - \gamma). \tag{105}$$

The second equation of (105) also defines the sign of the attenuation angle γ. See Fig. 1. Then (60) gives

$$p_1 = \sqrt{\tfrac{1}{2}W}(\sqrt{g+1}\sin i + \mathrm{i}\sqrt{g-1}\sin(i-\gamma)), \tag{106}$$

with

$$g = \sqrt{1 + Q^{-2}\cos^{-2}\gamma}, \quad W = \frac{2}{\mathcal{C}_H^2(1 + \sqrt{1+Q^{-2}})} = \frac{1}{V^2(1+Q^{-2})}. \tag{107}$$

Here V is the complex-valued velocity of incident plane wave, see (35) for P and S waves. Similarly, $\mathcal{C}_H$ is the phase velocity (also real-valued) of relevant homogeneous wave, see (55). For $Q \to \infty$ (low-loss media)

$$W \sim \frac{1}{V} \sim \frac{1}{\mathcal{C}_H}. \tag{108}$$

For any R/T wave, the tangential component $\tilde{p}_1$ of the complex-valued slowness vector equals p_1,

$$\tilde{p}_1 = p_1, \tag{109}$$

with p_1 given by the relation analogous to (106),

$$\tilde{p}_1 = \sqrt{\tfrac{1}{2}\tilde{W}}(\sqrt{\tilde{g}+1}\sin\tilde{i} + \mathrm{i}\sqrt{\tilde{g}-1}\sin(\tilde{i}-\tilde{\gamma})). \tag{110}$$

Here $\tilde{i}$ is the real-valued angle of reflection/transmission, $\tilde{\gamma}$ the attenuation angle of the R/T wave, and $\tilde{W}$, $\tilde{g}$ are given by relations

$$\tilde{g} = \sqrt{1+\tilde{Q}^{-2}\cos^{-2}\tilde{\gamma}}, \quad \tilde{W} = \frac{2}{\tilde{\mathcal{C}}_H^2(1+\sqrt{1+\tilde{Q}^{-2}})} = \frac{1}{\tilde{V}^2(1+\tilde{Q}^{-2})}. \tag{111}$$

Here $\tilde{Q}$, $\tilde{\mathcal{C}}_H$ and $\tilde{V}$ correspond to the selected R/T wave.

It may be interesting to separate the real and imaginary parts of (109). Using (106) and (110), we obtain

$$\begin{array}{lcl} \sqrt{\frac{1}{2}W}\sqrt{g+1}\sin i & = & \sqrt{\frac{1}{2}\tilde{W}}\sqrt{\tilde{g}+1}\sin\tilde{i} \\ \sqrt{\frac{1}{2}W}\sqrt{g-1}\sin(i-\gamma) & = & \sqrt{\frac{1}{2}\tilde{W}}\sqrt{\tilde{g}-1}\sin(\tilde{i}-\tilde{\gamma}). \end{array} \tag{112}$$

These two relations represent the Snell's law for an interface between two dissipative media, valid if the slowness vector plane Σ^S is perpendicular to the interface Σ. Equation (112) can be, in principle, used to compute $\tilde{i}$ and $\tilde{\gamma}$ from known i and γ, assuming $V, \tilde{V}, Q, \tilde{Q}$ are known. We must, however, remember that $\tilde{g}$ also includes $\tilde{\gamma}$. In this text, however, we shall use more efficient procedures to compute $\tilde{i}$ and $\tilde{\gamma}$ than (112). For more details on Snell's law in dissipative media see Wennerberg (1985).

Now we shall determine both components of the slowness vector of the generated wave, horizontal $\tilde{p}_1$ and vertical $\tilde{p}_3$. Using (83) we obtain

$$\tilde{p}_1 = p_1, \quad \tilde{p}_2 = 0, \quad \tilde{p}_3 = \pm\varepsilon(1/\tilde{V}_C^2 - p_1^2)^{\frac{1}{2}}, \tag{113}$$

as $a_1 = p_1, a_2 = a_3 = 0, n_1 = n_2 = 0, n_3 = 1$. Here ε is the orientation index (82), $\tilde{V}_C$ is the complex-valued velocity of the selected R/T wave. The upper sign corresponds to the transmitted waves, the lower sign to the reflected waves.

The sign of $(1/\tilde{V}_C^2 - p_1^2)^{\frac{1}{2}}$ must be determined using the continuation procedure, outlined in Section 3.2, part 3. For normal incidence ($i = 0$), we have

$$[1/\tilde{V}_C^2 - p_1^2]^{\frac{1}{2}} = \mathcal{P}.\mathcal{V}.[1/\tilde{V}_C^2 - p_1^2]^{\frac{1}{2}}. \tag{114}$$

For $i > 0$ and fixed γ, we use criteria (90) — (92). The only thing which remains to be specified is the determination of the discrete critical angles i^* and i^{**} of the incidence, if they exist.

4.1 Determination of discrete critical angles

We shall use (89), with $1/\tilde{V}_C^2 - a^2 = 1/\tilde{V}_C^2 - p_1^2$. For $1/\tilde{V}_C^2$, we use (57)

$$1/\tilde{V}_C^2 = \tilde{W}(1 + \mathrm{i}/\tilde{Q}). \tag{115}$$

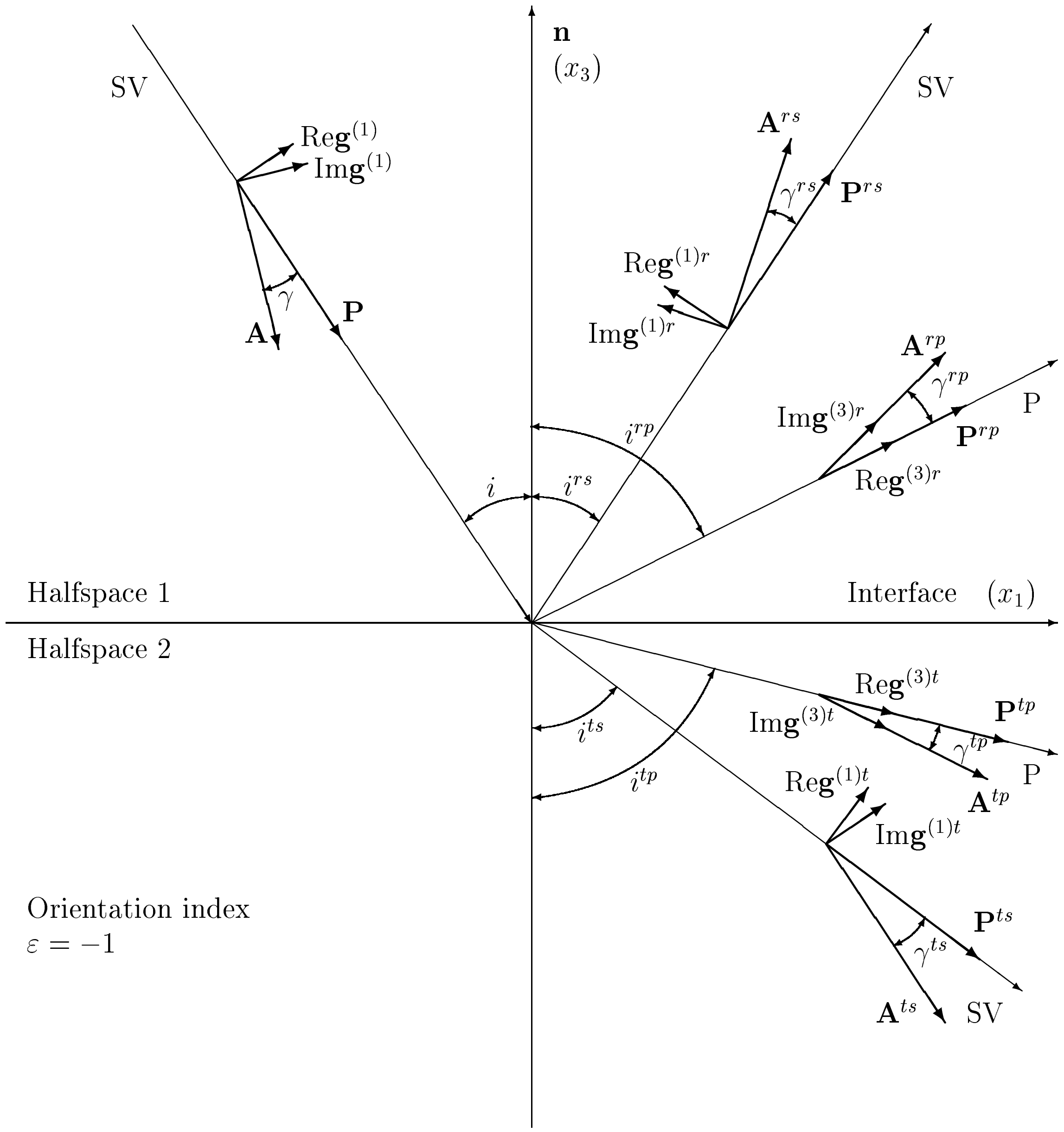

Figure 1: Reflection and transmission of an *inhomogeneous plane SV wave* on a plane interface between two isotropic dissipative halfspaces (schematically). The picture displays a simple situation that the propagation vector $\mathbf{P}$ and the attenuation vector $\mathbf{A}$ of the incident wave are coplanar with $\mathbf{n}$, the unit vector normal to the interface. In this case, the propagation and attenuation vectors of all generated R/T plane waves are situated in the same plane. The angle of incidence is denoted by i, and the attenuation angle of the incident wave by γ. The angles of reflection/transmission and the attenuation angles of all generated waves by the same symbols, with appropriate superscripts. The vectors $\mathbf{g}^{(1)}$ and $\mathbf{g}^{(3)}$ represent the complex-valued eigenvectors of SV and P plane waves. $\text{Re}\mathbf{g}^{(3)}$ and $\text{Im}\mathbf{g}^{(3)}$ are parallel to $\mathbf{P}$, $\mathbf{A}$ of P waves, and $\text{Re}\mathbf{g}^{(1)}$, $\text{Im}\mathbf{g}^{(1)}$ are perpendicular to relevant $\mathbf{P}$, $\mathbf{A}$ of SV waves. As the eigenvectors are complex-valued, the polarization of all waves is elliptical. Quite analogous picture would be obtained for the P incident wave, only the relevant eigenvector would be represented by $\mathbf{g}^{(3)}$ (with $\text{Re}\mathbf{g}^{(3)}$ parallel to $\mathbf{P}$ and $\text{Im}\mathbf{g}^{(3)}$ parallel to $\mathbf{A}$.)

Then(89) with (106) yield conditions for the discrete critical angle

$$\begin{array}{rcccl}\mathrm{Im}[1/\tilde{V}_C^2 - p_1^2] & = & \tilde{W}\tilde{Q}^{-1} - WQ^{-1}\cos^{-1}\gamma\sin i\sin(i-\gamma) & = & 0, \\ \mathrm{Re}[1/\tilde{V}_C^2 - p_1^2] & = & \tilde{W} - \frac{1}{2}W[(1+g)\sin^2 i - (g-1)\sin^2(i-\gamma)] & < & 0.\end{array} \tag{116}$$

We shall first solve the first equation of (116) for i. Writing it in the form $\tilde{W}\tilde{Q}^{-1} = WQ^{-1}\cos^{-1}\gamma\sin i\sin(i-\gamma)$ and taking squares of both sides of this equation, we obtain a quadratic equation for $\Omega = \sin^2 i$:

$$\Omega^2 - \Omega[(c+1)\cos^2\gamma + \sin^2\gamma] + \tfrac{1}{4}\cos^2\gamma(c+1)^2 = 0, \tag{117}$$

where

$$c = 2\frac{\tilde{W}Q}{W\tilde{Q}} - 1. \tag{118}$$

There are two roots of (117), Ω_1 and Ω_2

$$\Omega_{1,2} = \tfrac{1}{2} + \tfrac{1}{2}c\cos^2\gamma \pm \tfrac{1}{2}\sin\gamma\sqrt{1 - c^2\cos^2\gamma}. \tag{119}$$

We are interested only in real-valued roots (119). Such roots exist only if the discriminant is non-negative,

$$\cos^2\gamma < \frac{1}{c^2} = (2\frac{\tilde{W}Q}{W\tilde{Q}} - 1)^{-1}. \tag{120}$$

If the condition (120) is not satisfied, no critical angle exist. If it is satisfied, we can calculate two roots $\Omega_k, k = 1, 2$. None, one or two critical angles may exist, corresponding to the found Ω_k. For each k, we perform the following tests:
a) First test:

$$0 \le \Omega_k \le 1. \tag{121}$$

In this condition is satisfied, we can calculate the relevant angle if incidence i_k

$$i_k = \arcsin(\sqrt{\Omega_k}). \tag{122}$$

If (121) is not satisfied, Ω_k does not yield any critical angle.
b) Second test:

$$i_k > \gamma. \tag{123}$$

For $i_k < \gamma$, the first equation of (116) is not satisfied, as both terms are positive. (The root was computed from the equation $\tilde{W}^2\tilde{Q}^{-2} = W^2Q^{-2}\cos^{-2}\gamma\sin^2 i\sin^2(i-\gamma)$, not from the first equation of (116)).
c)Third test:

$$\mathrm{Re}(1/\tilde{V}_C^2 - p_1^2) < 0, \tag{124}$$

see the second equation of (116).

If any of conditions (120), (121), (123) and (124) is not satisfied, Ω_k does not represent a critical angle. The numerical implementation of these criteria is easy. It should be noted that the first critical angle is very common in practical computations, but the second critical angle exists only exceptionally.

To explain in a greater detail the behaviour of the square root $\sigma = [1/\tilde{V}_C^2 - p_1^2]^{\frac{1}{2}}$, we shall compare them for dissipative and non-dissipative media, and present several typical examples. See Fig. 2 for non-dissipative media and Fig. 3 for dissipative media. The left-hand columns in Figs. 2 and 3 display the values of $\mathrm{Re}\sigma^2$ and $\mathrm{Im}\sigma^2$, in dependence on the angle of incidence, $0^o \leq i \leq 90^o$. $\mathrm{Re}\sigma^2$ is shown by a continuous line, $\mathrm{Im}\sigma^2$ by a dashed line. The second column shows, by a bold line, a parametric graph of σ in a complex plane with $\mathrm{Re}\sigma$ along the real axis, and $\mathrm{Im}\sigma$ along the imaginary axis. The parameter of the curve is the angle of incidence i, varying from 0^o (denoted by $\times$) to 90^o (denoted by $\Box$). We shall use the following notations: 1) The angle of incidence, for which $\mathrm{Re}\sigma^2 = 0$, is denoted by i^R. 2) The angle of incidence, for which $\mathrm{Im}\sigma^2 = 0$, is denoted by i^I. In Figs. 2 and 3, the angle of incidence i^R (if it exists) is indicated by $\circ$, and the angle of incidence i^I (if it exist) is indicated by $\bullet$. If two angles i^I exist, both i_1^I and i_2^I are denoted by $\bullet$. Note that i^R (if it exists) separates the sub-critical region from the post-critical region, see Section 3.2, sub 3.

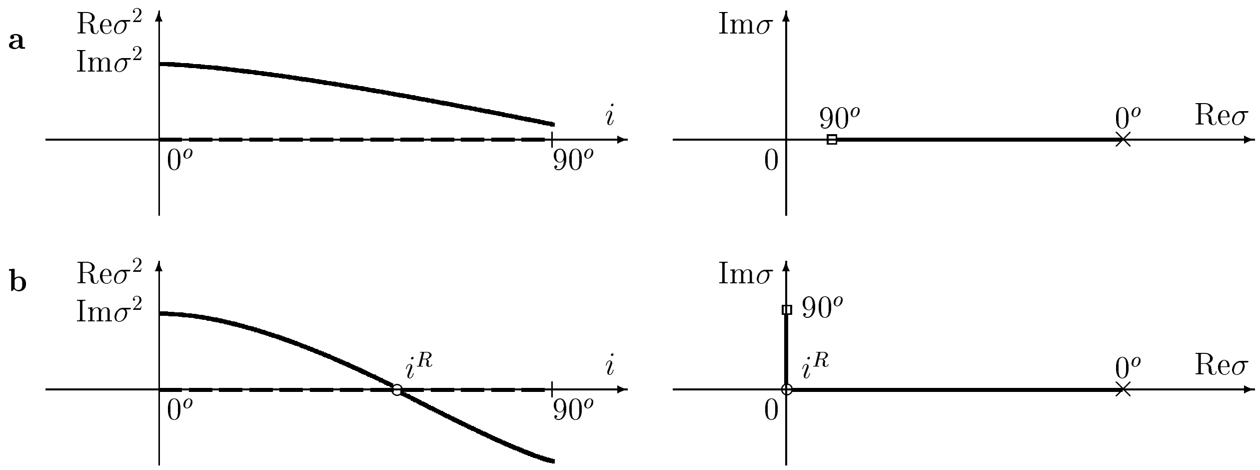

Figure 2: Square root σ for a non-dissipative medium (schematically). In the left-hand collumn, $\mathrm{Re}\sigma^2$ is shown by a continuous line, and $\mathrm{Im}\sigma^2$ by a dashed line. See text for other details.

Let us first briefly discuss *non-dissipative media*, see Fig. 2. The imaginary part of $1/\tilde{V}_C^2 - p_1^2$ is always zero in this case. There are two possibilities. a) $\mathrm{Re}\sigma^2 > 0$ in the whole range of angles of incidence, $0^o \leq i \leq 90^o$. Then i^R does not exist and σ is positive real-valued for all angles of incidence. See Fig. 2a . b) $\mathrm{Re}\sigma^2$ is positive for $i < i^R$, and negative for $i^R < i < 90^o$. Then σ is positive real-valued for $0 < i < i^R$, and positive imaginary for $i^R < i < 90^o$, see (87) and Fig. 2b.

For *dissipative media*, see Fig. 3. Figs. 3a, b consider no angle of incidence i^I, Figs. 3c, d, e one angle of incidence i^I, and Figs. 3f, g, h two angles of incidence i^I, denoted by i_1^I, i_2^I. The situation is considerably more complex than for non-dissipative media.

a) If both $\mathrm{Re}\sigma^2$ and $\mathrm{Im}\sigma^2$ are positive for the whole range of angles of incidence $0^o < i < 90^o$, σ is completely situated in the first quadrant. For $Q \to \infty$ and $\tilde{Q} \to \infty$, the curves 3a approach 2a for non-dissipative media.

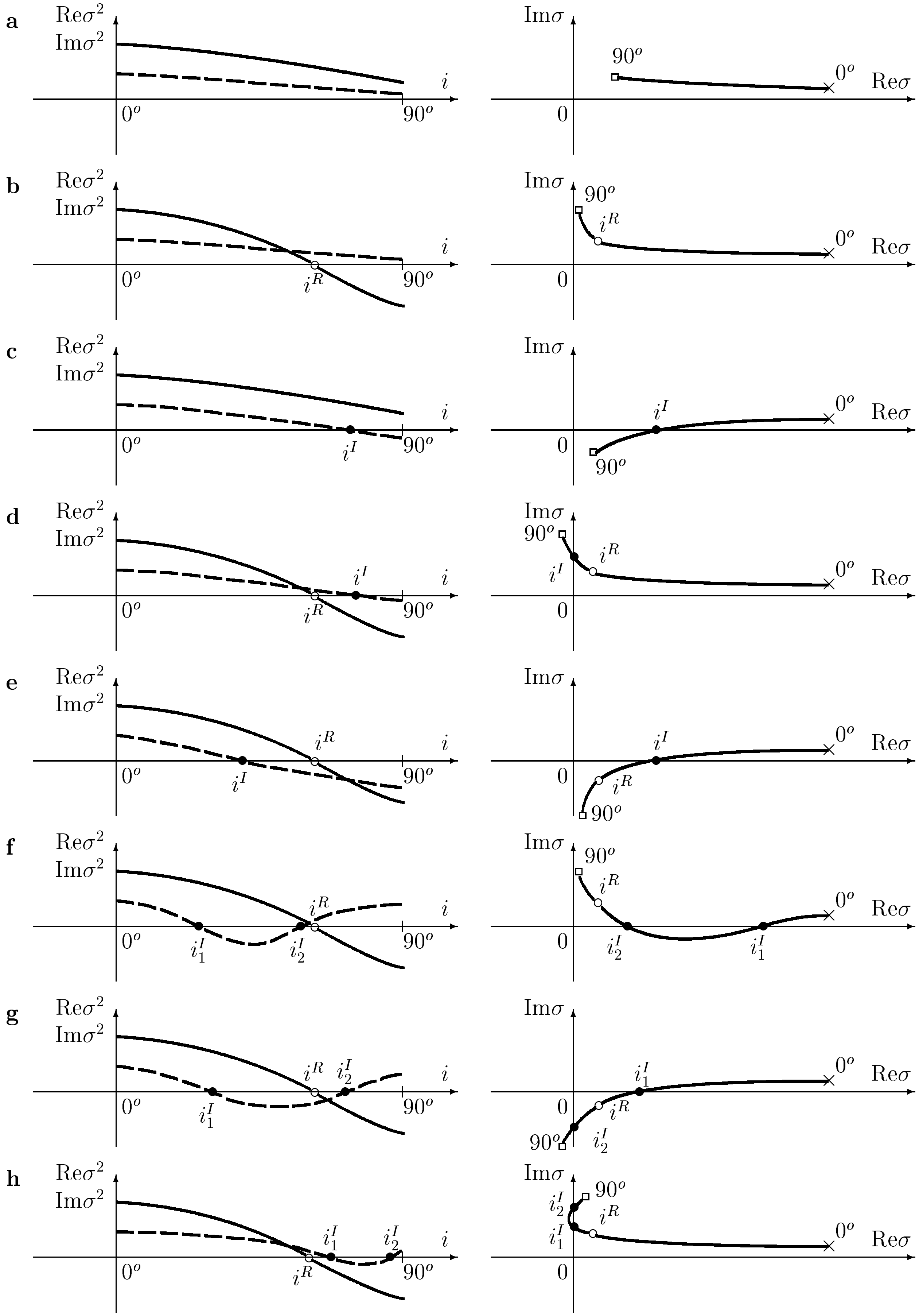

Figure 3: Square root σ for a dissipative medium (schematically). For other details, see text and caption of Fig. 2.

b) If $\mathrm{Im}\sigma^2 > 0$ for $0^o < i < 90^o$, but $\mathrm{Re}\sigma^2$ changes sign at i^R, $0^o < i^R < 90^o$, σ is again completely situated in the first quadrant. For $i > i^R$, σ is close to positive imaginary axis. See Fig. 3b. For $Q \to \infty$ and $\tilde{Q} \to \infty$, the curves 3b approach 2b for non-dissipative media.

c) If $\mathrm{Re}\sigma^2 > 0$ for $0^o < i < 90^o$, but $\mathrm{Im}\sigma^2$ changes sign at i^I, $0^o < i^I < 90^o$, σ is situated in the first and fourth quadrant. See Fig. 3c. For $Q \to \infty$ and $\tilde{Q} \to \infty$, the curves 3c approach 2a for non-dissipative media.

d) Assume that $\mathrm{Re}\sigma^2$ changes sign at $i = i^R$, $0^o < i^R < 90^o$, $\mathrm{Im}\sigma^2$ at $i = i^I$, and that $i^I > i^R$. See Fig. 3d. Then the angle of incidence i^I represents the critical angle i^*. The square root σ is situated in the first and second quadrant. For $i = i^I$, it intersects the positive imaginary axis, and, for $i^R < i < 90^o$, it is close to positive imaginary axis. For $Q \to \infty$ and $\tilde{Q} \to \infty$, the curve 3d approaches 2b for non-dissipative media.

e) Assume that $\mathrm{Re}\sigma^2$ changes sign at $i = i^R$, $0^o < i^R < 90^o$, and $\mathrm{Im}\sigma^2$ at i^I, $0^o < i^I < 90^o$. Contrary to the previous case, however, we assume that $i^I < i^R$. In this case, i^I *does not represent a critical angle.* It has, however, a different effect: It reverses the trend of σ in the $\mathrm{Re}\sigma$-$\mathrm{Im}\sigma$ plane from the positive imaginary axis to the negative imaginary axis. Compare Figs. 3d and 3e. In Fig. 3e, the square root σ is situated in the first and fourth quadrant and it is close to negative imaginary axis. For $Q \to \infty$ and $\tilde{Q} \to \infty$, it does not approach any of curves 2a or 2b known for dissipative media. Actually, it would be analogous to 2b, with the part $i^R < i < 90^o$ situated not along positive, but *along negative imaginary axis.* We shall speak of the *anomalous square root argument.* It should be noted that the argument is not anomalous in the concept of inhomogeneous waves in dissipative media. "Anomalous" is understood here in such a way that for $Q \to \infty$ and $\tilde{Q} \to \infty$ the argument will be different from that for non-dissipative medium.

f) Consider $0^o < i^R < 90^o$, and two angles i^I_1, i^I_2, in such a way that $0^o < i^I_1 < i^I_2 < i^R < 90^o$, see Fig. 3f. Then none of the angles i^I_1, i^I_2 represents a critical angle. The square root σ is situated in the first and fourth quadrants, but has a quite regular character. For $Q \to \infty$ and $\tilde{Q} \to \infty$, the curve 3f approaches the curve 2b for non-dissipative media.

g) Consider $0^o < i^R < 90^o$, and two angles i^I_1, i^I_2, in such a way that $0^o < i^I_1 < i_R < i^I_2 < 90^o$, see Fig. 3g. The angle i^I_2 represents a critical angle in this case, and the square root σ is situated in the first, fourth, and third quadrant. The σ curve intersects the positive real axis for $i = i^I_1$, and the negative imaginary axis for $i = i^I_2$. The argument of the square root is *anomalous* in this case. For $Q \to \infty$ and $\tilde{Q} \to \infty$, it approaches the negative imaginary axis for $i^R < i < 90^o$.

h) Consider $0^o < i^R < 90^o$, and two angles i^I_1, i^I_2, in such a way that $0^o < i^R < i^I_1 < i^I_2 < 90^o$, see Fig. 3h. In this case, the angles i^I_1, i^I_2 represent critical angles i^* and i^{**}. The square root σ is situated in the first and second quadrant. It intersects twice the positive imaginary axis, at $i = i^I_1$ and $i = i^I_2$. For $Q \to \infty$ and $\tilde{Q} \to \infty$, it approaches the curve 2b for dissipative media.

The behaviour of $\sigma = [1/\tilde{V}_C^2 - p_1^2]^{\frac{1}{2}}$ looks complicated, but the *general conclusions* are simple:

1) If i^R does not exist (i.e., $\mathrm{Re}(1/\tilde{V}_C^2 - p_1^2) > 0$ for all angles of incidence), no critical angles exist. Moreover, the argument of the square root is regular, and, for $Q \to \infty$, $\tilde{Q} \to \infty$, it approaches the argument known for non-dissipative medium. This conclusion

remains valid even if σ^2 changes sign for $0^o < i < 90^o$, and i^I or i_1^I and i_2^I exist.

2) If i^R and one angle i^I exist in such a way that $0^o < i^R < i^I < 90^o$, then i^I represents a critical angle. The argument of σ is regular in this case.

3) If i^R and one angle i^I exist in such a way that $0^o < i^I < i^R < 90^o$, then i^I does not represent a critical angle. It, however, indicates an anomalous argument of the square root.

4) If i^R and two angles i_1^I, i_2^I exist, the situation is analogous to 2 and 3:
a) For $0^o < i_1^I < i_2^I < i^R < 90^o$: No critical angle, regular argument.
b) For $0^o < i_1^I < i^R < i_2^I < 90^o$: One critical angle $i^* = i_2^I$; anomalous argument.
c) For $0^o < i_R < i_i^I < i_2^I < 90^o$: Two critical angles $i^* = i_1^I, i^{**} = i_2^I$; regular argument.

Finally it should be emphasized that the criterion for the choice of sign of σ, given by (90) – (92), is quite universal and remains valid in all cases discussed in Figs. 3a – h. the purpose of the discussion presented here is only to increase the understanding of certain properties of R/T coefficients for dissipative media, which will be studied in next sections.

4.2 σ^2-maps

It may be instructive to construct σ^2-maps, which display isolines of

$$\mathrm{Re}\sigma^2 = \mathrm{Re}[1/\tilde{V}_C^2 - p_1^2], \quad \mathrm{Im}\sigma^2 = \mathrm{Im}[1/\tilde{V}_C^2 - p_1^2], \tag{125}$$

for $0^o \le i \le 90^o, 0 \le \gamma \le 90^o$. The parameters of these maps are $V, \tilde{V}, Q, \tilde{Q}$, or, alternatively, $\mathcal{C}_H, \tilde{\mathcal{C}}_H, Q, \tilde{Q}$. Two such σ^2-maps are shown in Figs. 4 – 5. In both these figures, isolines of $\mathrm{Re}\sigma^2$ are continuous and isolines of $\mathrm{Im}\sigma^2$ dashed.

In Fig. 4, the model parameters are $\mathcal{C}_H = 1.44$ km/s, $\tilde{\mathcal{C}}_H = 2.08$ km/s, $Q = 13, \tilde{Q} = 22$. Thus, both the velocity and the Q factor of the incident wave are smaller than the same quantities of the generated wave. In Fig. 5, we use the same model, only $\tilde{Q}$ is changed from 22 to 5. Consequently, $\tilde{Q}$ of the generated wave is smaller than Q of the incident wave.

A general behaviour of σ^2-maps is as follows, see Figs. 4 – 5:
a) The isolines of $\mathrm{Re}\sigma^2$ are *roughly independent of* γ. Only for γ close to $\pm 90^o$, they have a more complicated behaviour. An important role is played by the isolines $\mathrm{Re}\sigma^2 = 0$ which are shown by bold lines. For high Q's, the isoline $\mathrm{Re}\sigma^2 = 0$ corresponds roughly to i^R, given by relation

$$i^R \sim \arcsin(\mathcal{C}_H/\tilde{\mathcal{C}}_H) \sim \arcsin(V/\tilde{V}). \tag{126}$$

In our case, $i^R \doteq 44^o$.
b) The isolines of $\mathrm{Im}\sigma^2$ are more complex. An important role is again played by the isolines $\mathrm{Im}\sigma^2 = 0$ which are shown by a bold dashed line. This line may run through all γ's, see Fig. 4, or only through some range of γ's, see Fig. 5.
c) It is simple to identify the critical angles i^* and i^{**} from σ^2-maps. The critical angles for different γ are determined by the curve $\mathrm{Im}\sigma^2 = 0$ for $i > i^R$. The curve $\mathrm{Im}\sigma^2 = 0$ for $i < i^R$ does not represent critical angles.
d) σ^2-maps can be also used to determine the square roots σ with *anomalous argument.* If a single root of $\mathrm{Im}\sigma^2$ is situated in the sub-critical region of angles of incidence, $0^o < i < i^R$, the argument of the square root is anomalous.

As we can see in Fig. 4, the line $\text{Re}\sigma^2 = 0$ intersects the line $\text{Im}\sigma^2 = 0$ at $\gamma = 21^o$ in Model 1. No discrete critical angle exists for $\gamma < 21^o$. For $\gamma < 21^o$, however, the argument of the square root will be anomalous. For $\gamma > 21^o$, one discrete critical angle i^* exists. It equals $i^* = 44^o$ for $\gamma = 21^o$ and increases to $i^* = 90^o$ for $\gamma \to 90^o$. For $\gamma > 21^o$, however, the argument of the square root is regular and is the same as for non-dissipative media for $Q \to \infty$ and $\tilde{Q} \to \infty$.

In the second model, the situation is quite different, see Fig. 5. For $\gamma > -48^o$, there is no discrete critical angle, and also the argument of the square root is regular. For $-57^o < \gamma < -48^o$, two discrete critical angles exist, and the argument of the square root is again not anomalous. Finally, for $-90^o < \gamma < -57^o$, one discrete critical angle exist. In addition, the argument of the square root is anomalous.

For $\mathcal{C}_H \leq \tilde{\mathcal{C}}_H$, the isoline $\text{Re}\sigma^2 = 0$ does not exist. Consequently, no critical angles of incidence would exist and the argument of the square root would be regular. See examples in Figs. 24, 36 and 37.

4.3 Determination of parameters of R/T inhomogeneous waves

The general expressions for R/T waves given in Section 3.2, sub 4, remain valid even in the special case of Σ^S perpendicular to Σ, but they are simplified. For the reader's convenience, we shall present here the most important of them.

The components of the complex-valued slowness vector of the R/T wave are given by (113), where p_1 is given by (106). Consequently, the components of the propagation vector $\tilde{\mathbf{P}}$ and the attenuation vector $\tilde{\mathbf{A}}$, with $\tilde{\mathbf{p}} = \tilde{\mathbf{P}} + \mathrm{i}\tilde{\mathbf{A}}$, are as follows

$$\begin{array}{rclrcl} \tilde{P}_1 &=& \sqrt{\frac{1}{2}W(g+1)}\sin i, & \tilde{A}_1 &=& \sqrt{\frac{1}{2}W(g-1)}\sin(i-\gamma), \\ \tilde{P}_2 &=& 0, & \tilde{A}_2 &=& 0, \\ \tilde{P}_3 &=& \pm\varepsilon \text{Re}[1/\tilde{V}_C^2 - p_1^2]^{\frac{1}{2}}, & \tilde{A}_3 &=& \pm\varepsilon \text{Im}[1/\tilde{V}_C^2 - p_1^2]^{\frac{1}{2}}. \end{array} \tag{127}$$

Here ε is the orientation index, given by (82), "+" is for transmitted waves, "$-$" for reflected waves. Moreover

$$\tilde{P} = [\tilde{P}_1^2 + \tilde{P}_3^2]^{\frac{1}{2}}, \quad \tilde{A} = [\tilde{A}_1^2 + \tilde{A}_3^2]^{\frac{1}{2}}. \tag{128}$$

Let us emphasize that the quantities without a tilde correspond to the incident wave, and p_1 is given by (106). The unit vectors along $\tilde{\mathbf{P}}$ and $\tilde{\mathbf{A}}$ are as follows

$$\begin{array}{rclrcl} \tilde{N}_1^R &=& \tilde{P}_1/\tilde{P}, & \tilde{N}_1^I &=& \tilde{A}_1/\tilde{A}, \\ \tilde{N}_2^R &=& 0, & \tilde{N}_2^I &=& 0, \\ \tilde{N}_3^R &=& \tilde{P}_3/\tilde{P}, & \tilde{N}_3^I &=& \tilde{A}_3/\tilde{A}. \end{array} \tag{129}$$

As $n_1 = n_2 = 0$ and $n_3 = 1$, (96) yields a simple expression for the angle $\tilde{i}$ of reflection/transmission

$$\cos\tilde{i} = \tilde{N}_3^R. \tag{130}$$

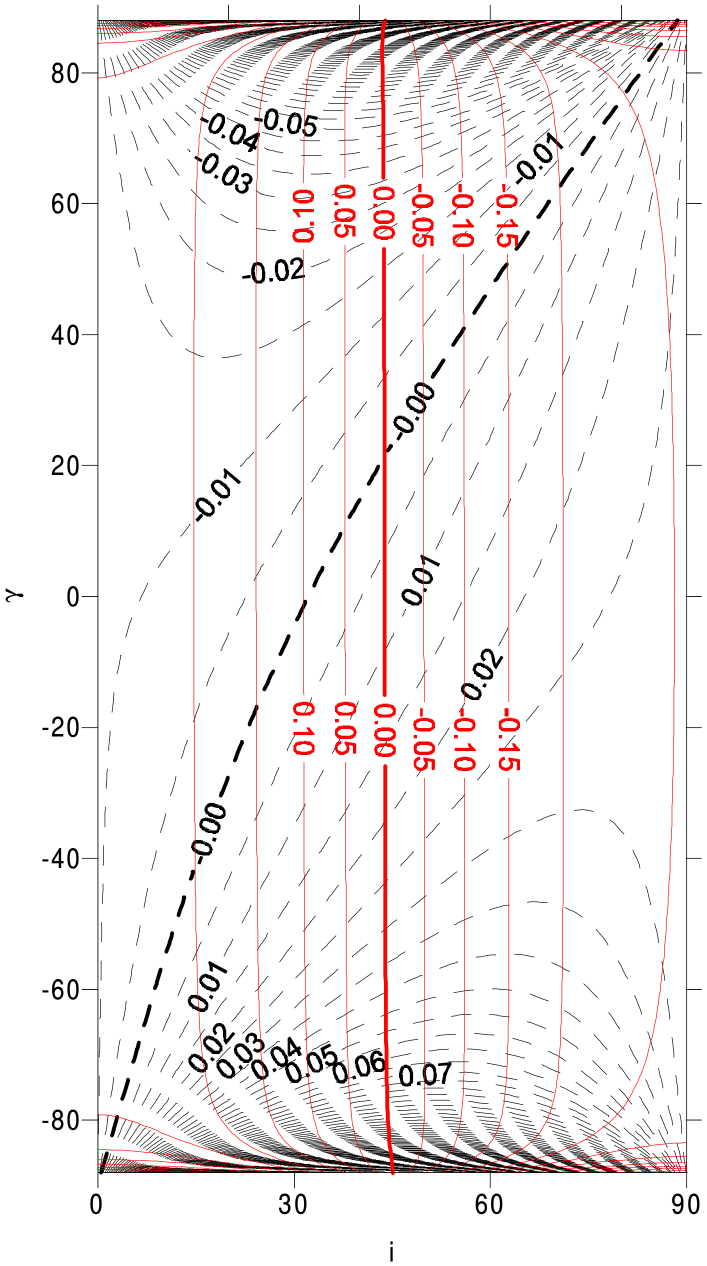

Figure 4: σ^2-map displays the isolines of $\mathrm{Re}\sigma^2 = \mathrm{Re}[1/\tilde{V}_C^2 - p_1^2]$ and $\mathrm{Im}\sigma^2 = \mathrm{Re}[1/\tilde{V}_C^2 - p_1^2]$, in a rectangular frame specified by the angle of incidence i and the attenuation angle γ. The model parameters are $\mathcal{C}_H = 1.44$ km/s, $\tilde{\mathcal{C}}_H = 2.08$ km/s, $Q = 13$, $\tilde{Q} = 22$. See details in text.

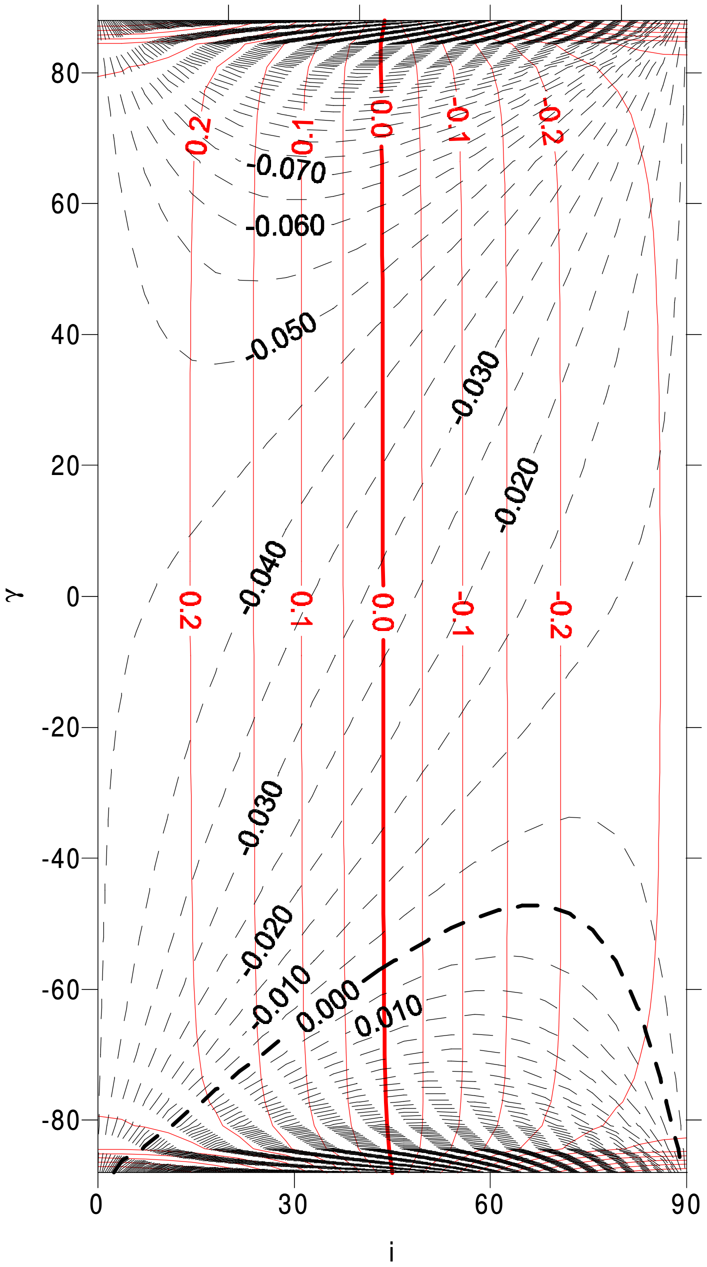

Figure 5: σ^2-map for model parameters $\mathcal{C}_H = 1.44$ km/s, $\tilde{\mathcal{C}}_H = 2.08$ km/s, $Q = 13$, $\tilde{Q} = 5$. See details in text.

As $\tilde{N}_3^R$ may be both positive and negative in dissipative media, we consider angle $\tilde{i}$ in the range $0^o \leq \tilde{i} \leq 180^o$. The attenuation angle of the R/T wave is given by (97),

$$\cos\tilde{\gamma} = \tilde{N}_1^R \tilde{N}_1^I + \tilde{N}_3^R \tilde{N}_3^I. \tag{131}$$

The expressions for the phase velocity $\tilde{\mathcal{C}}$ is again given by (98). Finally, the modified expression for the slowness vector (99) reads

$$\tilde{p}_1 = \tilde{\mathcal{C}}^{-1}(\tilde{N}_1^R + \mathrm{i}\tilde{b}\tilde{N}_1^I), \quad \tilde{p}_2 = 0, \quad \tilde{p}_3 = \tilde{\mathcal{C}}^{-1}(\tilde{N}_3^R + \mathrm{i}\tilde{b}\tilde{N}_3^I), \tag{132}$$

where $\tilde{b}$ is given by (100). Note that both $\tilde{\mathcal{C}}$ and $\tilde{b}$ depend also on the attenuation angle $\tilde{\gamma}$.

4.4 Homogeneous incident wave

When the incident wave is homogeneous ($\gamma = 0$), we can use all equations of Section 4, as the slowness vector plane Σ^S of the incident wave may be chosen arbitrarily, only it must contain the propagation vector $\mathbf{P}$ of the incident wave. We merely choose it as a plane of incidence, specified by the propagation vector $\mathbf{P}$ of the incident wave and by the normal $\mathbf{n}$ to the interface.

With the exception of the unconverted reflected wave and of isolated angles of incidence (e.g., the normal incidence), *all generated R/T waves are inhomogeneous* ($\tilde{\gamma} \neq 0$), although the incident wave is homogeneous, see Fig. 6. Both the propagation and attenuation vectors of all generated R/T waves, however, are situated in the plane of incidence. Consequently, the general system of six equations (76) can be *always* decomposed into a P-SV system of four equations (103) and SH system of two equations (104), if the incident wave is homogeneous.

The expression (106) for the tangential component of the slowness vector of the incident wave also simplifies

$$p_1 = \sqrt{\tfrac{W}{2}}\sin i(\sqrt{g+1} + \mathrm{i}\sqrt{g-1}), \quad g = \sqrt{1+Q^{-2}}. \tag{133}$$

As the simplification of all other relations for $\gamma = 0$ is very simple, we shall briefly discuss only the determination of *critical angles.* From (116), we obtain the conditions for the discrete critical angles in the following simple form:

$$\begin{array}{rclcl} \mathrm{Im}(1/\tilde{V}_C^2 - p_1^2) & = & \tilde{W}\tilde{Q}^{-1} - WQ^{-1}\sin^2 i & = & 0, \\ \mathrm{Re}(1/\tilde{V}_C^2 - p_1^2) & = & \tilde{W} - W\sin^2 i & < & 0. \end{array} \tag{134}$$

Equations (134) can be simply solved. They yield the conditions:
a) There is no critical angle for

$$\tilde{W}Q/W\tilde{Q} > 1. \tag{135}$$

b) For $\tilde{W}Q/W\tilde{Q} < 1$, the critical angle is given by the relation

$$\sin i^* = \tilde{W}Q/W\tilde{Q}, \quad \text{if} \quad \tilde{Q} < Q. \tag{136}$$

If $\tilde{Q} > Q$, no critical angle exist.
c) Two critical angles cannot exist for a homogeneous incident wave.

Similarly, we can make a conclusion related to the *anomalous arguments* of the square roots:

For a homogeneous incident wave, the argument of the square root is anomalous, if

$$\tilde{W}Q/W\tilde{Q} > 1 \quad \text{and} \quad \tilde{Q} > Q. \tag{137}$$

Otherwise, the argument is regular.

4.5 Strongly inhomogeneous incident plane wave

As explained in Section 2.3, inhomogeneous plane waves with the attenuation angle $\gamma = \pm\frac{1}{2}\pi$ cannot propagate in dissipative media; they do not satisfy the existence condition $p_i p_i = 1/V_C^2$. The phase velocity of such waves would be zero. For this reason, it has no sense to discuss the R/T coefficients on a plane interface between two dissipative media for the incident wave with the attenuation angle $\gamma = \pm\frac{1}{2}\pi$.

Here we shall make several comments not for $\gamma = \pm 90^o$, but for γ *close to* $\pm 90^o$. In this case, $\cos\gamma$ is high and $g \doteq 1/Q\cos\gamma$. This yields the following approximate expression for the tangential component of the slowness vector p_1 of the incident wave, see (106)

$$p_1 \;\doteq\; \sqrt{\tfrac{1}{2}W}(\sin i \pm \mathrm{i}\cos i)/Q\cos\gamma. \tag{138}$$

Consequently, $|p_1|$ is very high for γ close to $\pm 90^o$. Moreover, the square roots $[1/\tilde{V}_C^2 - p_1^2]^{\frac{1}{2}}$ simplify considerably, as for any R/T wave we obtain

$$[1/\tilde{V}_C^2 - p_1^2]^{\frac{1}{2}} \;\doteq\; [-p_1^2]^{\frac{1}{2}} \;=\; \sqrt{\tfrac{1}{2}W}(\cos i \mp \mathrm{i}\sin i)/Q\cos\gamma. \tag{139}$$

In (138) and (139), the upper sign is for γ close to 90^o, and the lower sign for γ close to -90^o. Equation (139) indicates that the square roots of all generated R/T waves are the same; they depend only on the parameters of the incident wave (W, Q), and not on the parameters of the R/T wave $(\tilde{W}, \tilde{Q})$.

From (138) and (139), we also obtain, see (127)

$$\tilde{P}_1 \doteq \sqrt{\tfrac{1}{2}W}\sin i/Q\cos\gamma, \quad \tilde{P}_3 \doteq \pm\varepsilon\sqrt{\tfrac{1}{2}W}\cos i/Q\cos\gamma, \quad \tilde{P} \doteq \sqrt{\tfrac{1}{2}W}/Q\cos\gamma.$$

This yields a very interesting result, see (130) and (129)

$$\cos\tilde{i} \doteq \pm\varepsilon\cos i. \tag{140}$$

If $\tilde{i}$ is defined as the *acute R/T angle*, (140) yields a simple Snell's law for strongly inhomogeneous plane wave (γ close to 90^o or to -90^o)

$$\tilde{i} \doteq i. \tag{141}$$

Thus, if the incident wave is strongly inhomogeneous, the angles of reflection/transmission of all generated waves equal approximately the angle of incidence. This is valid for all transmitted waves, and even for converted waves.

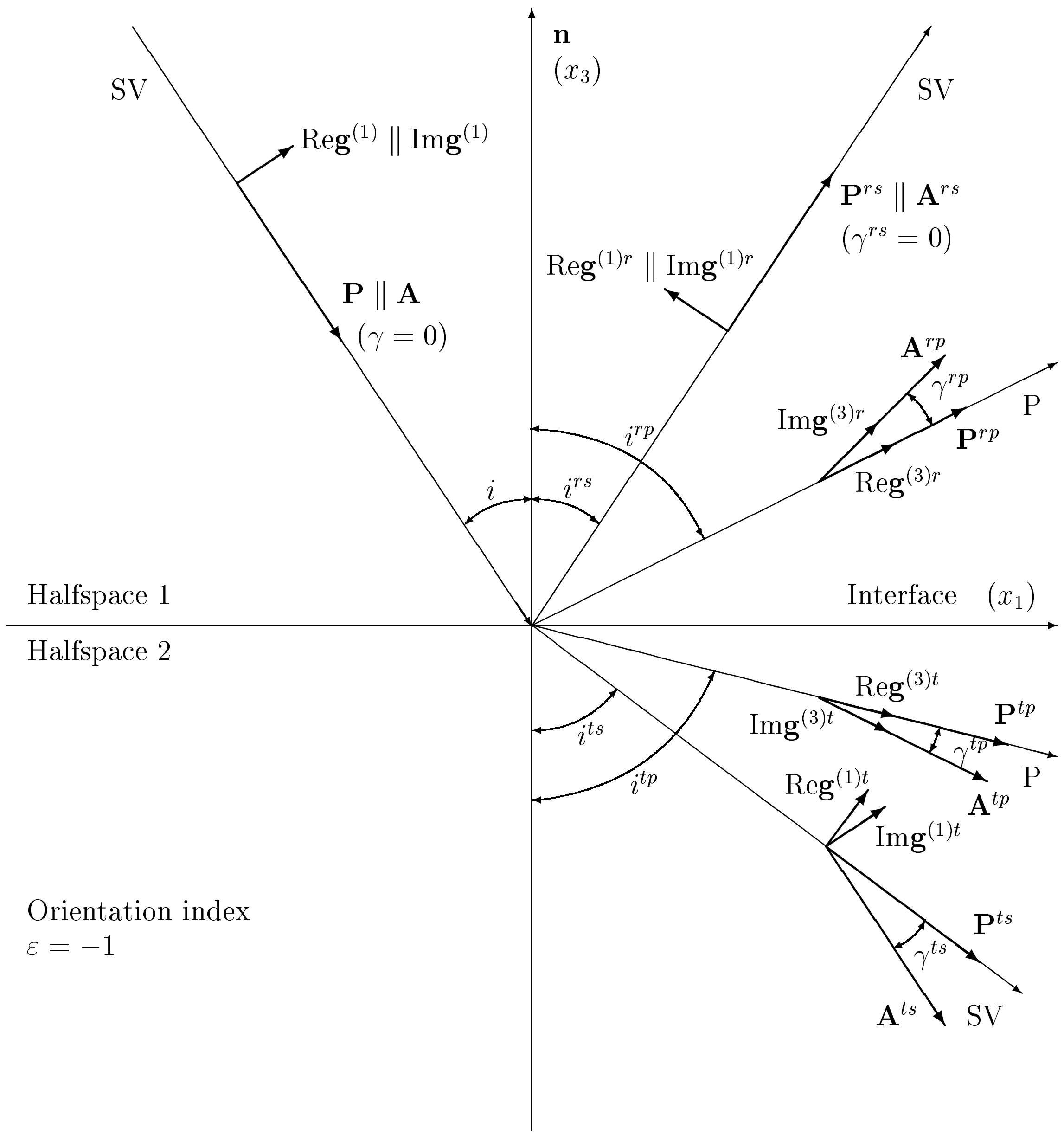

Figure 6: Reflection and transmission of a *homogeneous plane SV wave* on a plane interface between two isotropic dissipative halfspaces (schematically). Although the incident wave is homogeneous, all generated R/T waves, with the exception of unconverted reflected wave, are inhomogeneous. Quite analogous picture would be obtained even for an incident P wave. For more details, see the caption to Fig. 1.

The R/T coefficients also behave anomalously for γ close to 90^o or -90^o. This can be simply seen on R/T coefficients for SH waves, see (104). We merely use $Z_2 = \varepsilon\mu_1 p_3, Z_2^r = -\varepsilon\mu_1 p_3, Z_2^t = \varepsilon\mu_2 p_3$, where μ_1, μ_2 are complex-valued moduli of torsion, and obtain

$$C^r \doteq \frac{\mu_1 - \mu_2}{\mu_1 + \mu_2}, \quad C^t \doteq \frac{2\mu_1}{\mu_1 + \mu_2} \tag{142}$$

Thus, both reflection and transmission coefficients of SH waves are complex-valued constants, independent of the angle of incidence.

4.6 Incident wave with $i = \gamma$

For $i = \gamma$, the tangential component p_1 of the slowness vector of the incident wave (106) simplifies,

$$p_1 = \sqrt{\tfrac{1}{2}W(g+1)}\sin i. \tag{143}$$

Thus, p_1 is **real-valued**. Equation (109) then shows that also the tangential components $\tilde{p}_1$ of all generated R/T waves are real-valued, and $\tilde{i} = \tilde{\gamma}$. See Fig. 7. Consequently, even many other relations simplify. It is not difficult to show that there is no critical angle for $i = \gamma$. This is also nicely seen in the σ^2-maps in Figs. 4 and 5. Note that g in (143) is given by the relation $g = \sqrt{1 + Q^{-2}\cos^{-2} i}$ in this case.

For $Q \cos i \gg 1$, Eq. (143) simplifies even more

$$p_1 \quad = \quad \sqrt{\tfrac{1}{2}W}\sin i \doteq \sin i/V. \tag{144}$$

Assuming that $\tilde{Q}\cos\tilde{i} \gg 1$ is also satisfied for all generated waves, we obtain the Snell's law

$$\sqrt{\tfrac{1}{2}\tilde{W}}\sin\tilde{i} \quad = \quad \sqrt{\tfrac{1}{2}W}\sin i. \tag{145}$$

For high Q's and angles of incidence i not too close to 90^o, this yields a standard Snell's law, as known from non-dissipative media

$$\sin\tilde{i}/\tilde{V} = \sin i/V. \tag{146}$$

5 Computer routine COEF52

Computer routine COEF52 is a generalization of the computer routine COEF51, described by Brokešová and Červený (1997). In COEF51, routines RTMAT and RTMATQ from the reflectivity program written by G. Müller (1985) were used (with the author's permission). Similarly as COEF51, the routine COEF52 is designed for the computation of displacement reflection/transmission coefficients of plane waves of various types at a plane interface between two homogeneous dissipative solid media and at a thin transition layer between two homogeneous dissipative media, simulated by a stack of homogeneous dissipative sublayers. Also the pressure and particle velocity R/T coefficients at an interface between two liquid halfspaces and at a thin liquid transition layer may be computed.

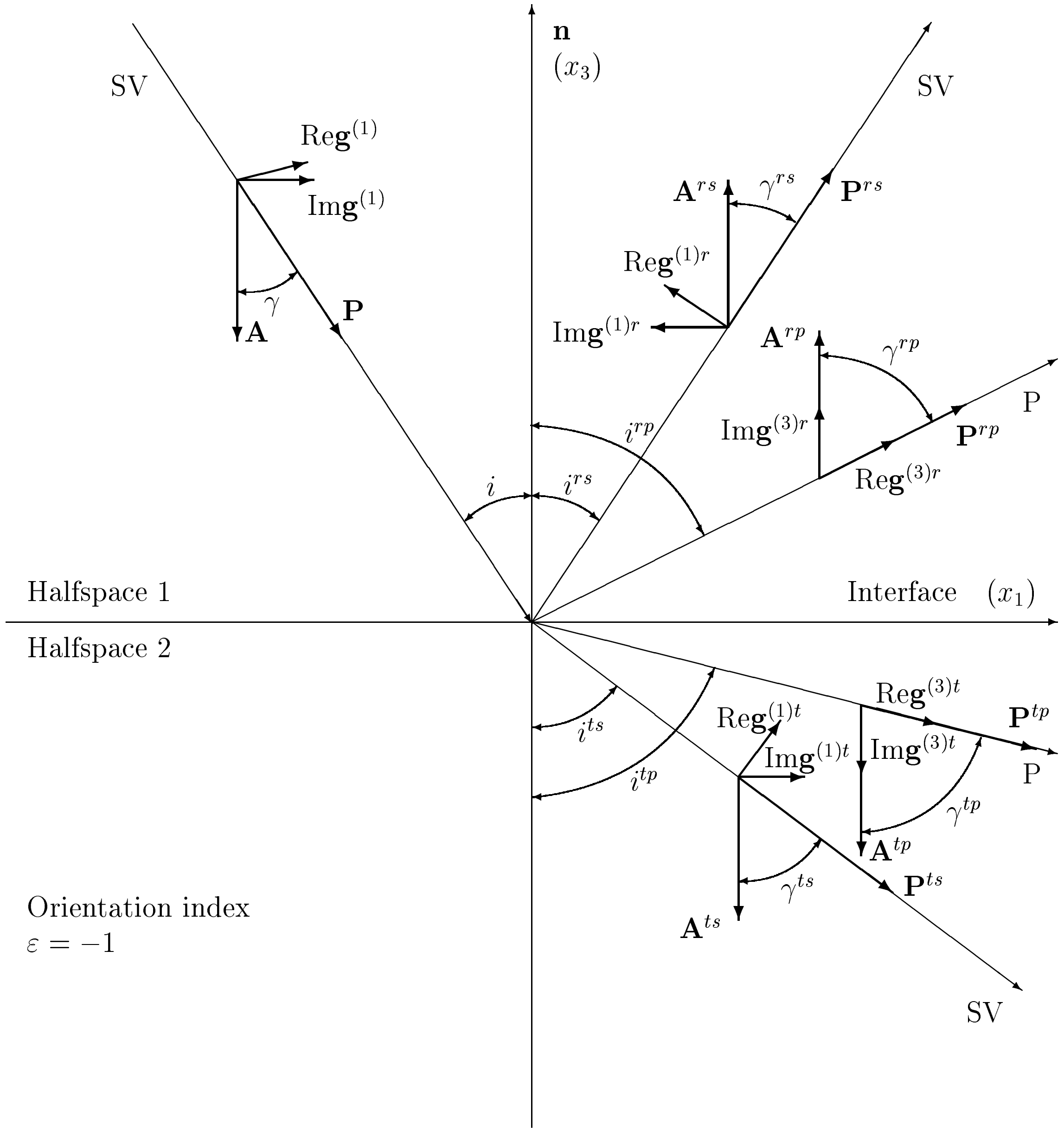

Figure 7: Reflection and transmission of an *inhomogeneous plane SV wave with* $i = \gamma$ on a plane interface between two isotropic dissipative halfspaces (schematically). As $i = \gamma$, the attenuation vector of the incident wave is parallel to the x_3-axis. In this case, the attenuation vectors of all generated waves are also parallel to the normal $\mathbf{n}$ to the interface. Quite analogous picture would be obtained for an incident inhomogeneous plane P wave with $i = \gamma$. For more details, see the caption to Fig. 1.

The routine COEF52, however, considers an arbitrary *inhomogeneous incident plane wave*, with an arbitrary attenuation angle γ. Homogeneous plane waves ($\gamma = 0$) are considered as a special case. Consequently, the ray parameter is complex-valued in COEF52. In the computer routine COEF51, the ray parameter was real-valued. Thus, the computations by COEF51 corresponded only to a special case of an inhomogeneous incident plane wave, with the attenuation angle γ equal to the angle of incidence i, see Section 4.6. Another generalization of COEF52 is that all computations are exact, valid not only for low-loss media (high Q's), but also for highly dissipative media (low Q's).

A special care in COEF52 is devoted to the computation of critical angles, which are needed in the determination of correct branches of roots corresponding to all R/T waves, see Section 4.1. In COEF51, such computations were not necessary, as the ray parameter was presumably real-valued.

Also the input parameters are changed. Instead of real-valued velocities, V_P and V_S, given by (35), the phase velocities of corresponding homogeneous waves, C_P and C_S, are used. The differences between V_P, V_S and C_P, C_S are negligible in low-loss media (high Q's), but may be more distinct in highly dissipative media, see the general relation (55). There are two reasons why this change is made. First, the phase velocities of homogeneous waves C_P, C_S are more traditional in the theoretical literature devoted to the subject of inhomogeneous plane waves in viscoelastic media, see Borcherdt (1977, 1982), Krebes (1984). Second, C_P and C_S are also used as parameters in most numerical examples known in seismological literature, see Krebes (1983, 1984). It should be, however, emphasized, that the difference is only formal; it would be simple to use optionally either C_P, C_S or V_P, V_S as input parameters.

Similarly as COEF51, even the routine COEF52 is limited only to isotropic media, and to the decomposed systems of equations (103) and (104) for R/T coefficients, see Section 4. In other words, it is assumed that the propagation vector $\mathbf{P}$ and the attenuation vector $\mathbf{A}$ of the incident wave are *coplanar with the normal* $\mathbf{n}$ to the interface. The fully general case of $\mathbf{P}, \mathbf{A}, \mathbf{n}$ not coplanar cannot be treated by COEF52. For this case it would be necessary to design a completely new routine, based on the system of six equations (76).

The routine COEF52 was supplemented by an independent routine for the calculation of σ^2-maps, see section 4.2. These maps may find useful applications both in the correct understanding and in the discussion of computed R/T coefficients.

6 Numerical examples of R/T coefficients and their discussion

Routine COEF52 is very general. The numerical examples which will be presented here emphasize only several aspects of possible computations. We are particularly interested in the influence of the attenuation angle γ of the incident wave and of the quality factors Q's in both halfspaces on the R/T coefficients.

For this reason, we shall not exploit the broad possibilities of COEF52, and consider only the following special cases:
a)We shall consider only the R/T coefficients at a *plane interface* between two halfspaces, not on a transition layer between two halfspaces. Thus, the thickness of the transition

layer is fixed in all computations and equals zero.
b) We shall discuss only the so-called *reference R/T coefficients*, see Brokešová and Červený (1997). Under the reference R/T coefficients, we understand the R/T coefficients, computed for a fixed frequency, equal to the reference frequency f_r of the model (the frequency for which the velocities for dissipative model are specified). Note that the reference R/T coefficients are frequency-independent. For a more detailed discussion of frequency-dependent R/T coefficients, see Brokešová and Červený (1997).

As the model parameters, the following quantities are taken in all computations:
1) First halfspace: CP1, CS1, RHO1, QP1, QS1.
2) Second halfspace: CP2, CS2, RHO2, QP2, QS2.
The meaning of all quantities is apparent. CP and CS are phase velocities of homogeneous P and S waves, RHO are densities, QP and QS are the quality factors of P and S waves.

For each R/T coefficient, two pictures are presented. The lower shows the modulus of the R/T coefficient, and the upper the phase of the R/T coefficient. The type of the R/T coefficient is mostly shown above the upper figure. The phases are displayed in angles, from -180^o to 180^o. The figures of phases sometimes contain vertical lines, from the bottom to the top of the figure. These vertical lines have only a formal meaning and correspond to a smooth transition of the phase through 180^o (the drum effect). The vertical axis for pictures of the modulus is mostly from 0 to 1, but it is not the same in all cases. The reason is that certain R/T coefficients differ considerably in magnitude. Even the moduli of non-converted reflected waves may be greater than unity in post-critical regions in dissipative media ! See more details in Section 5, sub 5d.

The horizontal axes of all figures correspond to the angle of incidence, varying from 0^o to 90^o.

For comparison, the relevant R/T coefficients for non-dissipative media are also displayed in all figures, by bold dotted lines. For non-dissipative media, the incident wave and most of generated R/T waves are homogeneous. Only for higher (post-critical) angles of incidence certain R/T waves may be inhomogeneous. The regions of corresponding angles of incidence, for which the generated R/T wave in non-dissipative medium is inhomogeneous, is shadowed in the pictures. Note that the propagation vector $\mathbf{P}$ is parallel to the interface and the attenuation vector $\mathbf{A}$ perpendicular to it in this case. In dissipative medium, the shadowing has, more or less, only a formal meaning. It only indicates the extension of the post-critical region, corresponding to the square root appearing in the exponential function representing the generated R/T wave under consideration. The angles $\tilde{i}$ of reflection/transmission, corresponding to the selected generated R/T wave, may be less than 90^o even for angles of incidence corresponding to the shadow zone.

6.1 Variations of R/T coefficients with the attenuation angle γ of the incident wave

In this section, we shall discuss the dependence of several R/T coefficients on the attenuation angle γ of the incident wave. We shall consider γ in a broad range, $-90^o < \gamma < 90^o$. On two simple examples, we shall also explain several typical features of R/T coefficients (behaviour in a post-critical region, behaviour close to the Brewster angle, anomalous phases due to the anomalous arguments of square roots, etc.).

We shall consider the following **Model 1**:

Model 1
CP1 = 2.5 km/s, CS1 = 1.44 km/s, RHO1 = 2.000 kg m^{-3}, QP1 = 30, QS1 = 13,
CP2 = 3.6 km/s, CS2 = 2.08 km/s, RHO2 = 2.000 kg m^{-3}, QP2 = 50, QS2 = 22.

First we shall discuss the *SH reflection coefficients*, see Fig. 8. The σ^2-map of the appropriate square root is shown in Fig. 4. The boundary angle i^R between the sub-critical and post-critical region equals approximately $i^R = 44^o$. Upper part of Fig. 8 displays the SH reflection coefficients for non-positive γ: $\gamma = 0^o$ (homogeneous wave, bold line), $\gamma = -25^o, -50^o, -75^o, -89.99^o$. Similarly, the lower part of Fig. 8 is for positive γ: $\gamma = 25^o, 50^o, 75^o$ and 89.99^o. In both parts, the dotted curves correspond to the non-dissipative case. Note that the Brewster angle, for which the SH reflection coefficient for non-dissipative media vanishes, equals 35^o approximately.

As we can see in Fig. 8, the *moduli of SH reflection coefficients* for dissipative and non-dissipative media are practically undistinguishable for small (subcritical) angles of incidence, and for $-75^o < \gamma < 75^o$. In critical ($i \doteq i^R$) and post-critical ($i > i^R$) regions, and in the vicinity of the Brewster angle, the differences between the moduli of SH reflection coefficients for dissipative and non-dissipative models are greater. Even in these regions, however, the differences between the moduli of R/T coefficients for dissipative and non-dissipative media are not too pronounced for $-50^o < \gamma < 50^o$. With increasing $|\gamma|$, the moduli of R/T coefficients become smoother, with respect to the angles of incidence. We speak of the *smoothing effect of* γ. For $\gamma = \pm 89.99^o$, the coefficients become constant, independent of the angle of incidence i.

Let us now briefly discuss the *phases of the SH reflection coefficients* in Fig. 8, particularly the relation between phases of these coefficients for dissipative and non-dissipative media. The smoothing effect of γ is well observable even in the phases. There is, however, an additional effect, connected with the anomalous phases of square roots. The phase of the SH reflection coefficient is influenced mainly by the argument of the relevant square root, see the σ^2-map in Fig. 4. As we can see in Fig. 4, the argument of the square root is *anomalous* for $\gamma < 20^o$, and regular for $\gamma > 20^o$. Thus the phase of the SH reflection coefficients for dissipative media are close to the (dotted) phase of the SH reflection coefficient for the non-dissipative medium for $\gamma > 20^o$ only, see the lower part of Fig. 8. Contrary to it, the phases have the opposite signs than the phases for the non-dissipative medium for $\gamma < 20^o$, see the upper part of Fig. 8. This can be nicely seen mainly on the phase for the homogeneous incident wave (bold line) and for the non-dissipative medium (dotted line) in the upper part of Fig. 8.

Now we shall discuss the *P1P1 reflection coefficients*, again for Model 1, see Fig. 9. As CP1/CP2 $\doteq$ CS1/CS2 and QP1/QP2 $\doteq$ QS1/QS2 in Model 1, the σ^2-map of the square root corresponding to P1 incident and P2 generated wave is practically the same as the σ^2-map for the square root of SH waves, see Fig. 4. The boundary angle i^R between the sub-critical and post-critical regions equals again 44^o. Other two square roots (incident P1 – generated S1, incident P1 – generated S2) do not influence the results considerably, as the relevant angles i^R do not exist. See also Fig. 24.

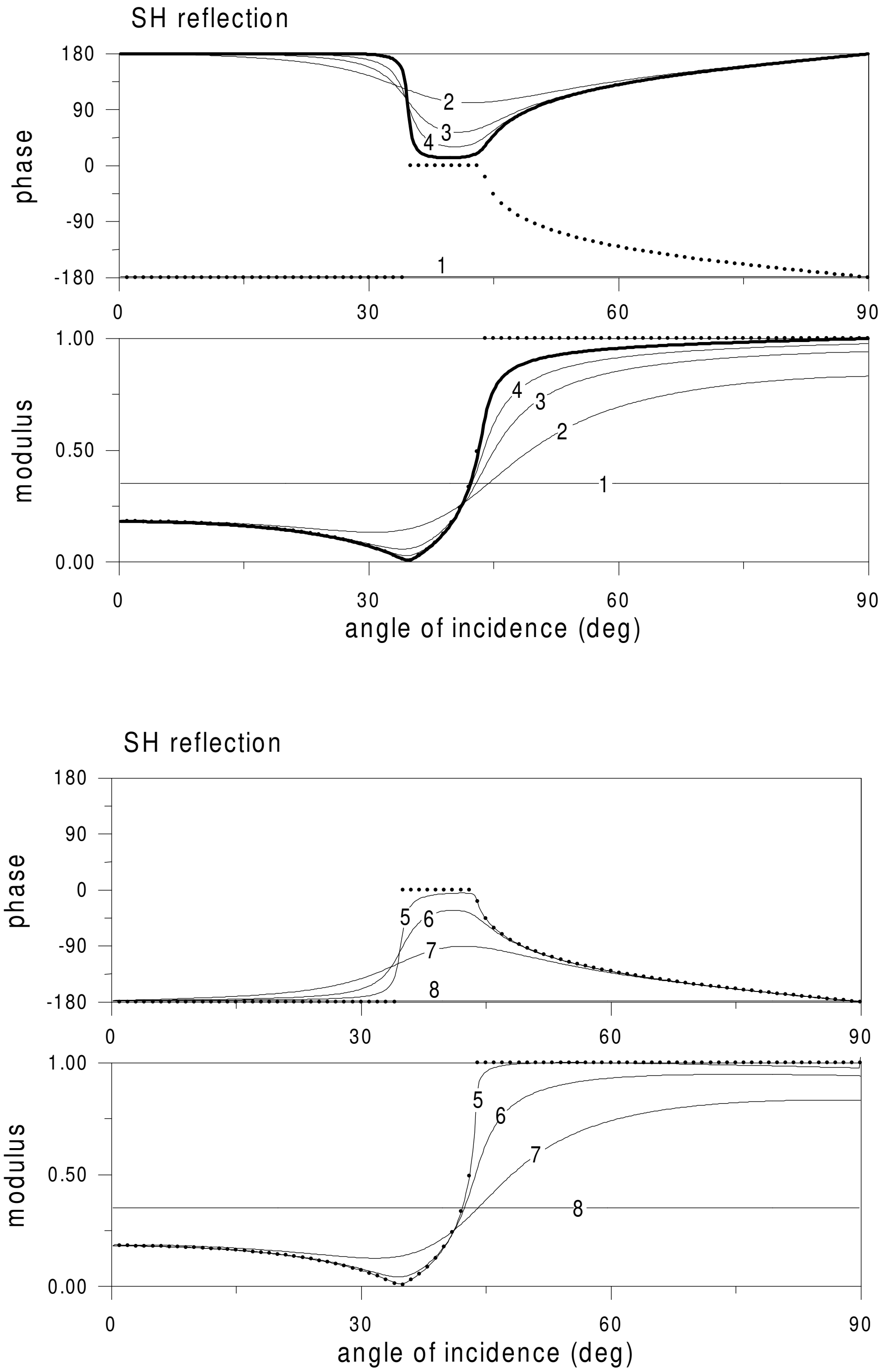

Figure 8: Model 1: Displacement SH reflection coefficient in non-dissipative medium (dotted line) is compared with that in dissipative medium for homogeneous incident wave ($\gamma = 0^o$, bold line) and for inhomogeneous incident waves with different attenuation angles: $\gamma = -89.99^o$ (1), $\gamma = -75^o$ (2), $\gamma = -50^o$ (3), $\gamma = -25^o$ (4), $\gamma = 25^o$ (5), $\gamma = 50^o$ (6), $\gamma = 75^o$ (7) and $\gamma = 89.99^o$ (8).

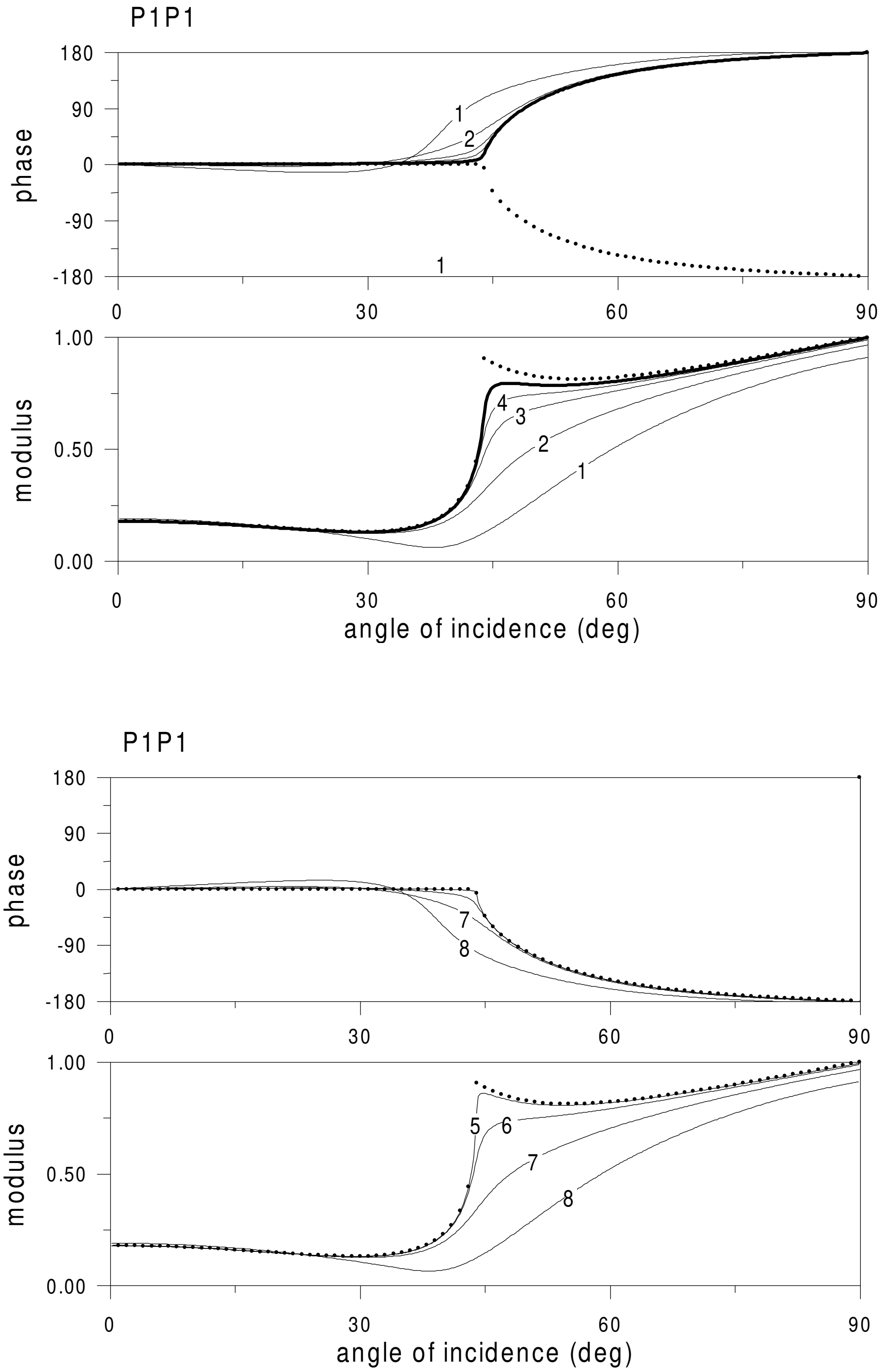

Figure 9: Model 1: Displacement P1P1 reflection coefficient in non-dissipative medium (dotted line) is compared with that in dissipative medium for homogeneous incident wave ($\gamma = 0^o$, bold line) and for inhomogeneous incident waves with different attenuation angles: $\gamma = -85^o$ (1), $\gamma = -75^o$ (2), $\gamma = -50^o$ (3), $\gamma = -25^o$ (4), $\gamma = 25^o$ (5), $\gamma = 50^o$ (6), $\gamma = 75^o$ (7) and $\gamma = 85^o$ (8).

The attenuation angles γ of the incident waves are chosen similarly as in Fig. 8 for SH waves, and the conclusions are also analogical. The anomalous phase of the P1P1 reflection coefficient can be observed for $\gamma > 20^o$ only, see the upper part of Fig. 9. The phases have opposite signs than those for a non-dissipative medium in this case. See, e.g., the bold line for the homogeneous incident wave in a dissipative medium, and the dotted line for a non-dissipative medium in the upper part of Fig. 9.

6.2 Complete set of R/T coefficients for Model 1

In this section, we shall present and discuss the complete set of all possible displacement R/T coefficients for Model 1. They are displayed in Figs. 10 – 23. For completness, we also include the pressure and particle velocity R/T coefficients at an interface between two liquid halfspaces, and the conversion coefficients at a free surface.

a) P-SV displacement R/T coefficients at a structural interface, Figs. 10 – 13. They include: reflection coefficients P1P1, P1S1, S1P1 and S1S1 (Figs. 10, 11), and transmission coefficients P1P2, P1S2, S1P2, S1S2 (Figs. 12, 13).

b) SH displacement R/T coefficients at a structural interface, Fig. 14. They include: reflection coefficient S1S1 (top) and transmission coefficient S1S2 (bottom). The model data CP1, CP2, QP1, QP2 are redundant in this case and do not influence the results.

c) Pressure R/T coefficients at an interface between two liquid halfspaces, Fig. 15. They include: reflection coefficient P1P1 (top) and transmission coefficient P1P2 (bottom). The model data CS1, CS2, QS1, QS2 are redundant in this case and do not influence the results.

d) Particle velocity R/T coefficients at an interface between two liquid halfspaces, Fig. 16. They include: reflection coefficient P1P1 (top) and transmission coefficient P1P2 (bottom). The model data CS1, CS2, QS1, QS2 are redundant in this case and do not influence the results. Note that the reflection P1P1 coefficients in c) and d) are the same, but the transmission P1P2 coefficients differ.

e) P-SV displacement reflection coefficients at the surface of elastic Earth, Figs. 17 and 18. They include: reflection coefficients P1P1, P1S1 (Fig. 17), and reflection coefficients S1P1, S1S1 (Fig. 18). The model data CP2, CS2, RHO2, QP1 and QS2 are redundant in this case and do not influence the results.

f) SH displacement reflection coefficients at the surface of the elastic Earth, Fig. 19, upper part. It equals $+1$ for all angles of incidence.

g) Pressure coefficients at the surface of a liquid halfspace, Fig 19, lower part. It equals -1 for all angles of incidence.

h) Coefficients of conversion at the surface of elastic Earth, Figs. 20 and 21. They include: PX, PZ (Fig. 20), and SX, SZ (Fig. 21). The model data CP2, CS2, RHO2, QP2 and QS2 are redundant in this case and do not influence the results.

i) SH conversion coefficient SY at the surface of elastic Earth, Fig. 22, upper part. It equals $+2$ for all angles of incidence.

j) Pressure conversion coefficient PZ at the surface of a liquid halfspace, Fig. 22, lower part.

k) Particle velocity reflection coefficient P1P1 at the surface of a liquid halfspace, Fig. 23, upper part. It equals -1 for all angles of incidence.

l) Particle velocity conversion coefficient PZ at the surface of a liquid halfspace, Fig. 23, lower part.

Note that the coefficients f), g), i) and k) are constant, independent of the angle of incidence. They are universal, independent of model data. The coefficients j) and l) are not constant, but they are also practically independent of the model data.

All figures display four curves:

1) R/T coefficients for non-dissipative media. Shown by dotted line.

2) R/T coefficients for dissipative media, for a homogeneous incident wave ($\gamma = 0$). shown by a bold continuous line.

3) R/T coefficients for dissipative media, for inhomogeneous incident wave ($\gamma \neq 0$):

3a) The attenuation angle of the incident wave $\gamma = 30^o$. Shown by a thin continuous line.

3b) The attenuation angle of the incident wave $\gamma = -30^o$. Shown by a thin dashed line.

The values of the attenuation angles γ of the incident wave, $\gamma = 0^o$, 30^o, and -30^o, were selected to appreciate the influence of the attenuation angle γ on R/T coefficients. The broader range of γ's would make the pictures less transparent.

Before we discuss individual R/T coefficients, we shall present several conclusions following from the σ^2-maps. The σ^2-maps for all possible square roots related to Model 1 are shown in Fig. 24. Three σ^2-maps correspond to the incident P wave (P1P2, P1S2, P1S1, see the upper row of pictures in Fig. 24), and three to the incident S wave (S1P2, S1S2, S1P1, see the lower row of pictures in Fig. 24). The σ^2-maps may be also plotted for P1P1 and S1S1 square rots, but they would not yield any information important for us. The σ^2-maps show clearly the angles i^R (for which $\mathrm{Re}\sigma^2 = 0$, bold continuous lines) and i^I (for which $\mathrm{Im}\sigma^2 = 0$, bold dashed lines).

The square roots P1S1 and P1S2 do not contain the isolines $\mathrm{Re}\sigma^2 = 0$, so that i^R does not exist in these cases. For other square roots, the angles i^R are as follows: P1P2 ... $i^R = 44^o$, S1P2 ... $i^R = 23^o$, S1S2 ... $i^R = 44^o$, S1P1 ... $i^R = 35^o$.

Consider first the incident P wave. Then only the square root P1P2 plays an important role, with $i^R = 44^o$. For $\gamma > 20^o$, there is one critical angle, and the argument of the square root behaves regularly (as $i^I > i^R$). For $\gamma < 20^o$, there is no critical angle, but the argument of the square root behaves anomalously (as $i^I < i^R$).

For incident S waves, the situation is more complex. The σ^2-map for the S1S2 square root is similar to the σ^2-map of the square root P1P2. For S1P1 square root, $i^R = 35^o, i^R > i^I$ for $\gamma < 22^o$, and $i^R < i^I$ for $\gamma > 22^o$. Finally, for S1P2 square root, $i^R = 24^o, i^R > i^I$ for $\gamma < 18^o$, and $i^R < i^I$ for $\gamma > 18^o$. Thus, the argument of the square root S1S2 behave anomalously for $\gamma < 20^o$, S1P2 for $\gamma < 18^o$, and S1P1 for $\gamma < 22^o$.

Discussion of R/T coefficients for Model 1

The differences between the R/T coefficients for dissipative and non-dissipative models are mostly very small or even negligible. This applies particularly to the moduli of all transmission coefficients, to the moduli of reflection coefficients of converted waves (in the whole range of angles of incidence), and to the moduli of reflection coefficients of non-converted waves for sub-critical angles of incidence. Only in exceptional cases, the differences in moduli of R/T coefficients are greater. The differences may be more pronounced in phases of R/T coefficients.

In the following, we shall briefly discuss these differences. Moreover, we shall also discuss certain pecularities of R/T coefficients for dissipative models, which are different from those of non-dissipative models.

1) **R/T coefficients in critical and post-critical regions.** The differences between the R/T coefficients for dissipative and non-dissipative models may be greater in critical and post-critical regions, mainly for non-converted reflected waves (S1S1, P1P1), for small Q's and greater γ's. The differences are usually more prominent for negative γ, and increase with increasing $|\gamma|$. Mostly, the sharp changes of R/T coefficients in the critical regions, typical for non-dissipative models, are removed in dissipative models, and the R/T coefficients for dissipative models become smoother. See Figs. 11 and 18 for S1S1 reflection coefficients, and Figs. 10, 17 for P1P1 reflection coefficients. See also Figs. 8 and 9.

2) **R/T coefficients in the vicinity of Brewster angles.** Similar smoothing effects can be observed in the vicinity of Brewster angles of incidence, at which the R/T coefficients for non-dissipative media vanish. The R/T coefficients for non-dissipative media change fastly with the change of the angle of incidence in the vicinity of an Brewster angle, but the changes are smoother in dissipative models. For example, see the P1P1 reflection coefficient at the free surface in Fig. 17, which contains two Brewster angles, 60^o and 77^o. The smoothing effect is particularly nicely displayed in the phases of this R/T coefficient. See also S1S1 reflection coefficient from the free surface in Fig. 18, the conversion coefficient SZ, Fig. 21.

3) **Anomalous phases of R/T coefficients.** The phases of R/T coefficients for certain attenuation angles γ of the incident wave in dissipative media behave anomalously in post-critical regions. This means that they are strongly different from those for non-dissipative media, even for Q's arbitrarily high. Mostly, they have opposite signs.

For *P waves incident on a structural interface*, the phases of reflection coefficients P1P1, P1S1, and of transmission coefficients P1P2, P1S2, are the same for non-dissipative media and dissipative media only for $\gamma = 30^o$. For $\gamma = 0^o$ and -30^o, they have (roughly) opposite signs, see Figs. 10, 12. This is simply understandable from σ^2-map, see Fig. 24. The reason is the anomalous argument of the square root P1P2 for $\gamma < 20^o$.

For *S waves incident on a structural interface*, three square roots influence the R/T coefficients, S1P1, S1P2 and S1S2, and all of these square roots have anomalous arguments for certain γ. In resulting R/T coefficients, the effect of anomalous arguments of individual square roots then overlap. The most distinct is the influence of the square root S1S2. As the σ^2-maps for S1S2 and P1P2 square roots are very similar, the final conclusions are similar to that for the incident P wave. The phases of reflection coefficients S1S1, S1P1 and transmission coefficients S1S2, S1P2 for non-dissipative media and dissipative media are close to each other for $\gamma = 30^o$ only. For $\gamma = 0^o$ and $\gamma = -30^o$, they have (roughly) opposite signs. See Figs. 11, 13.

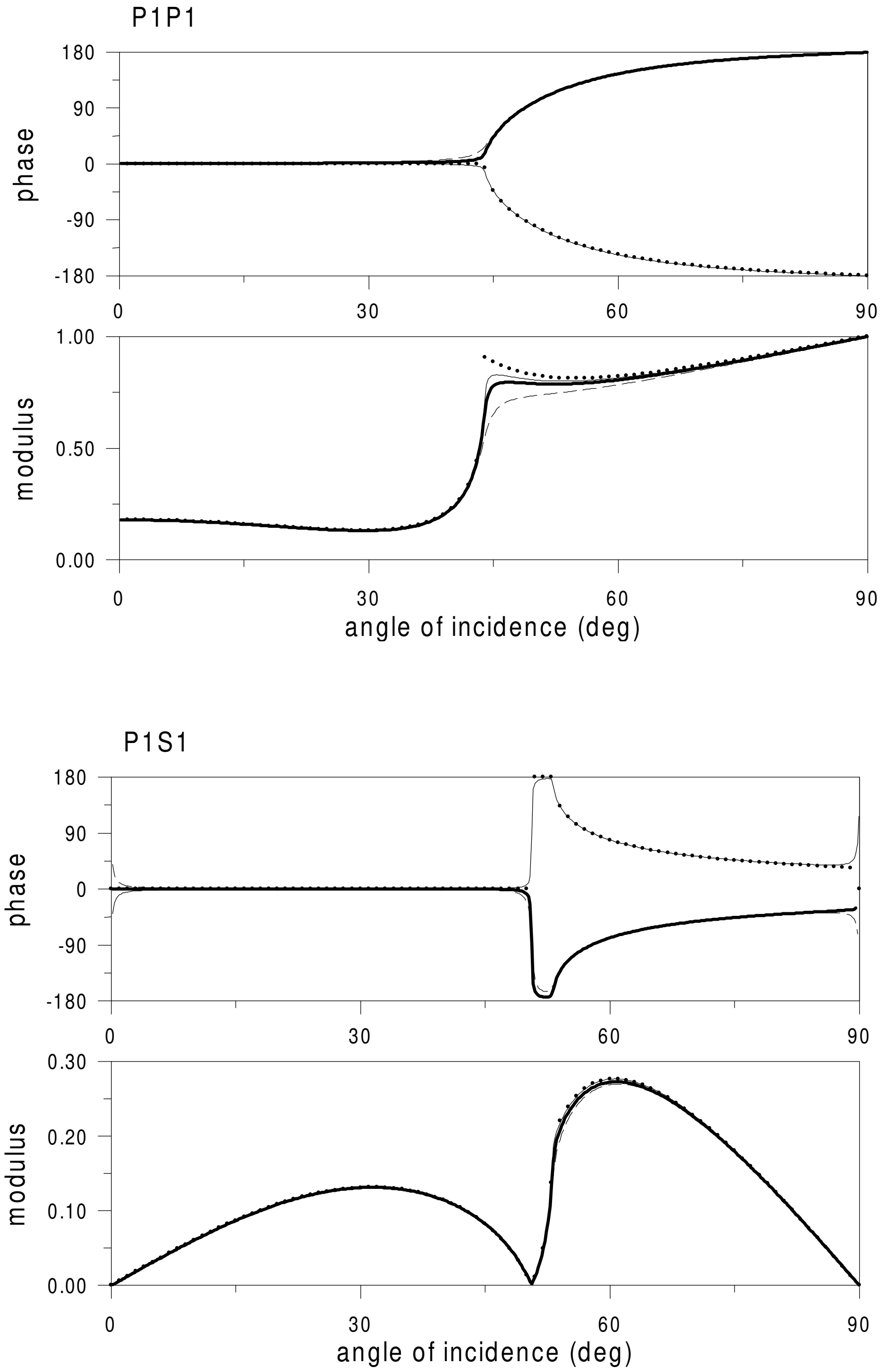

Figure 10: Model 1: Displacement reflection coefficients P1P1 and P1S1 at the interface between two solid halfspaces. (Non-dissipative media: bold dotted line; dissipative media: bold continuous line for $\gamma = 0^o$, thin continuous line for $\gamma = 30^o$, thin dashed line for $\gamma = -30^o$.)

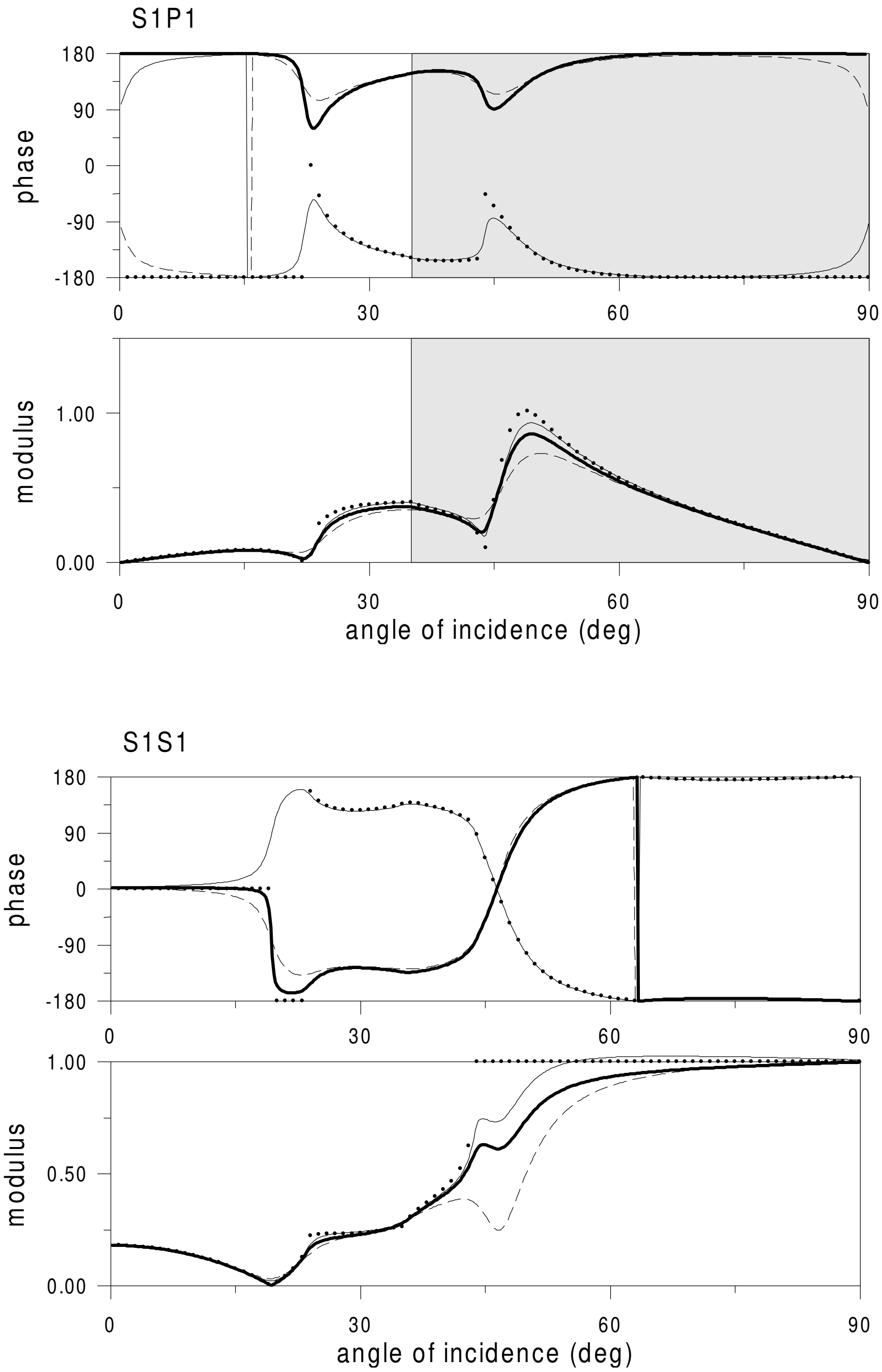

Figure 11: Model 1: displacement reflection coefficients S1P1 and S1S1 at the interface between two solid halfspaces. (Non-dissipative media: bold dotted line; dissipative media: bold continuous line for $\gamma = 0^o$, thin continuous line for $\gamma = 30^o$, thin dashed line for $\gamma = -30^o$.)

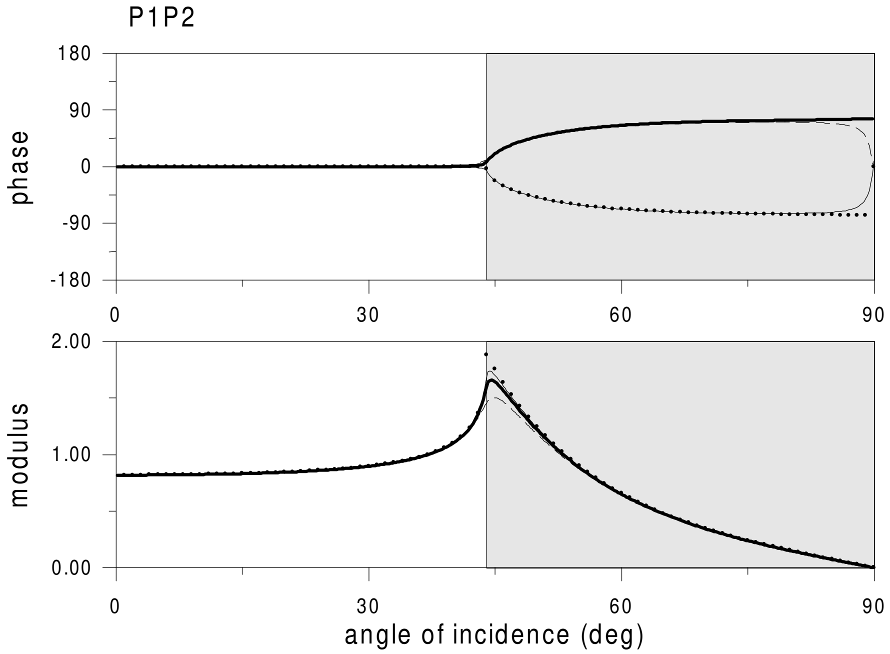

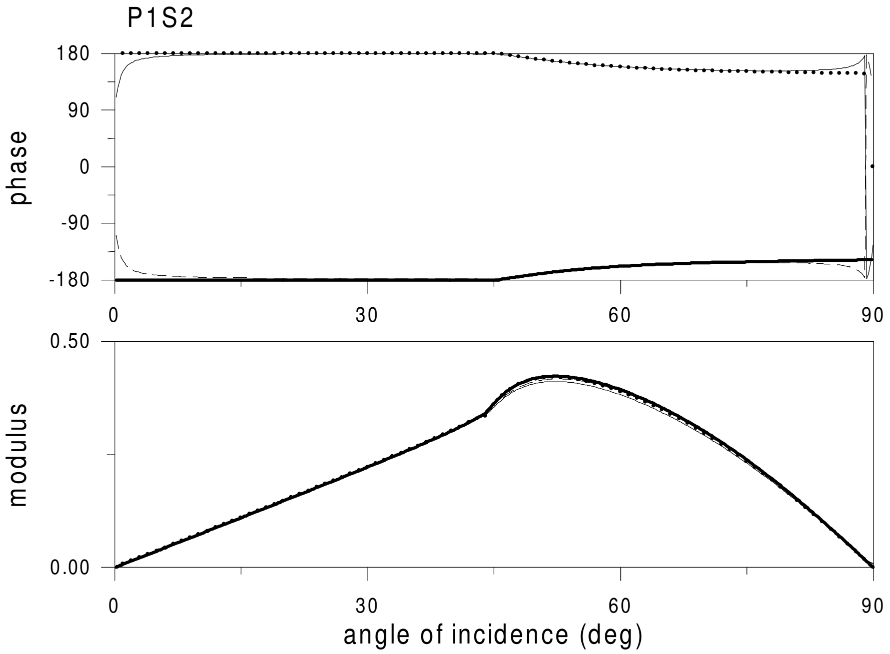

Figure 12: Model 1: Displacement transmission coefficients P1P2 and P1S2 at the interface between two solid halfspaces. (Non-dissipative media: bold dotted line; dissipative media: bold continuous line for $\gamma = 0^o$, thin continuous line for $\gamma = 30^o$, thin dashed line for $\gamma = -30^o$.)

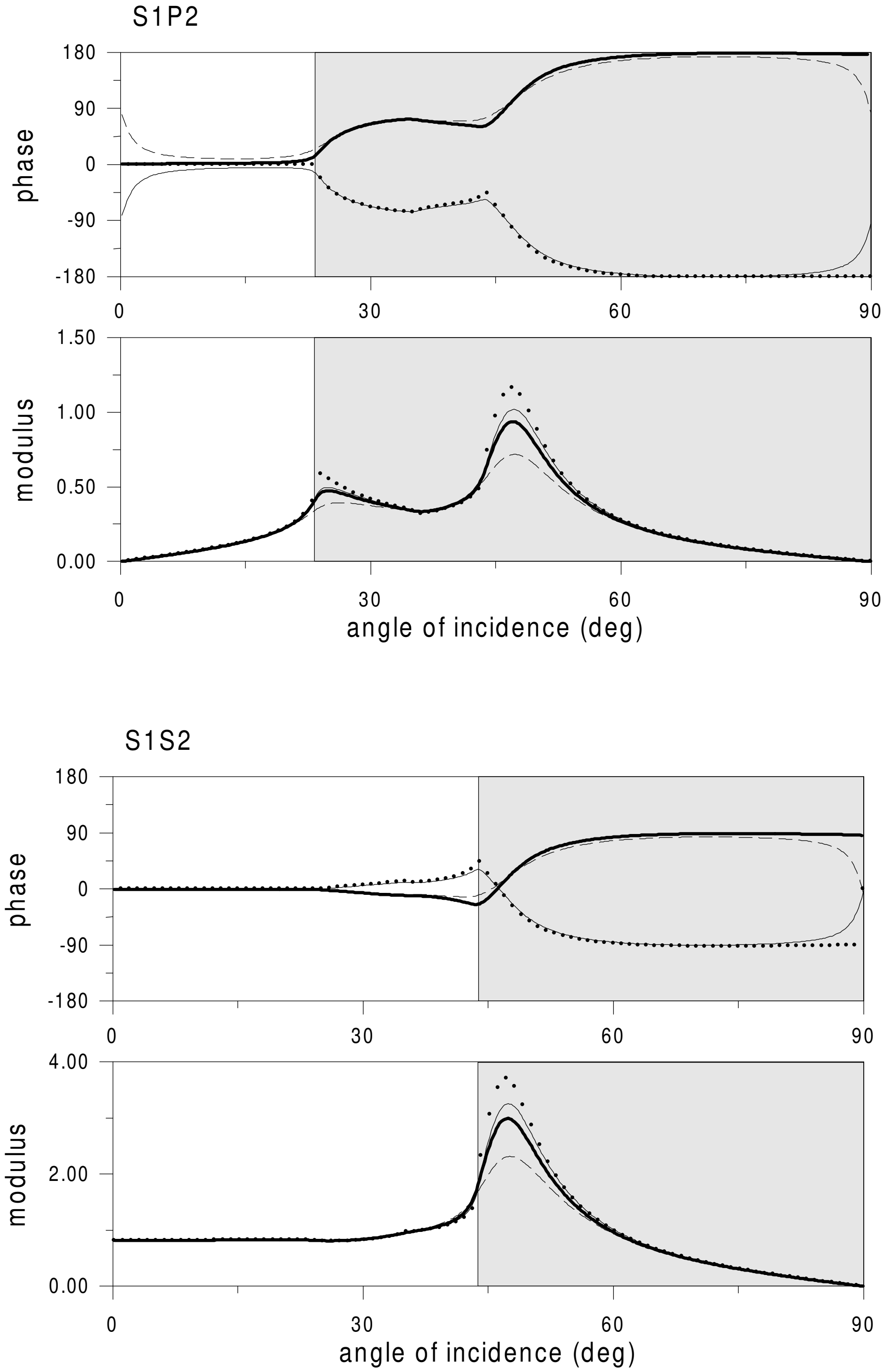

Figure 13: Model 1: Displacement transmission coefficients S1P2 and S1S2 at the interface between two solid halfspaces. (Non-dissipative media: bold dotted line; dissipative media: bold continuous line for $\gamma = 0^o$, thin continuous line for $\gamma = 30^o$, thin dashed line for $\gamma = -30^o$.)

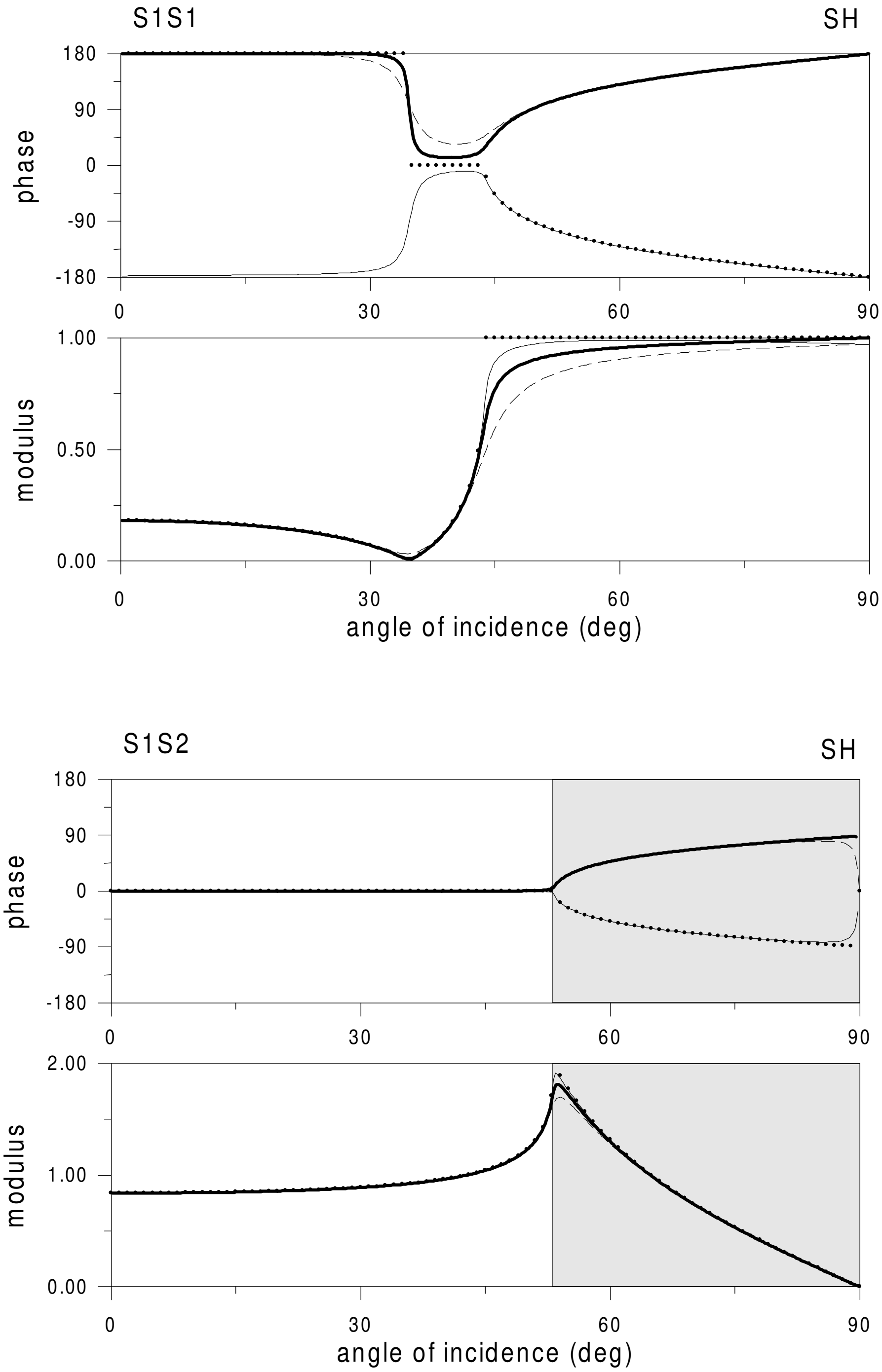

Figure 14: Model 1: Displacement SH R/T coefficients at the interface between two solid halfspaces. (Non-dissipative media: bold dotted line; dissipative media: bold continuous line for $\gamma = 0^o$, thin continuous line for $\gamma = 30^o$, thin dashed line for $\gamma = -30^o$.)

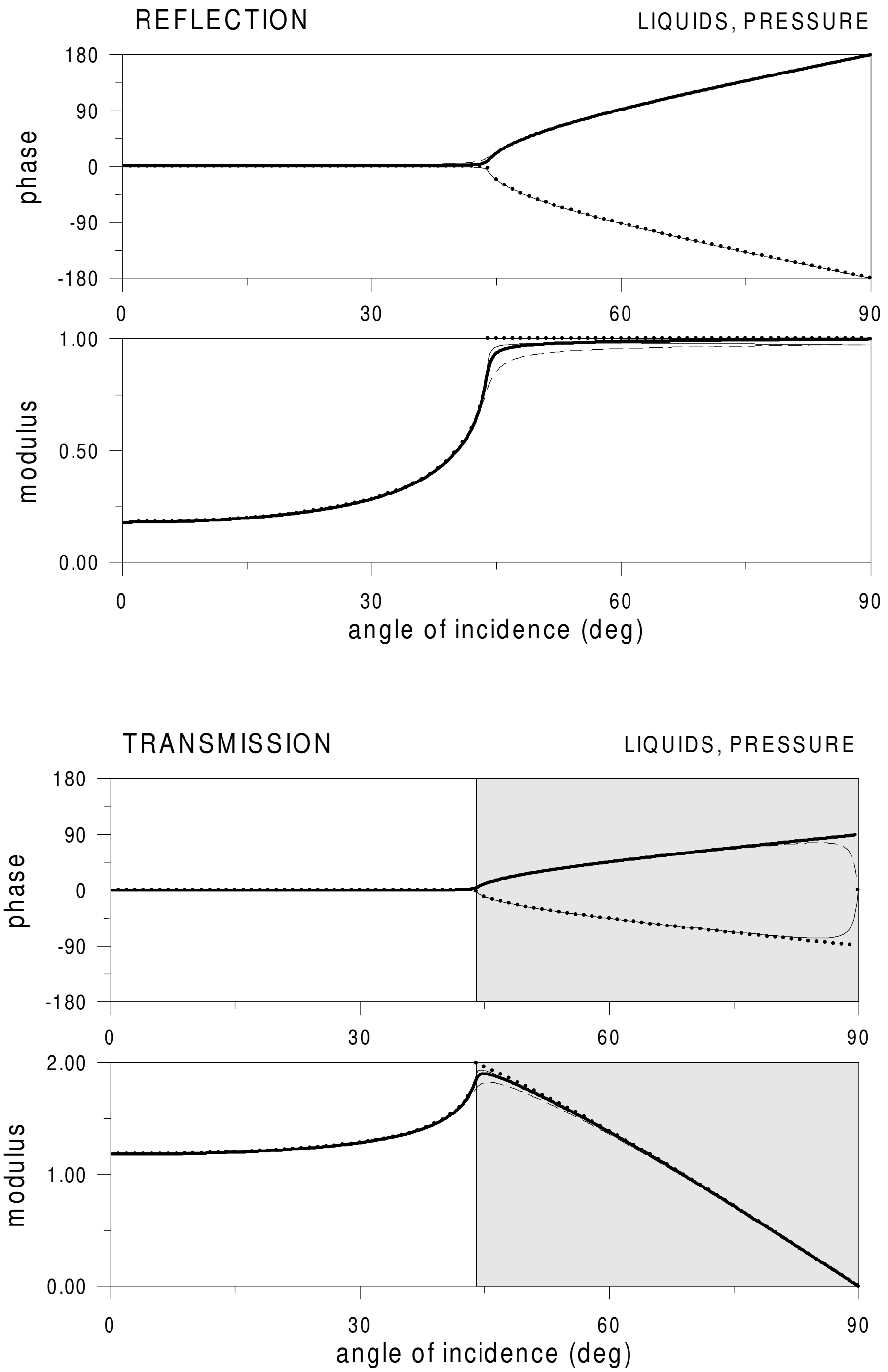

Figure 15: Model 1: Pressure R/T coefficients at the interface between two liquid halfspaces. (Non-dissipative media: bold dotted line; dissipative media: bold continuous line for $\gamma = 0^o$, thin continuous line for $\gamma = 30^o$, thin dashed line for $\gamma = -30^o$.)

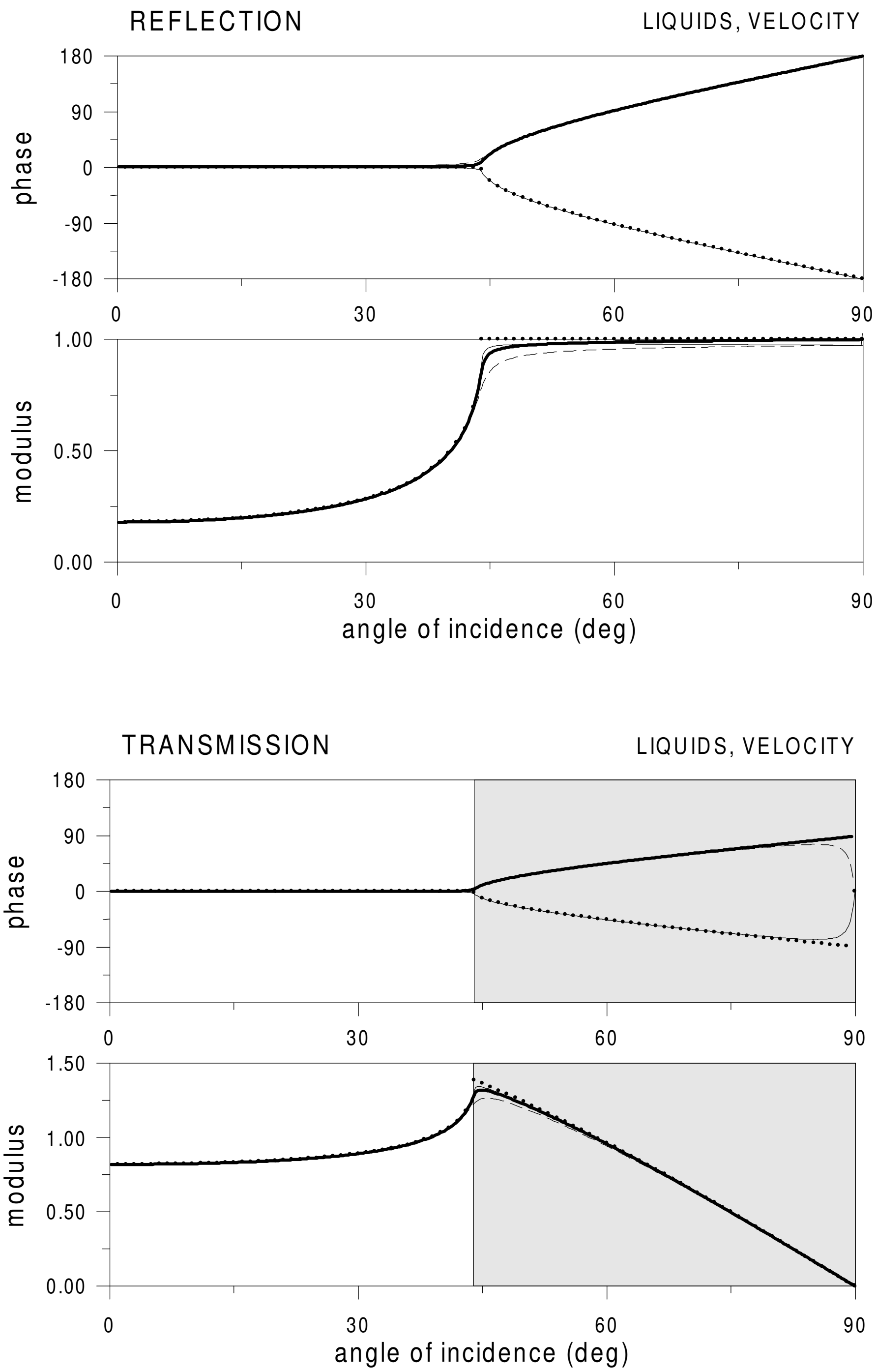

Figure 16: Model 1: Particle velocity R/T coefficients at the interface between two liquid halfspaces. Compare the transmission particle velocity coefficient with the transmission pressure coefficient in Fig. 15. (Non-dissipative media: bold dotted line; dissipative media: bold continuous line for $\gamma = 0^o$, thin continuous line for $\gamma = 30^o$, thin dashed line for $\gamma = -30^o$.)

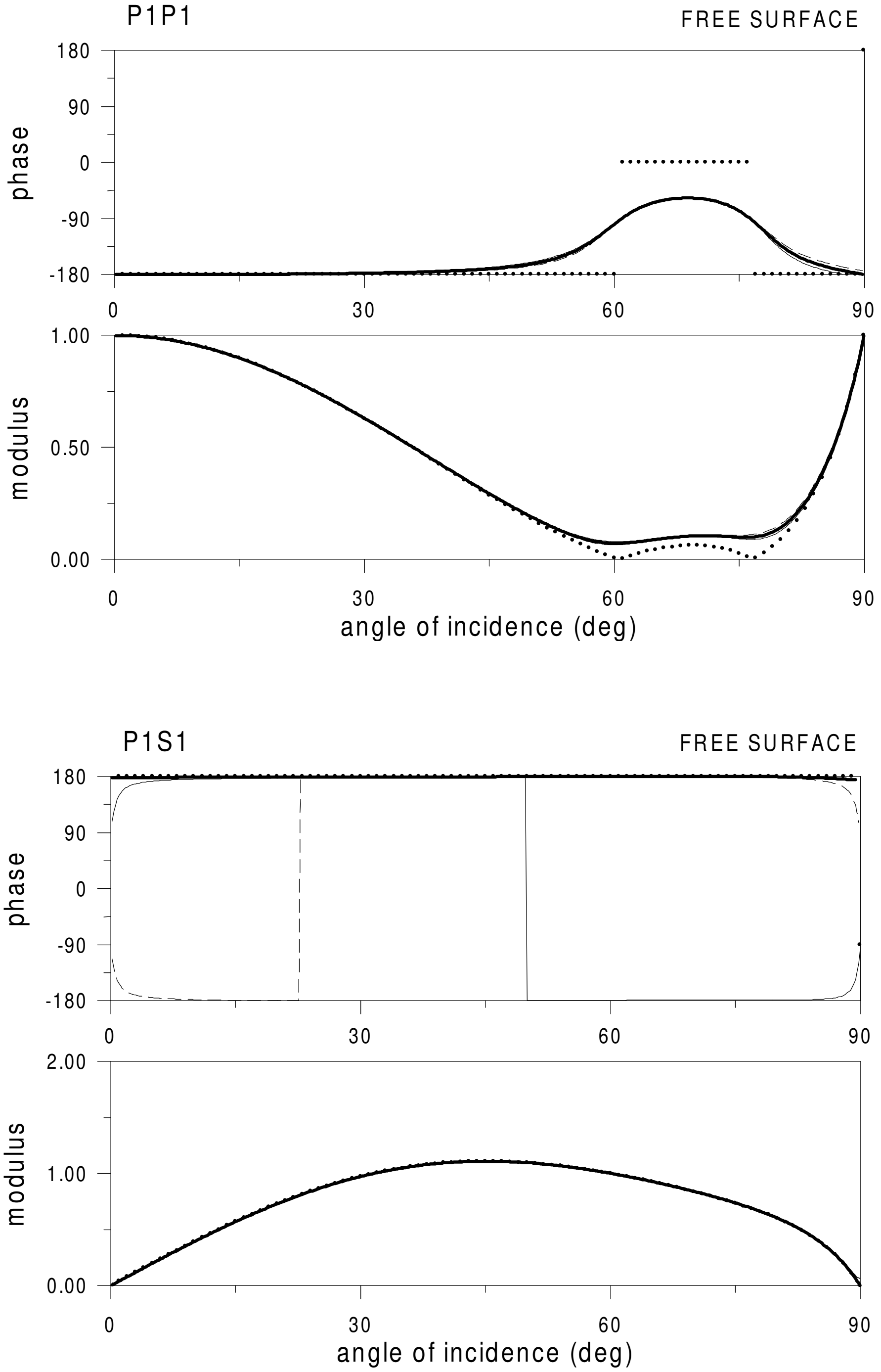

Figure 17: Model 1: Displacement reflection coefficients P1P1 and P1S1 at the free surface of a solid halfspace. (Non-dissipative media: bold dotted line; dissipative media: bold continuous line for $\gamma = 0^o$, thin continuous line for $\gamma = 30^o$, thin dashed line for $\gamma = -30^o$.)

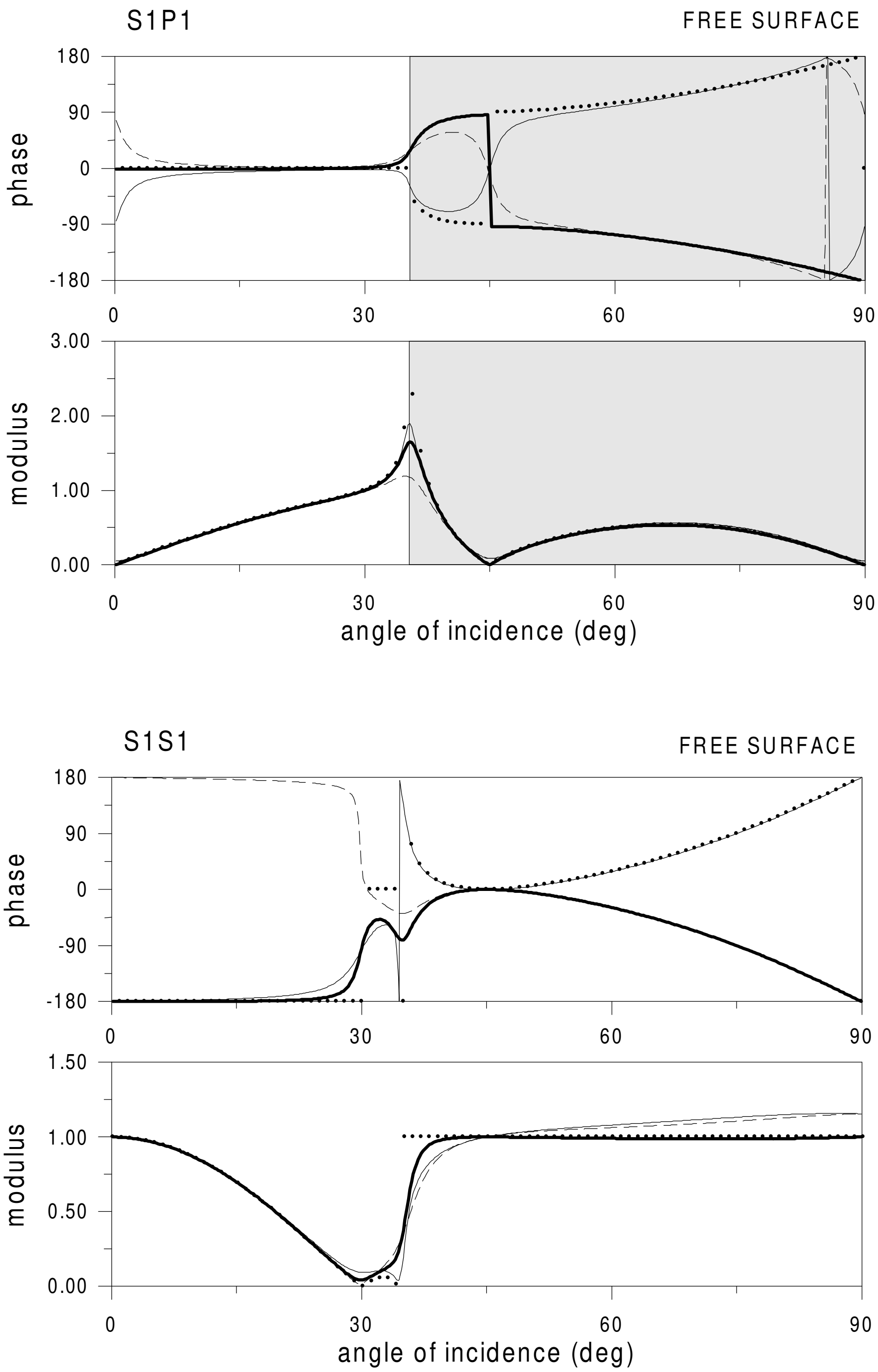

Figure 18: Model 1: Displacement reflection coefficients S1P1 and S1S1 at the free surface of a solid halfspace. (Non-dissipative media: bold dotted line; dissipative media: bold continuous line for $\gamma = 0^o$, thin continuous line for $\gamma = 30^o$, thin dashed line for $\gamma = -30^o$.)

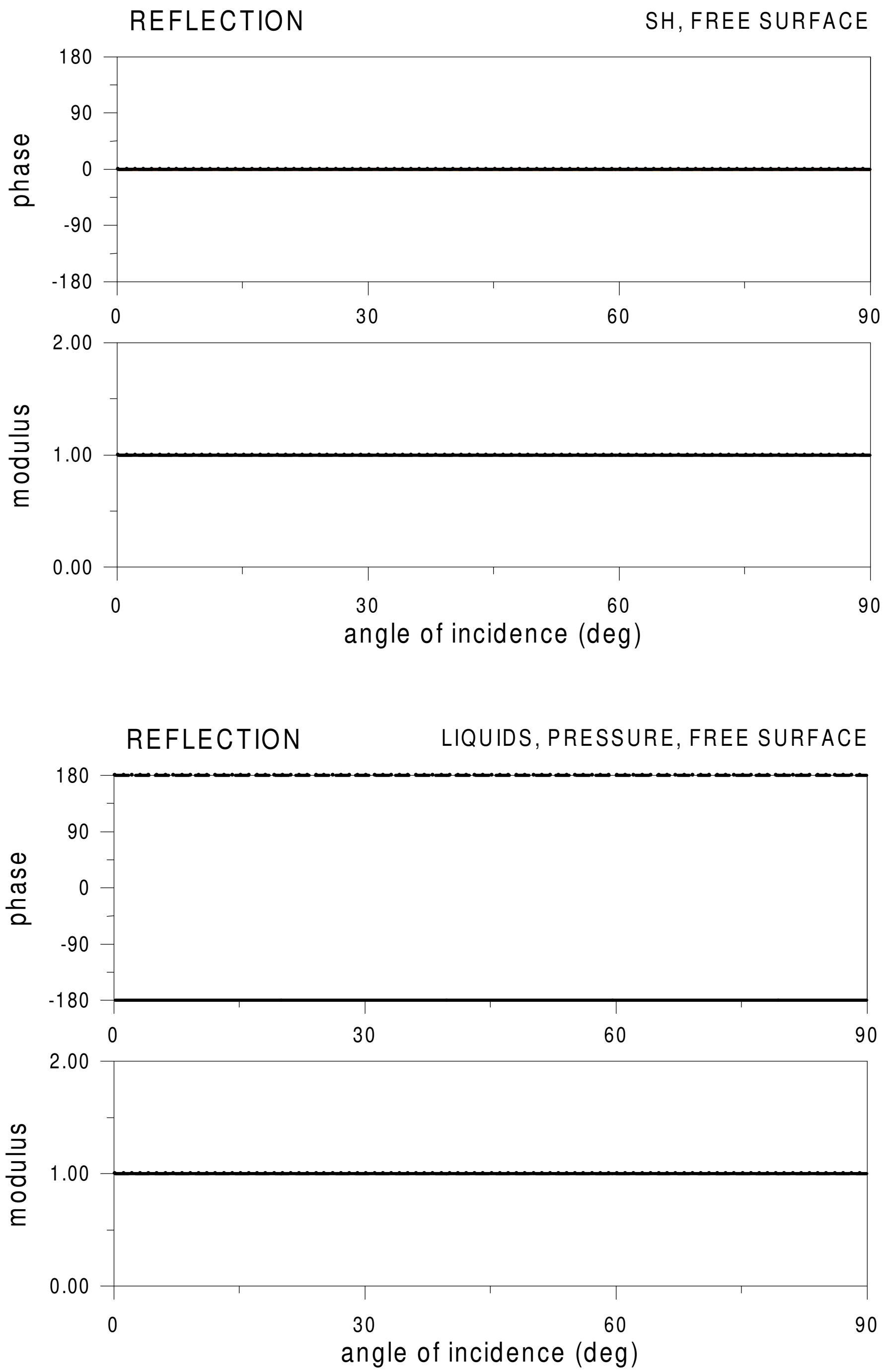

Figure 19: Model 1: Displacement SH reflection coefficient at the free surface of a solid halfspace (top) and pressure reflection coefficient at the free surface of a liquid halfspace (bottom). (Non-dissipative media: bold dotted line; dissipative media: bold continuous line for $\gamma = 0^o$, thin continuous line for $\gamma = 30^o$, thin dashed line for $\gamma = -30^o$.)

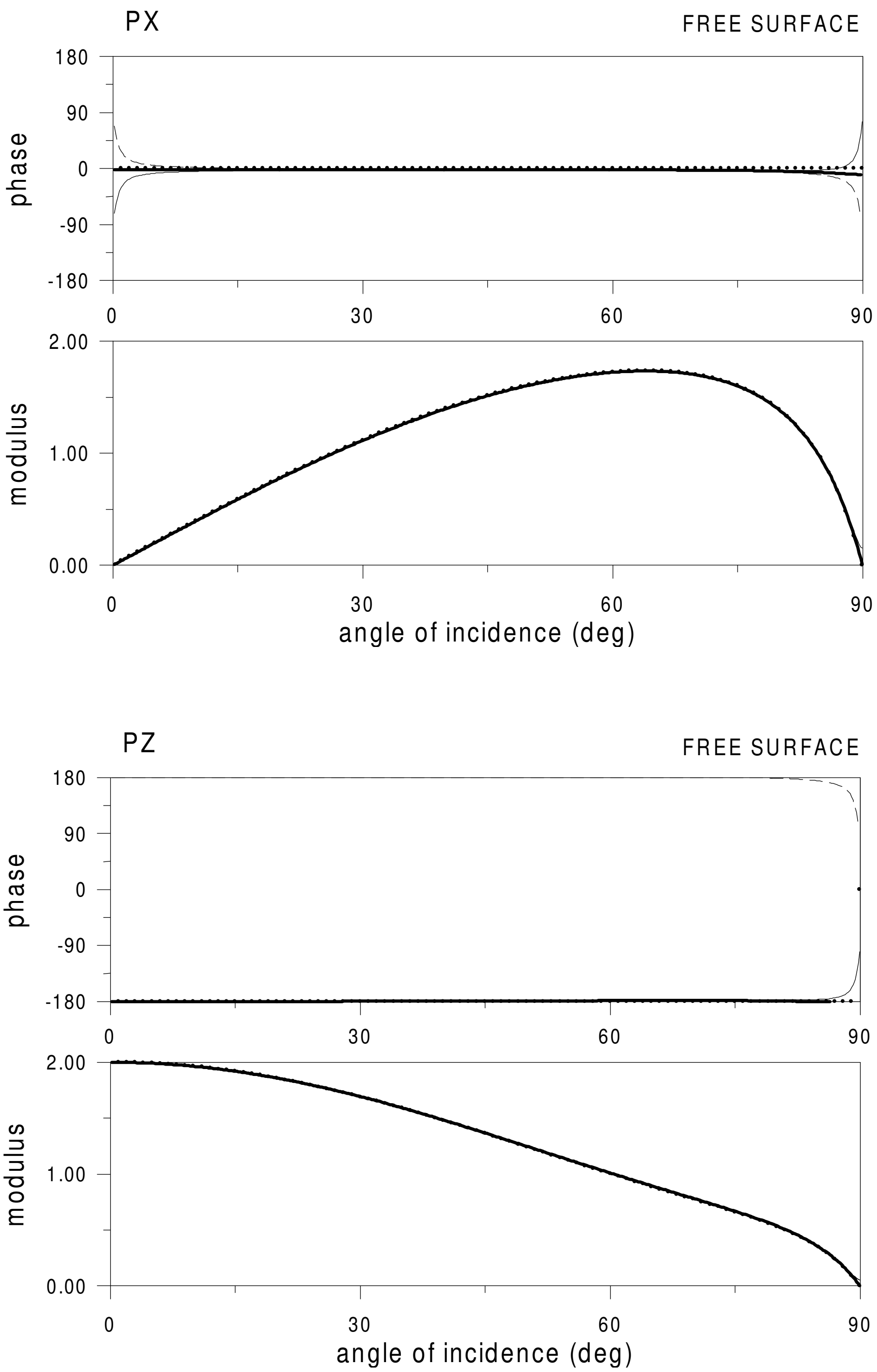

Figure 20: Model 1: Coefficients of conversion PX and PZ at the free surface of a solid halfspace. (Non-dissipative media: bold dotted line; dissipative media: bold continuous line for $\gamma = 0^o$, thin continuous line for $\gamma = 30^o$, thin dashed line for $\gamma = -30^o$.)

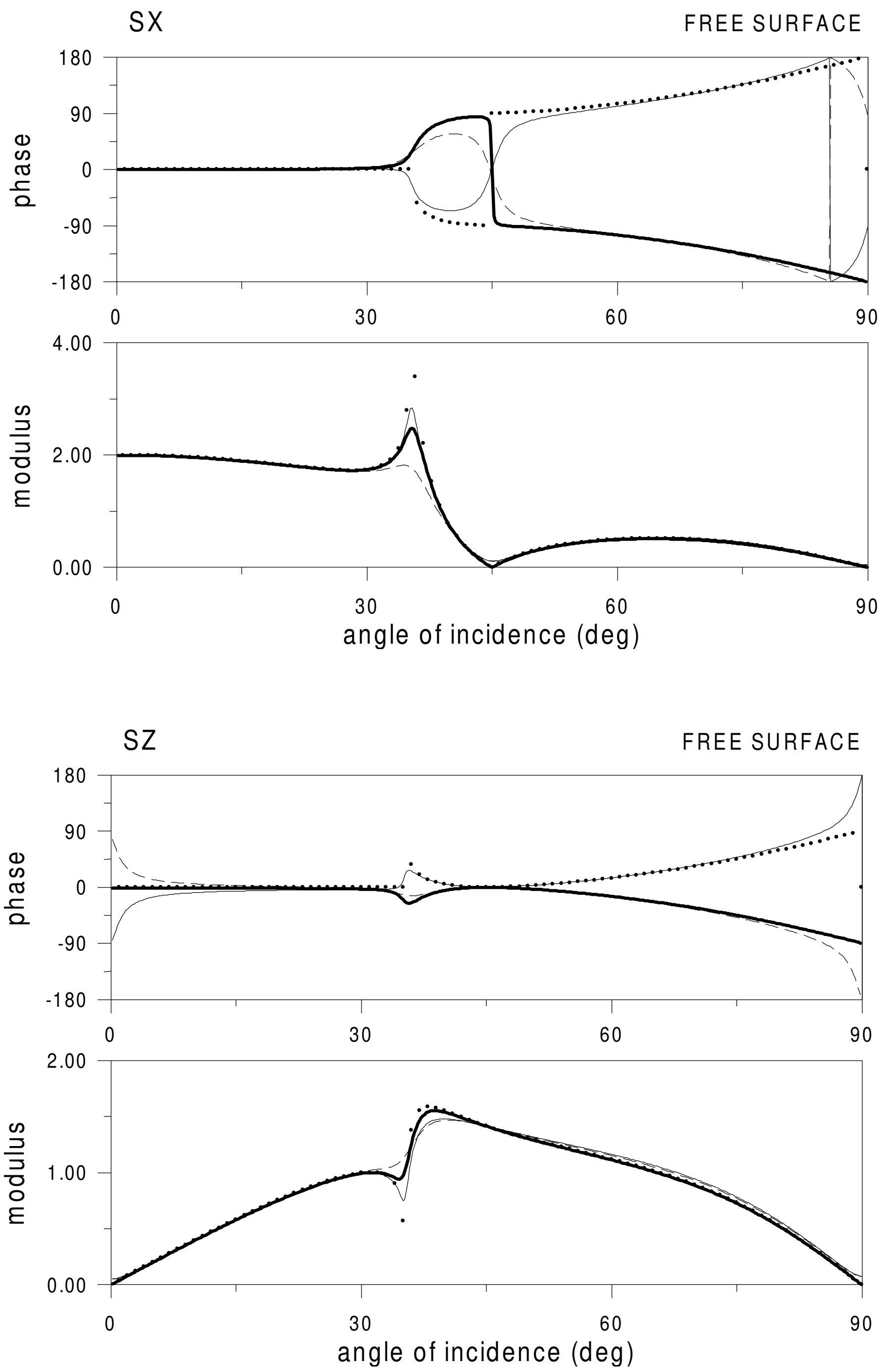

Figure 21: Model 1: Coefficients of conversion SX and SZ at the free surface of a solid halfspace. (Non-dissipative media: bold dotted line; dissipative media: bold continuous line for $\gamma = 0^o$, thin continuous line for $\gamma = 30^o$, thin dashed line for $\gamma = -30^o$.)

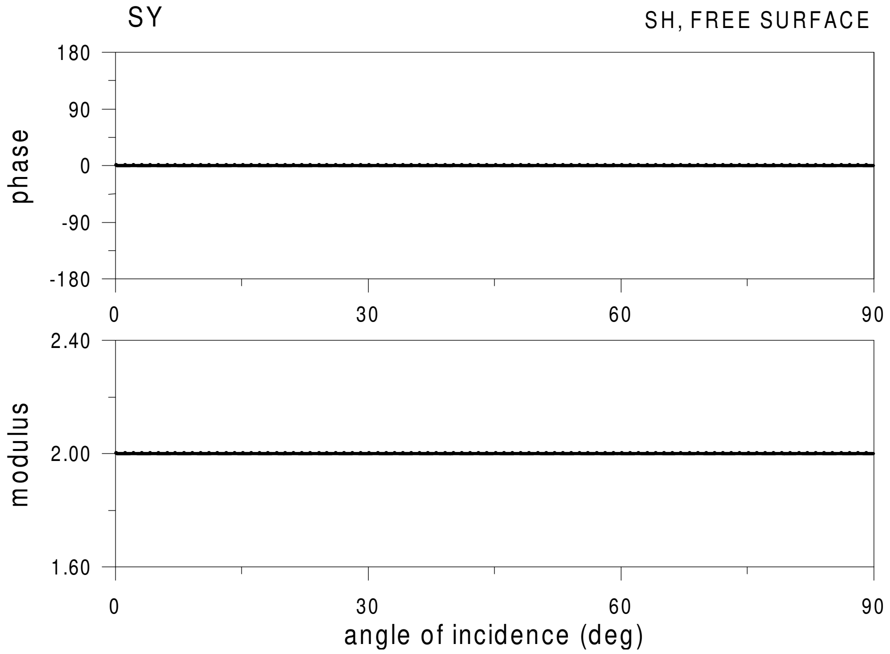

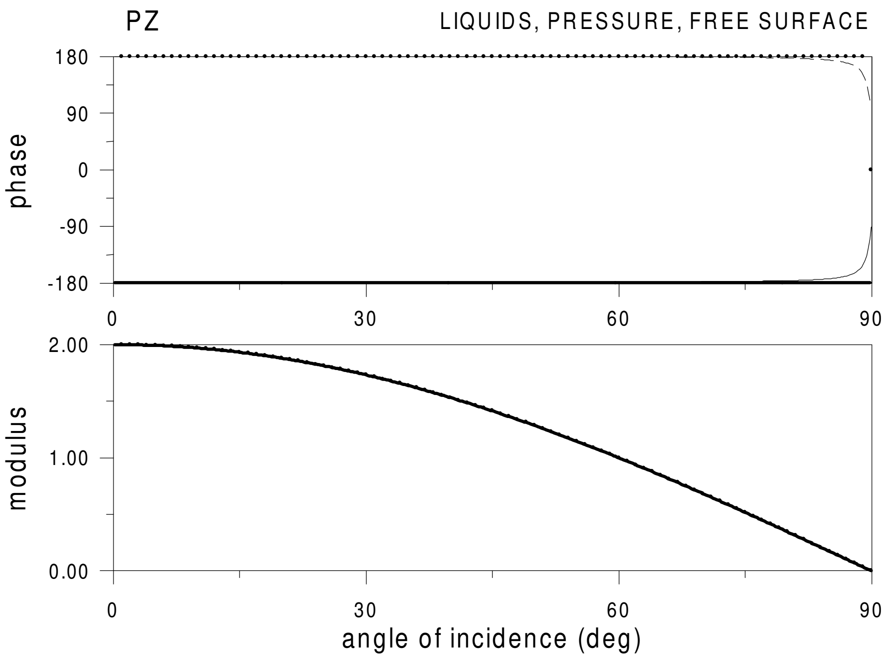

Figure 22: Model 1: Displacement SH coefficient of conversion at the free surface of a solid halfspace (top) and pressure coefficient of conversion at the free surface of a liquid halfspace (bottom). (Non-dissipative media: bold dotted line; dissipative media: bold continuous line for $\gamma = 0^o$, thin continuous line for $\gamma = 30^o$, thin dashed line for $\gamma = -30^o$.)

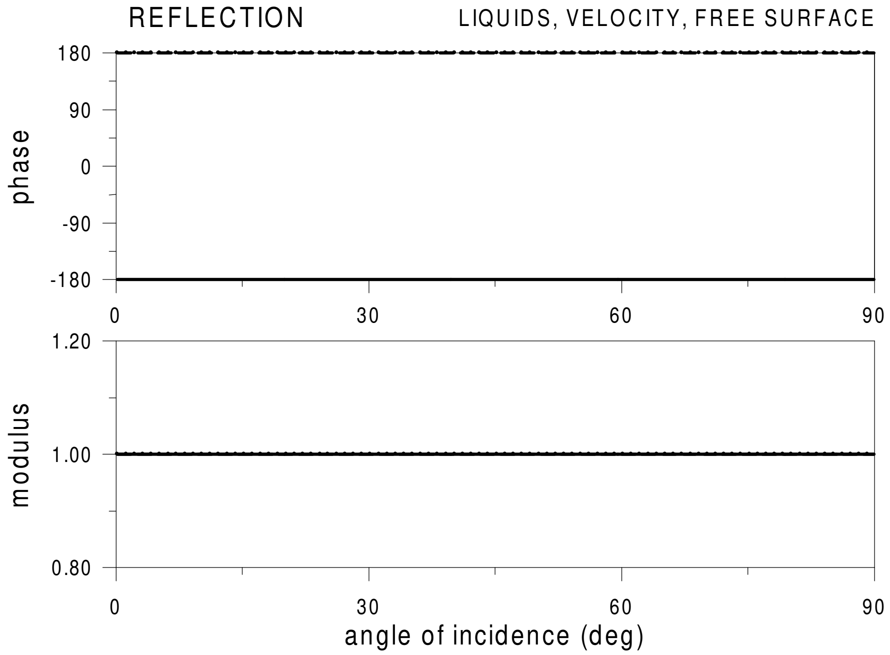

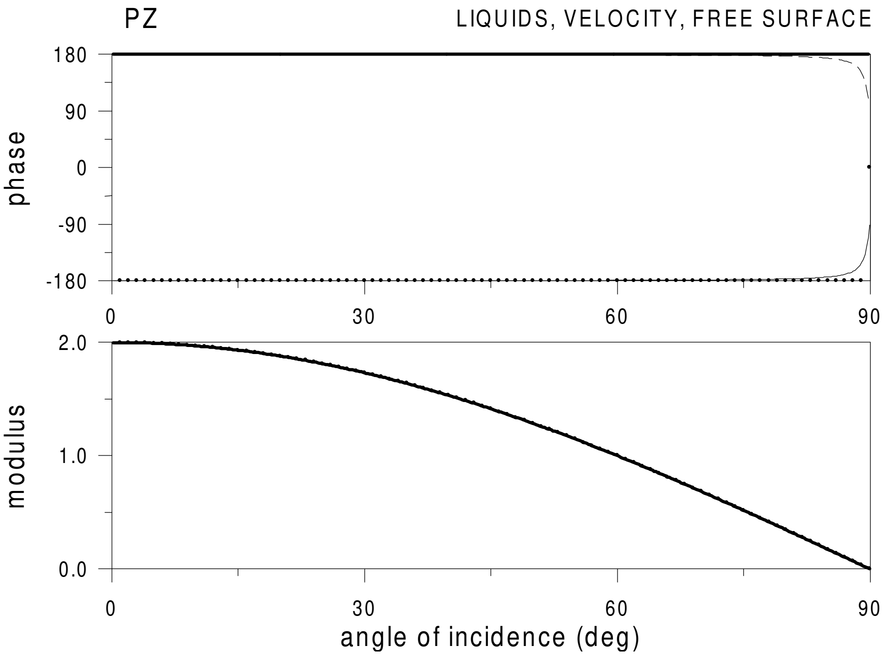

Figure 23: Model 1: Particle velocity reflection coefficient (top) and particle velocity coefficient of conversion (bottom) at the free surface of a liquid halfspace. (Non-dissipative media: bold dotted line; dissipative media: bold continuous line for $\gamma = 0^o$, thin continuous line for $\gamma = 30^o$, thin dashed line for $\gamma = -30^o$.)

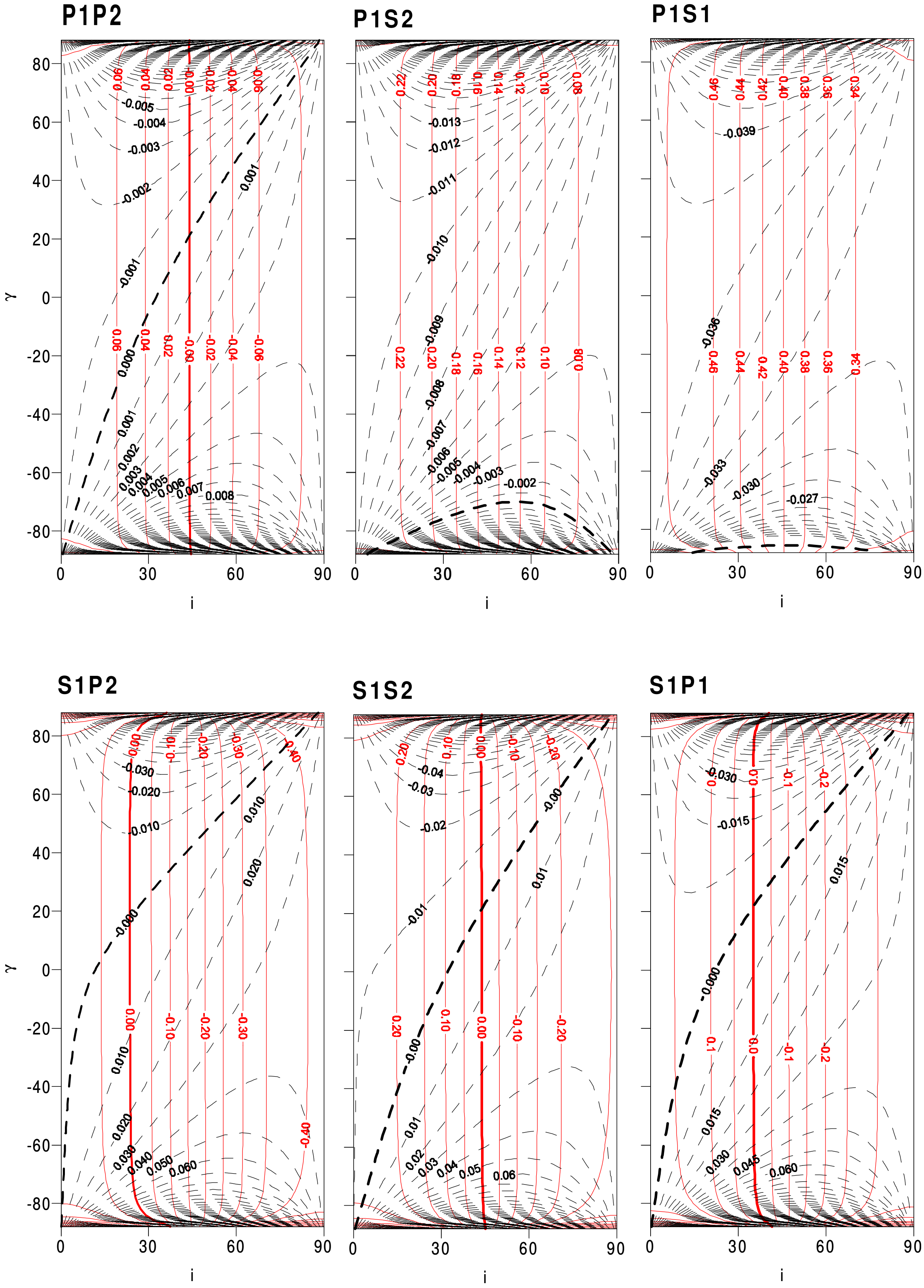

Figure 24: Model 1: σ^2-maps

For *R/T coefficients on a free surface*, the conclusions are simpler. The R/T coefficients from the free surface include only P1S1 and S1P1 square roots, see σ^2-maps in Fig. 24. As the P1S1 square root is always regular, the phases of R/T coefficients in dissipative media and non-dissipative media are always close to each other for incident P wave, for all γ. See P1P1 and P1S1 reflection coefficients in Fig. 17, and also PX and PZ conversion coefficients in Fig. 20. For an incident S wave, however, the situation is different, as the square root S1P1 plays a decisive role in this case. As we can see in Fig. 24, the argument of the square root S1P1 is anomalous for $\gamma < 22^o$. Consequently, the phases of S1P1 and S1S1 of reflection coefficients from the free surface for dissipative and non-dissipative media are close to each other only for $\gamma = 30^o$, see Fig. 18. For $\gamma = 0^o$ and $\gamma = -30^o$, they are approximately opposite. The same conclusion is valid even for the conversion coefficients SX and SZ, see Fig. 21.

4) **Moduli of post-critical non-converted reflections.** In non-dissipative media, the moduli of reflection coefficients of *unconverted reflected waves* in post-critical region do not exceed unity. In many cases they exactly equal unity. See the S1S1 reflection coefficient for $i > 44^o$ in Fig. 11, the SH reflection coefficient in Fig. 14, the P1P1 reflection coefficients at an interface between two liquids, Figs. 15 and 16, and the S1S1 reflection coefficient at a free surface in Fig. 18. In dissipative media, these moduli *may exceed unity.* The explanation is given in Section 3.2., sub 5d. In the computations presented in Figs. 10 – 23, this effect can be observed in two cases, both of them for S1S1 reflection coefficients. See Fig. 11 for $\gamma = 30^o$, and Fig. 18 for $\gamma = 30^o$ and $\gamma = -30^o$.

5) **The phases of R/T coefficients for near-normal incidence of an inhomogeneous plane wave.** The phases of R/T coefficients in dissipative media for $\gamma \neq 0^o$, the moduli of which vanish for the normal incidence (or are very close to zero), differ from the phases of R/T coefficients for non-dissipative media for small angles of incidence. This applies to coefficients of converted reflected waves P1S1, S1P1 (Figs. 10, 11, 17, 18), of converted transmitted waves P1S2 and S1P2 (Figs. 12, 13), and to conversion coefficients PX, SZ (Figs. 20, 21). The phase is not zero (or $\pm 180^o$) for the normal incidence, but equals either $+90^o$ or -90^o. With increasing angle of incidence, the phase goes to zero (or to $\pm 180^o$). The explanation is simple. For normal incidence of an inhomogeneous plane wave, the real part of the R/T coefficient vanishes, but the imaginary part not (even though it is very small and does not influence visibly the pictures of R/T coefficients). Thus, for the normal incidence of an inhomogeneous plane wave, the phase is $+90^o$ or -90^o, depending on the sign of the imaginary part. As the real part of the R/T coefficient increases with increasing i in the near-normal region, the phase fastly approaches zero (or $\pm 180^o$). It should be noted that this effect does not appear for an incident homogeneous plane wave ($\gamma = 0^o$). In this case, the phases of R/T coefficients for the near-normal incidence are the same for non-dissipative and dissipative media.

6) **The phases of R/T coefficients for near-grazing incidence of an inhomogeneous plane wave.** Similar effect to that described sub 5) can be also observed for the grazing incidence, $i \to 90^o$, when the modulus of the R/T coefficient under consideration vanishes for $i = 90^o$ (or is very close to zero). See pictures of all R/T coefficients named sub 5), but also the transmission coefficients P1P2 (Fig. 12), S1S2 (Fig. 13), and the conversion coefficients PZ, SX (Figs. 20, 21). The explanation is the same as sub 5).

6.3 Complete set of R/T coefficients for Model 2

Here we shall present and discuss a complete set of R/T coefficient for **Model 2**. Whereas Model 1 is typical for shallow structures, Model 2 is more representative for deeper crustal structures. It is as follows:

Model 2
CP1 = 6.4 km/s, CS1 = 3.698 km/s, RHO1 = 2.980 kg m^{-3}, QP1 = 100, QS1 = 50,
CP2 = 8.0 km/s, CS2 = 4.618 km/s, RHO2 = 3.300 kg m^{-3}, QP2 = 150, QS2 = 75.

As we can see, the quality factors in Model 2 are higher than in Model 1, so that Model 2 is less dissipative than Model 1. Note that Model 2 corresponds also to Model 2 in Brokešová and Červený (1997).

The R/T coefficients are displayed in Figs. 25 – 35. They are organized in the same way as in Section 6.2, see a) – l). The only difference is that the R/T coefficients f), g), i), j), k) and l) are not presented here, as they are the same as in Model 1 (they do not depend on model data). Four curves are displayed in any picture: a) R/T coefficient for a non-dissipative medium (dotted line), b) R/T coefficients for a dissipative medium, for $\gamma = 0^o$ (bold continuous line), $\gamma = 30^o$ (thin continuous line) and $\gamma = -30^o$ (thin dashed line).

The σ^2-maps for Model 2 are shown in Fig. 36. The explanation of the σ^2-maps is analogous to that in Section 6.2 for Model 1. The angles i^R, if they exist, are as follows: P1P2 ... $i^R = 53^o$, S1P2 ... $i^R = 27^o$, S1S2 ... $i^R = 53^o$, S1P1 ... $i^R = 35^o$. The behaviour of σ^2-maps in Fig. 36 is very similar to σ^2-maps in Fig. 24 for Model 1. Most important are the σ^2-maps of P1P2 and S1S2 square roots. In both cases, $i^R = 53^o$. For $\gamma > 24^o$, there is one critical angle, and the argument of the square root behaves regularly (as $i^I > i^R$). For $\gamma < 24^o$, there is no critical angle, but the argument of the square root behaves anomalously.

The discussion of all R/T coefficients for Model 2 is quite analogous to that for Model 1, see Section 6.2. The only difference in Model 2 is that quality factors in Model 2 are higher than in Model 1, so that the dissipative effects are weaker than for Model 1. Consequently, the moduli of all R/T coefficients for dissipative media are closer to the moduli of relevant R/T coefficients for non-dissipative media. In principle, the same conclusion is valid even for phases of R/T coefficients, but the phases of some R/T coefficients for certain γ in post-critical region have opposite signs than for dissipative media. The phases of R/T coefficients in dissipative and non-dissipative media in post-critical regions are close to each other only for $\gamma = 30^o$. For $\gamma = 0^o$ and $\gamma = -30^o$, they have opposite signs.

6.4 R/T coefficients for Model 2 with exchanged Q's

Certain features of R/T coefficients depend considerably on mutual relation of $\tilde{Q}$'s corresponding to generated waves to the Q of the incident wave. For example, for a homogeneous incident wave, the anomalous behaviour of arguments of square roots is completely controlled by $\tilde{Q}/Q$, where $\tilde{Q}$ corresponds to the generated wave and Q to the incident wave. See (136). Thus, we can expect that the anomalous phases of R/T coefficients in

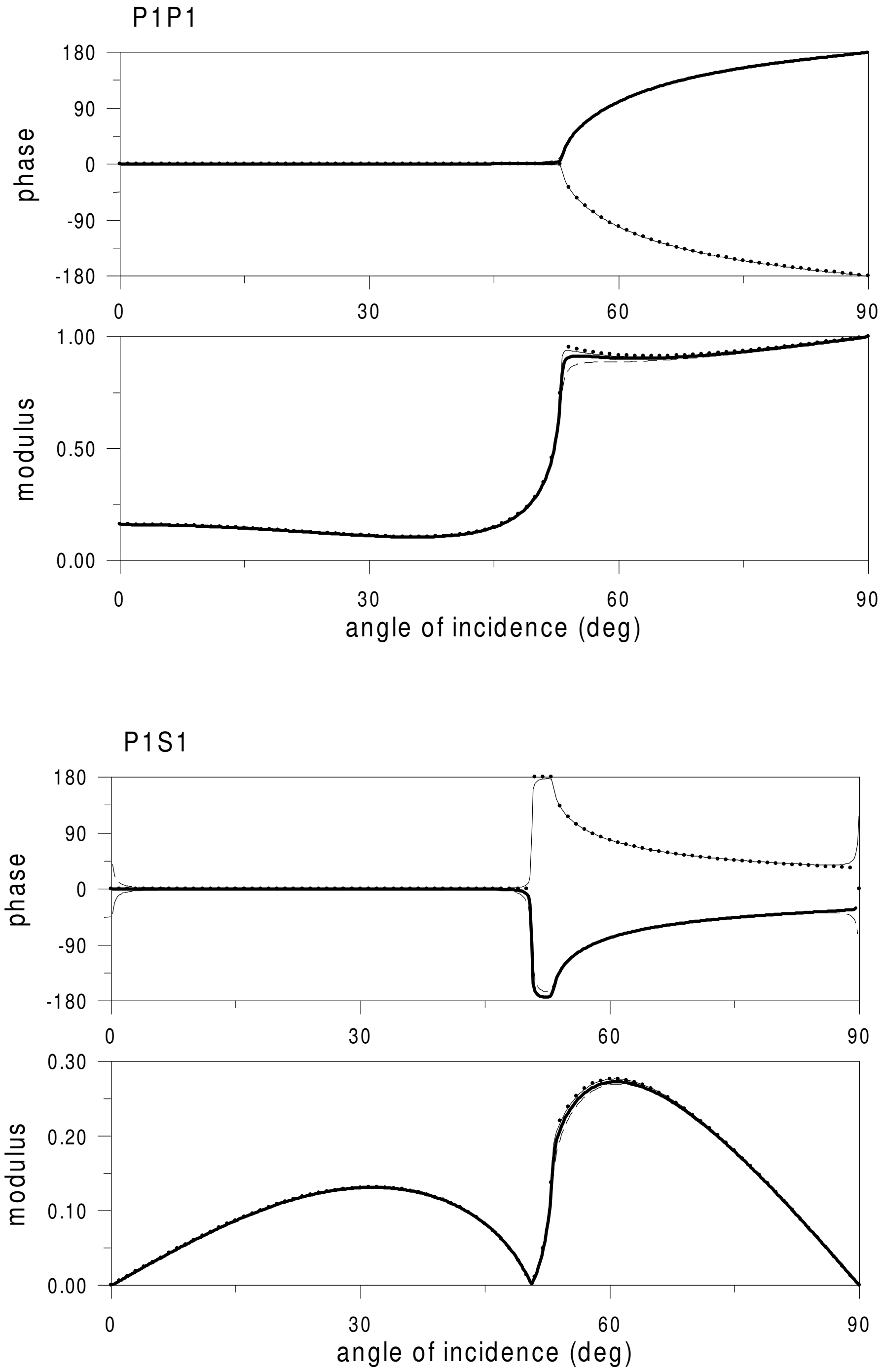

Figure 25: Model 2: Displacement reflection coefficients P1P1 and P1S1 at the interface between two solid halfspaces. (Non-dissipative media: bold dotted line; dissipative media: bold continuous line for $\gamma = 0^o$, thin continuous line for $\gamma = 30^o$, thin dashed line for $\gamma = -30^o$.)

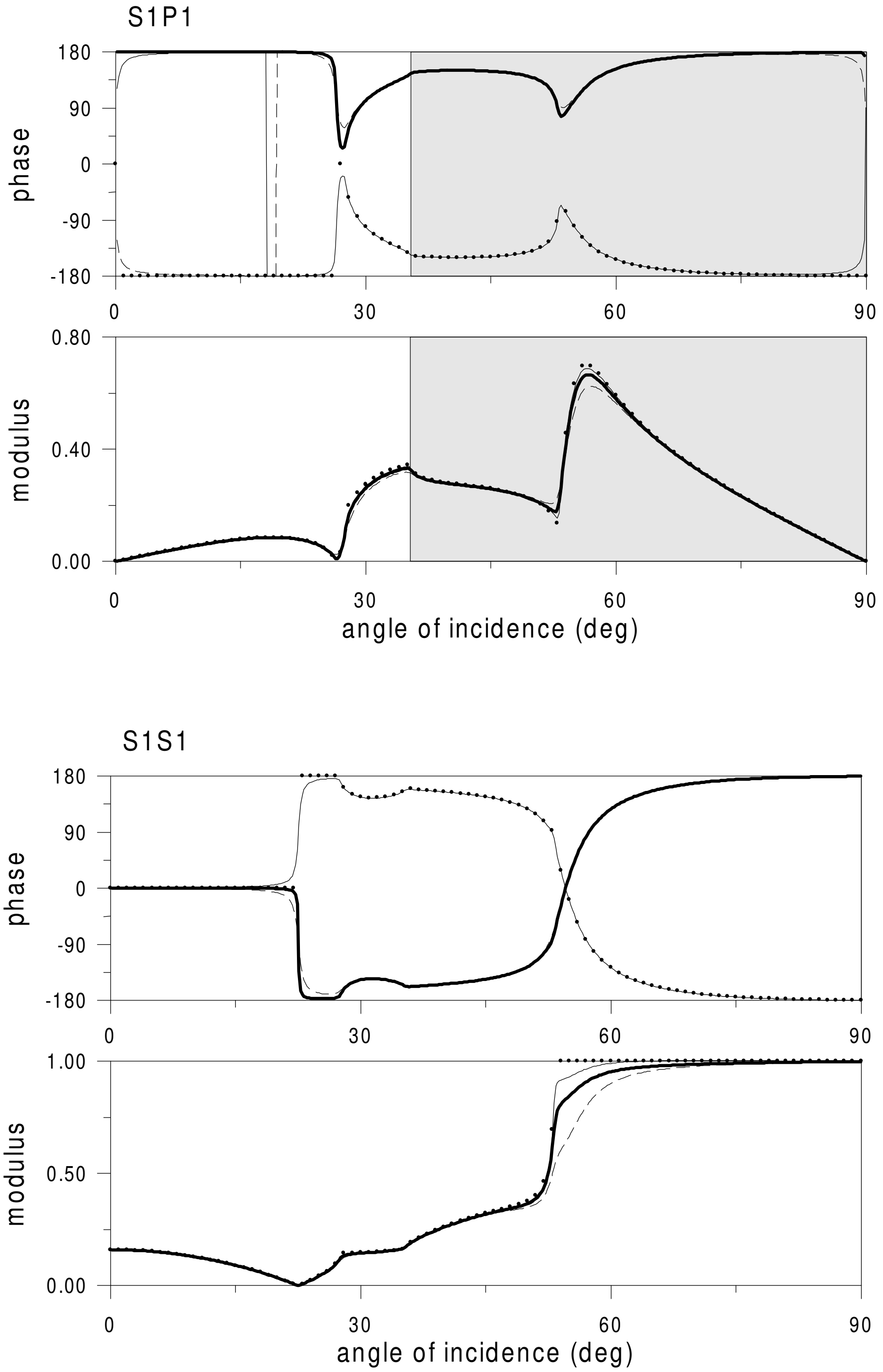

Figure 26: Model 2: Displacement reflection coefficients S1P1 and S1S1 at the interface between two solid halfspaces. (Non-dissipative media: bold dotted line; dissipative media: bold continuous line for $\gamma = 0^o$, thin continuous line for $\gamma = 30^o$, thin dashed line for $\gamma = -30^o$.)

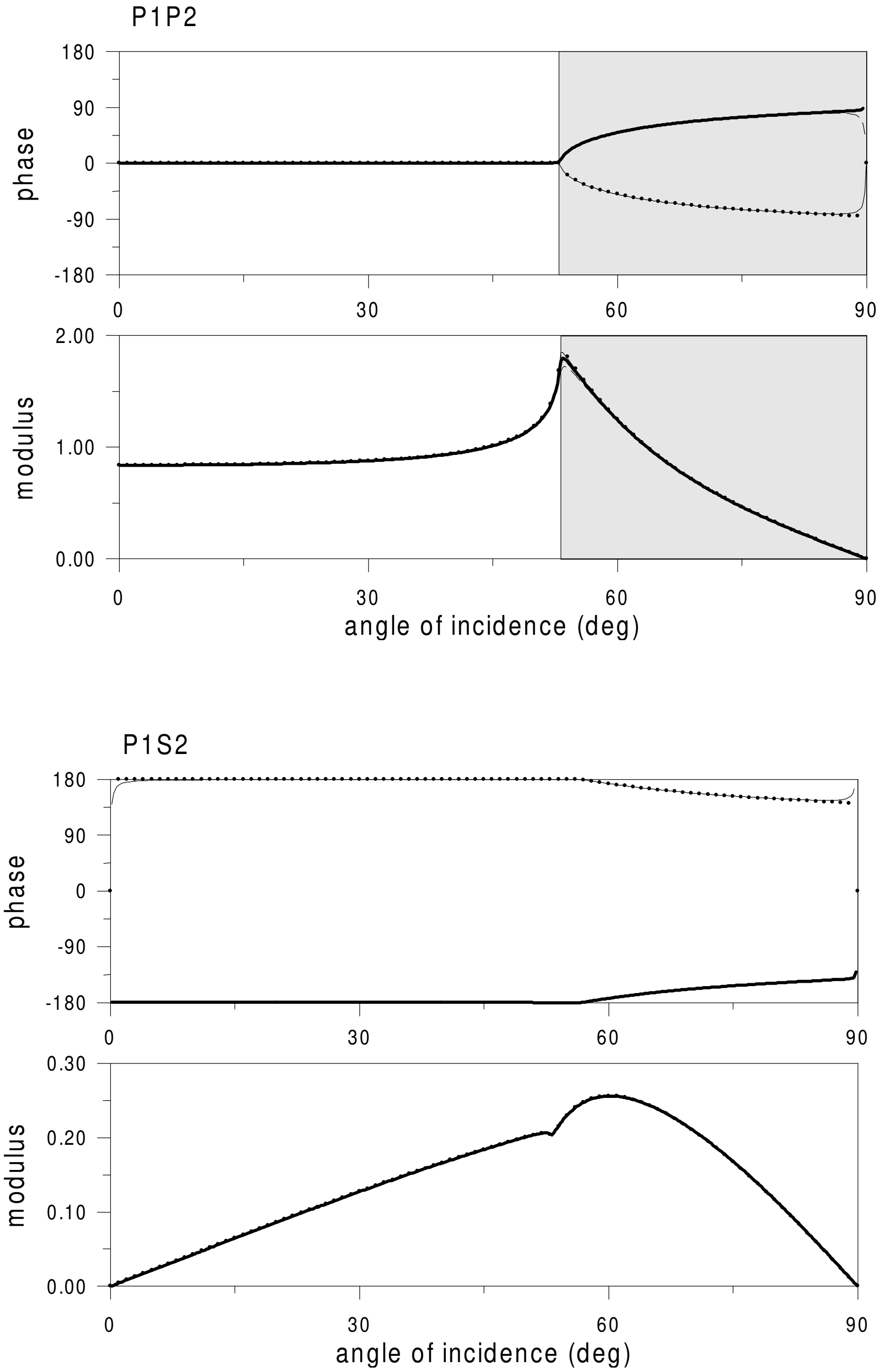

Figure 27: Model 2: Dispalcement transmission coefficients P1P2 and P1S2 at the interface between two solid halfspaces. (Non-dissipative media: bold dotted line; dissipative media: bold continuous line for $\gamma = 0^o$, thin continuous line for $\gamma = 30^o$, thin dashed line for $\gamma = -30^o$.)

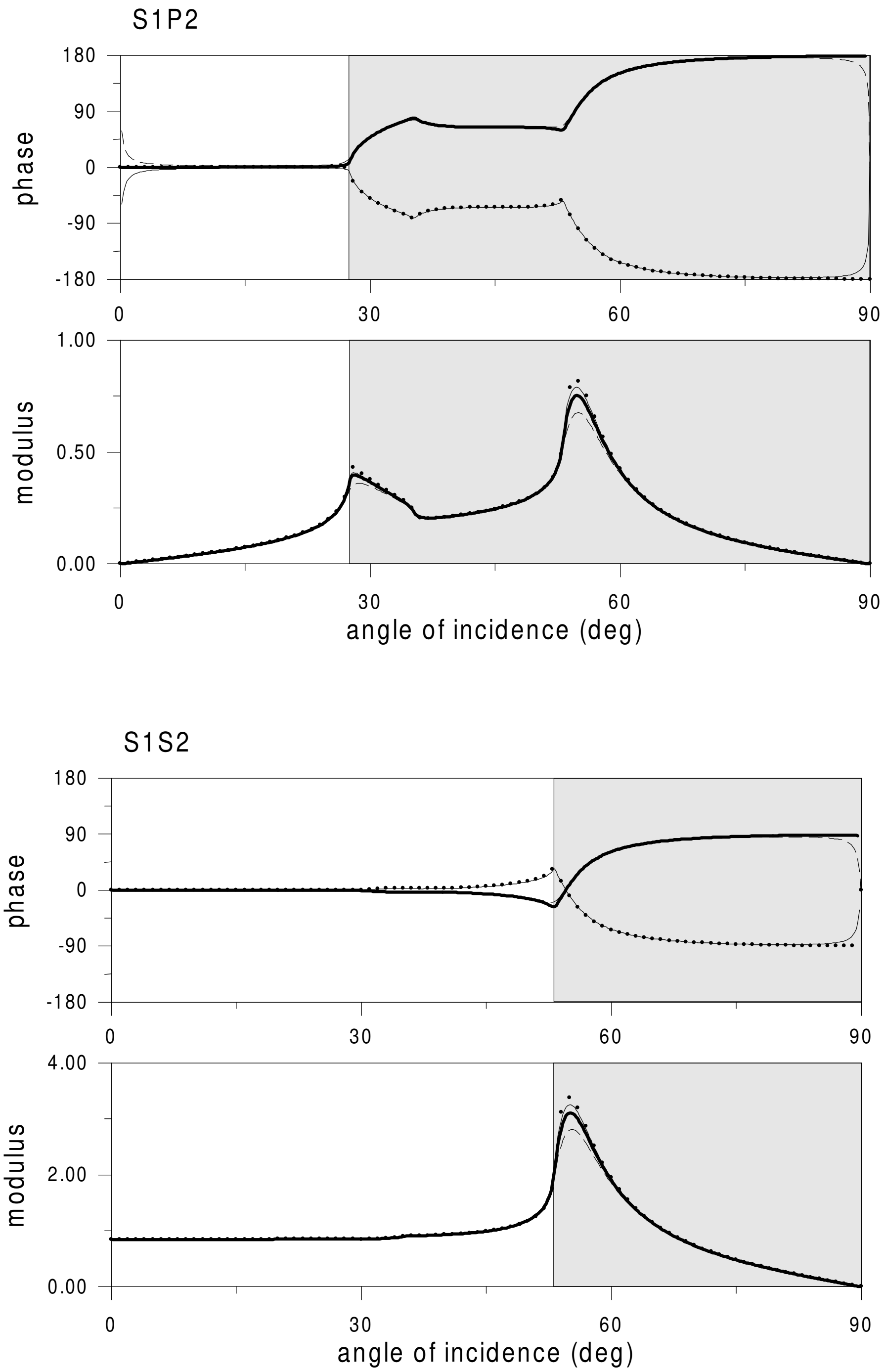

Figure 28: Model 2: Displacement transmission coefficients S1P2 and S1S2 at the interface between two solid halfspaces. (Non-dissipative media: bold dotted line; dissipative media: bold continuous line for $\gamma = 0^o$, thin continuous line for $\gamma = 30^o$, thin dashed line for $\gamma = -30^o$.)

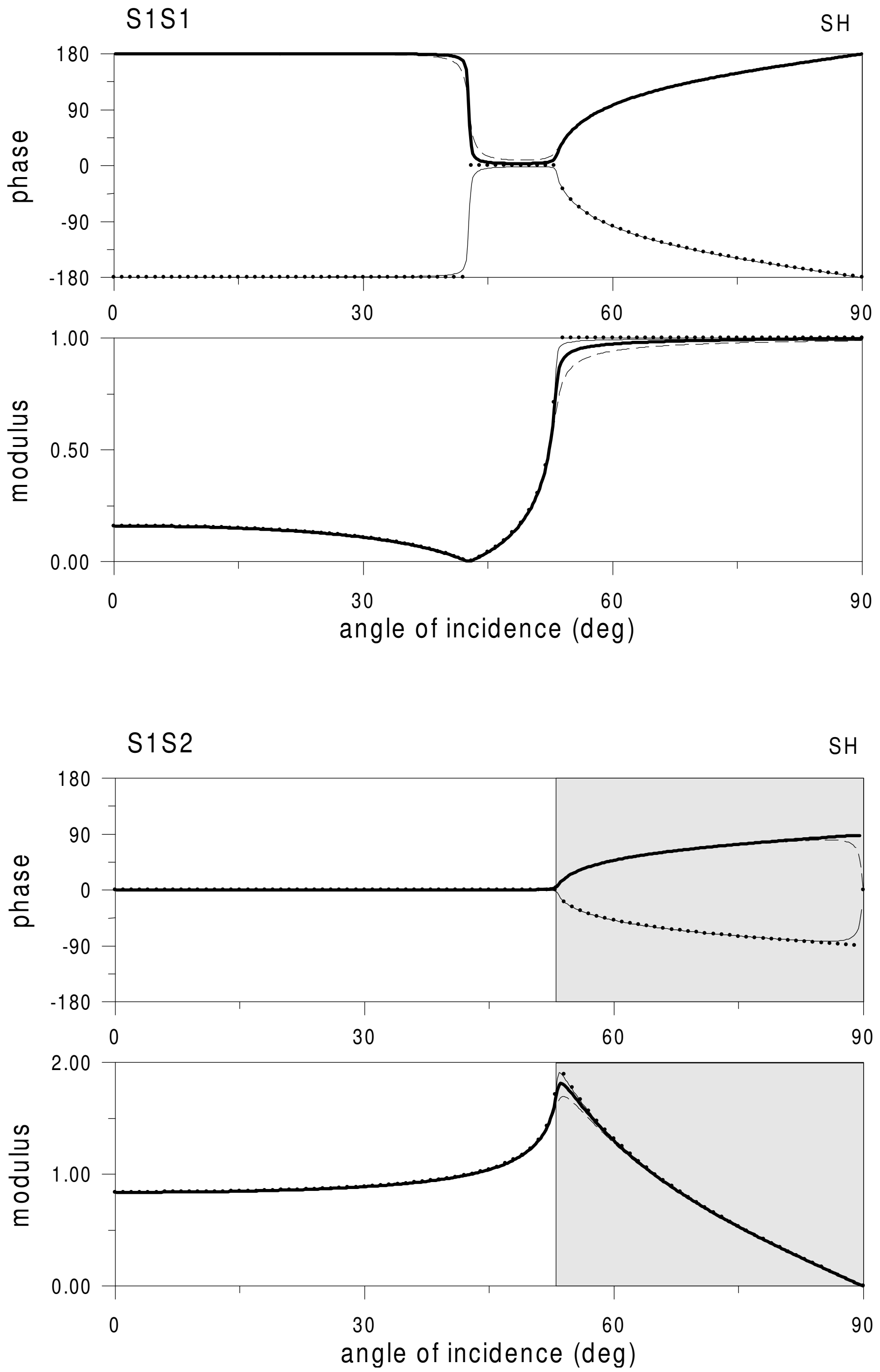

Figure 29: Model 2: Displacement SH R/T coefficients at the interface between two solid halfspaces. (Non-dissipative media: bold dotted line; dissipative media: bold continuous line for $\gamma = 0^o$, thin continuous line for $\gamma = 30^o$, thin dashed line for $\gamma = -30^o$.)

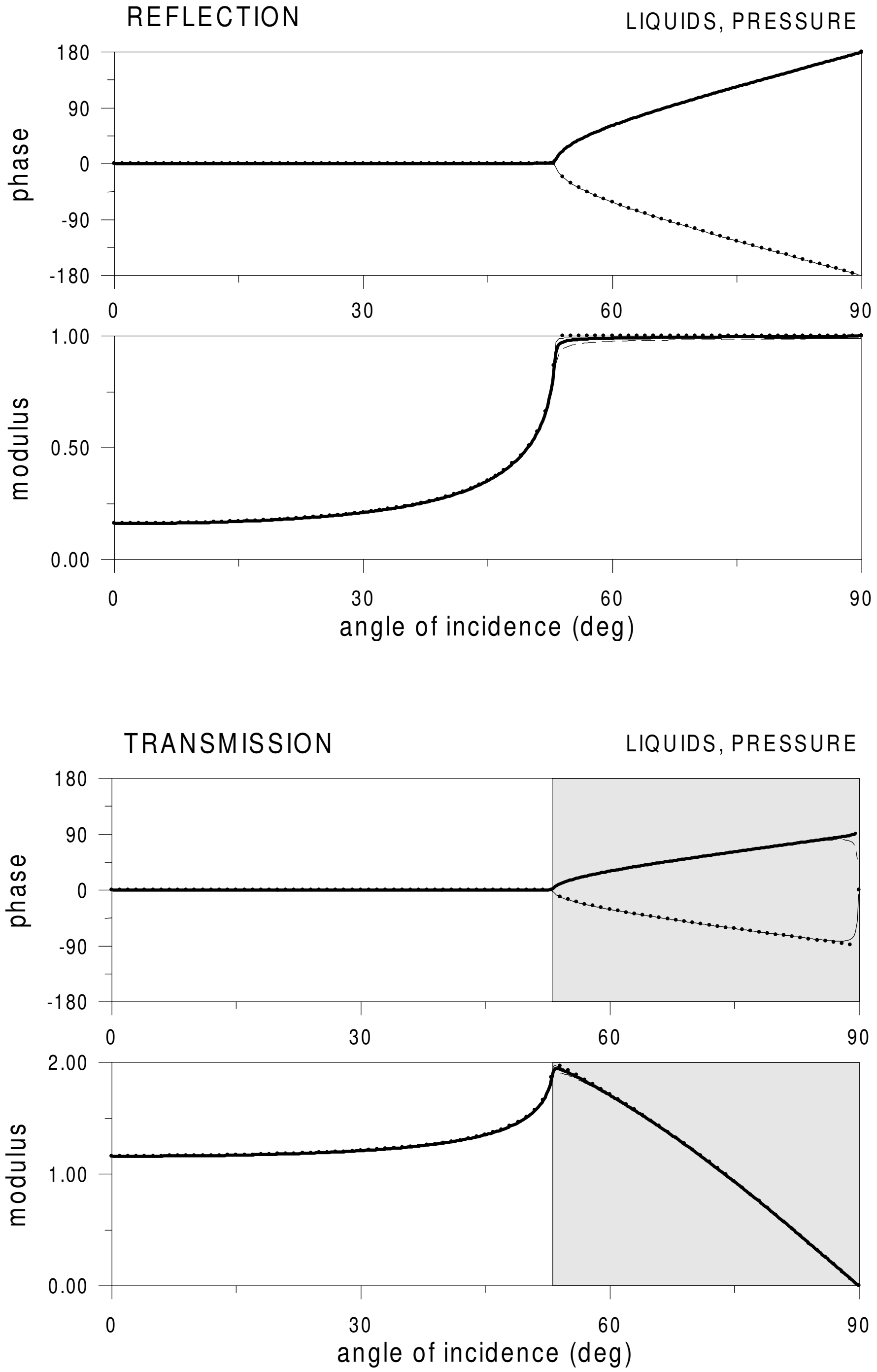

Figure 30: Model 2: Pressure R/T coefficients at the interface between two liquid halfspaces. (Non-dissipative media: bold dotted line; dissipative media: bold continuous line for $\gamma = 0^o$, thin continuous line for $\gamma = 30^o$, thin dashed line for $\gamma = -30^o$.)

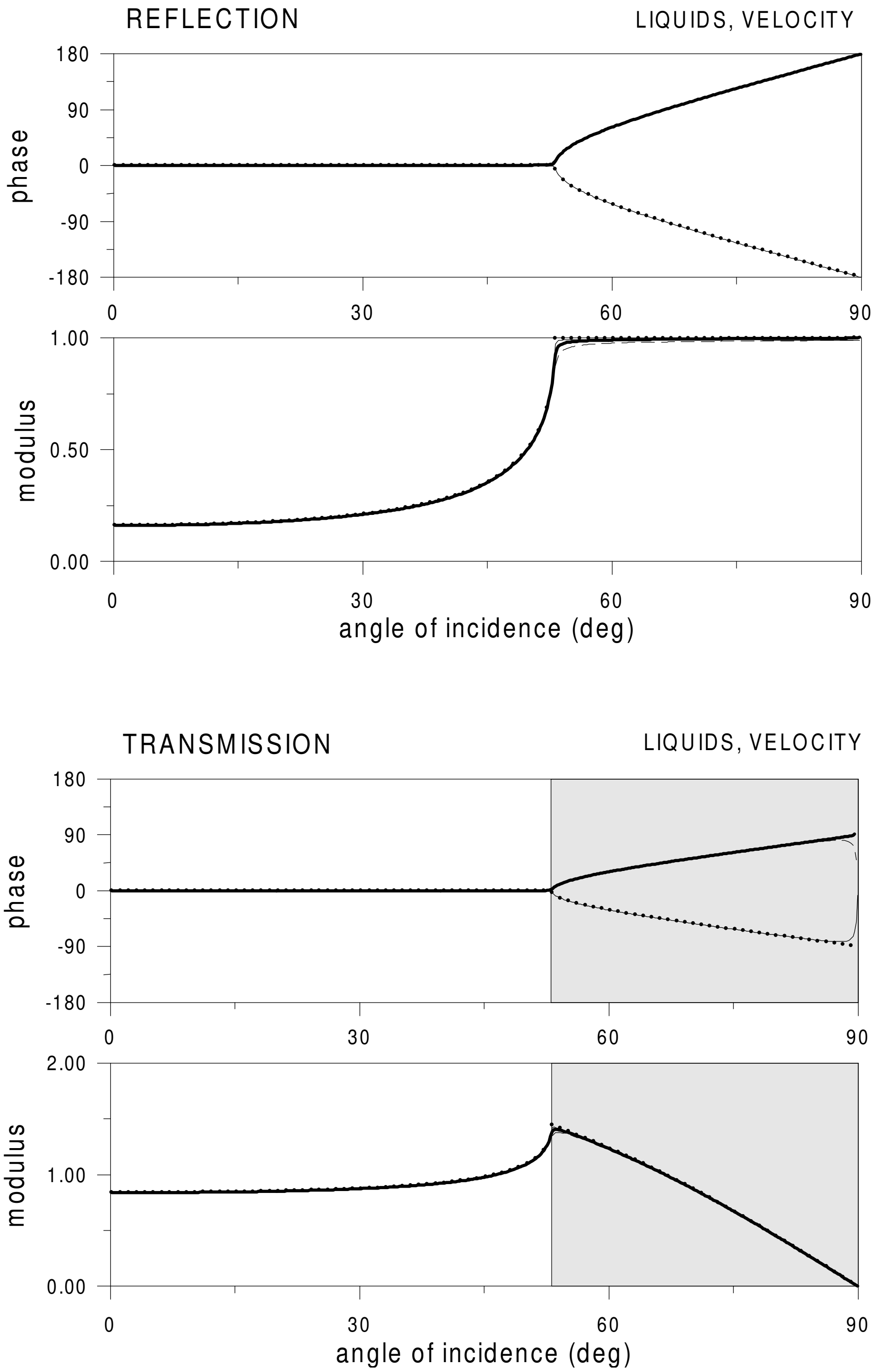

Figure 31: Model 2: Particle velocity R/T coefficients at the interface between two liquid halfspaces. Compare the transmission particle velocity coefficient with the transmission pressure coefficient in Fig. 30. (Non-dissipative media: bold dotted line; dissipative media: bold continuous line for $\gamma = 0^o$, thin continuous line for $\gamma = 30^o$, thin dashed line for $\gamma = -30^o$.)

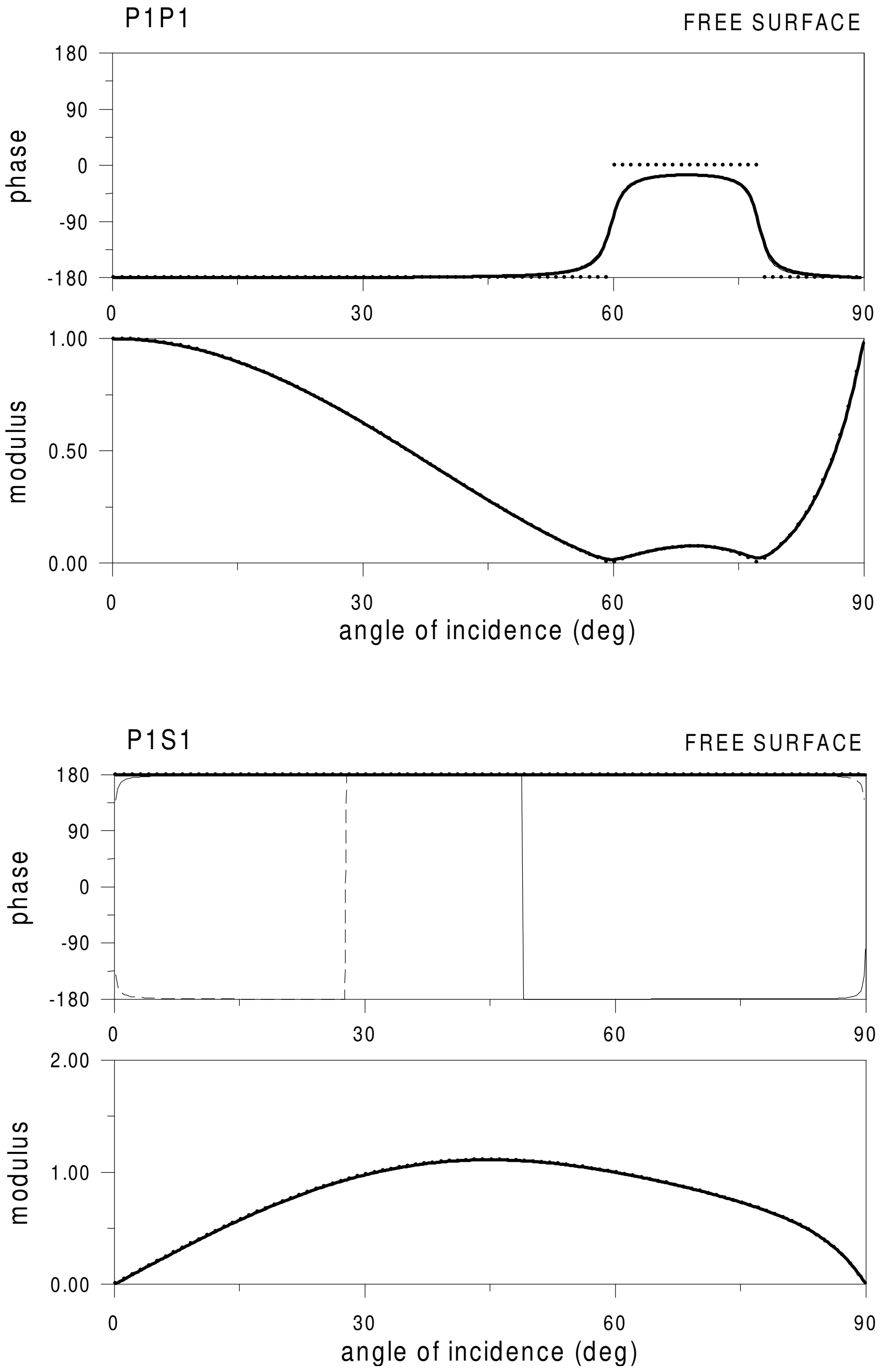

Figure 32: Model 2: Displacement reflection coefficients P1P1 and P1S1 at the free surface of a solid halfspace. (Non-dissipative media: bold dotted line; dissipative media: bold continuous line for $\gamma = 0^o$, thin continuous line for $\gamma = 30^o$, thin dashed line for $\gamma = -30^o$.)

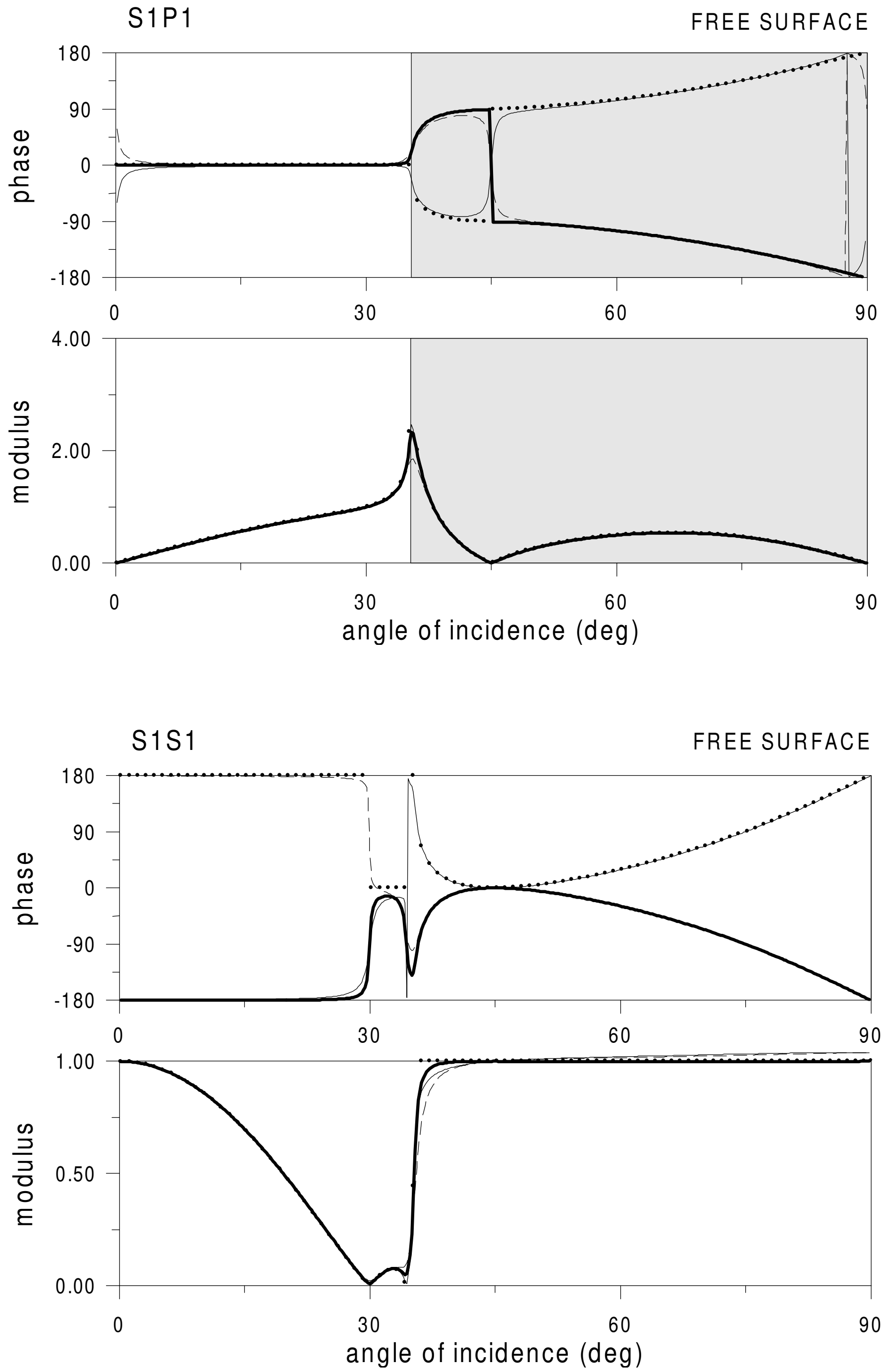

Figure 33: Model 2: Displacement reflection coefficients S1P1 and S1S1 at the free surface of a solid halfspace. (Non-dissipative media: bold dotted line; dissipative media: bold continuous line for $\gamma = 0^o$, thin continuous line for $\gamma = 30^o$, thin dashed line for $\gamma = -30^o$.)

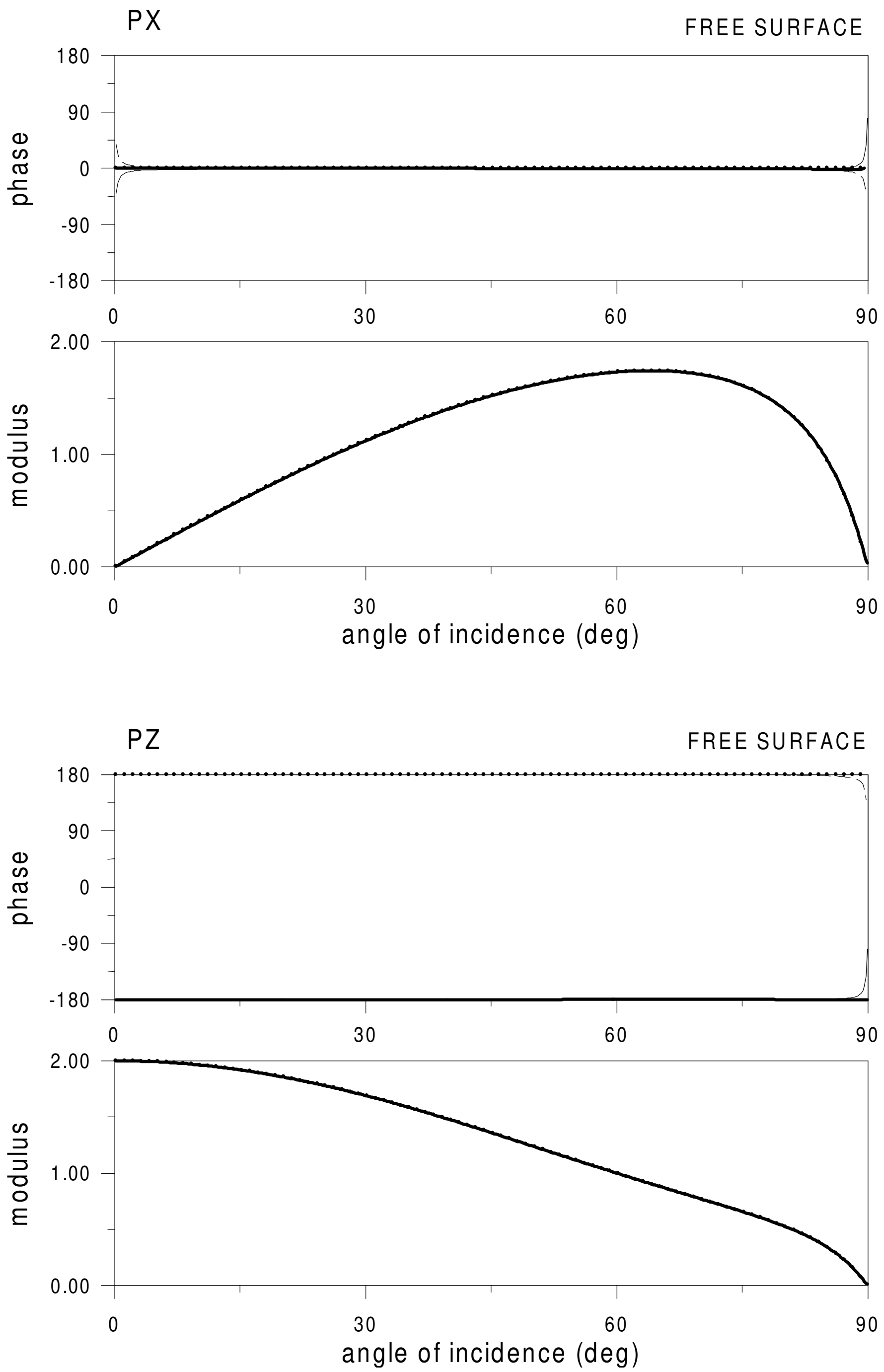

Figure 34: Model 2: Coefficients of conversion PX and PZ at the free surface of a solid halfspace. (Non-dissipative media: bold dotted line; dissipative media: bold continuous line for $\gamma = 0^o$, thin continuous line for $\gamma = 30^o$, thin dashed line for $\gamma = -30^o$.)

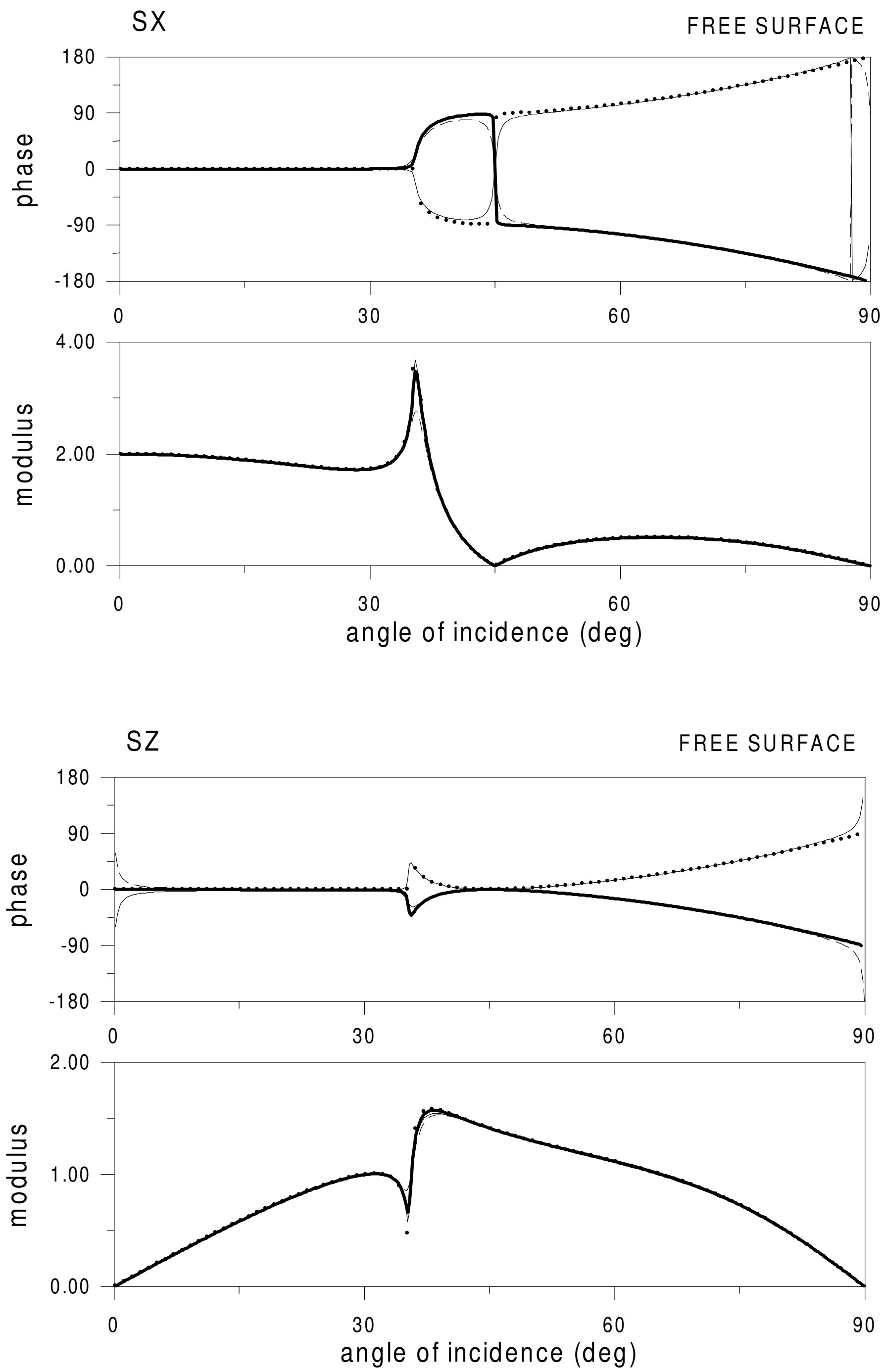

Figure 35: Model 2: Coefficients of conversion SX and SZ at the free surface of a solid halfspace. (Non-dissipative media: bold dotted line; dissipative media: bold continuous line for $\gamma = 0^o$, thin continuous line for $\gamma = 30^o$, thin dashed line for $\gamma = -30^o$.)

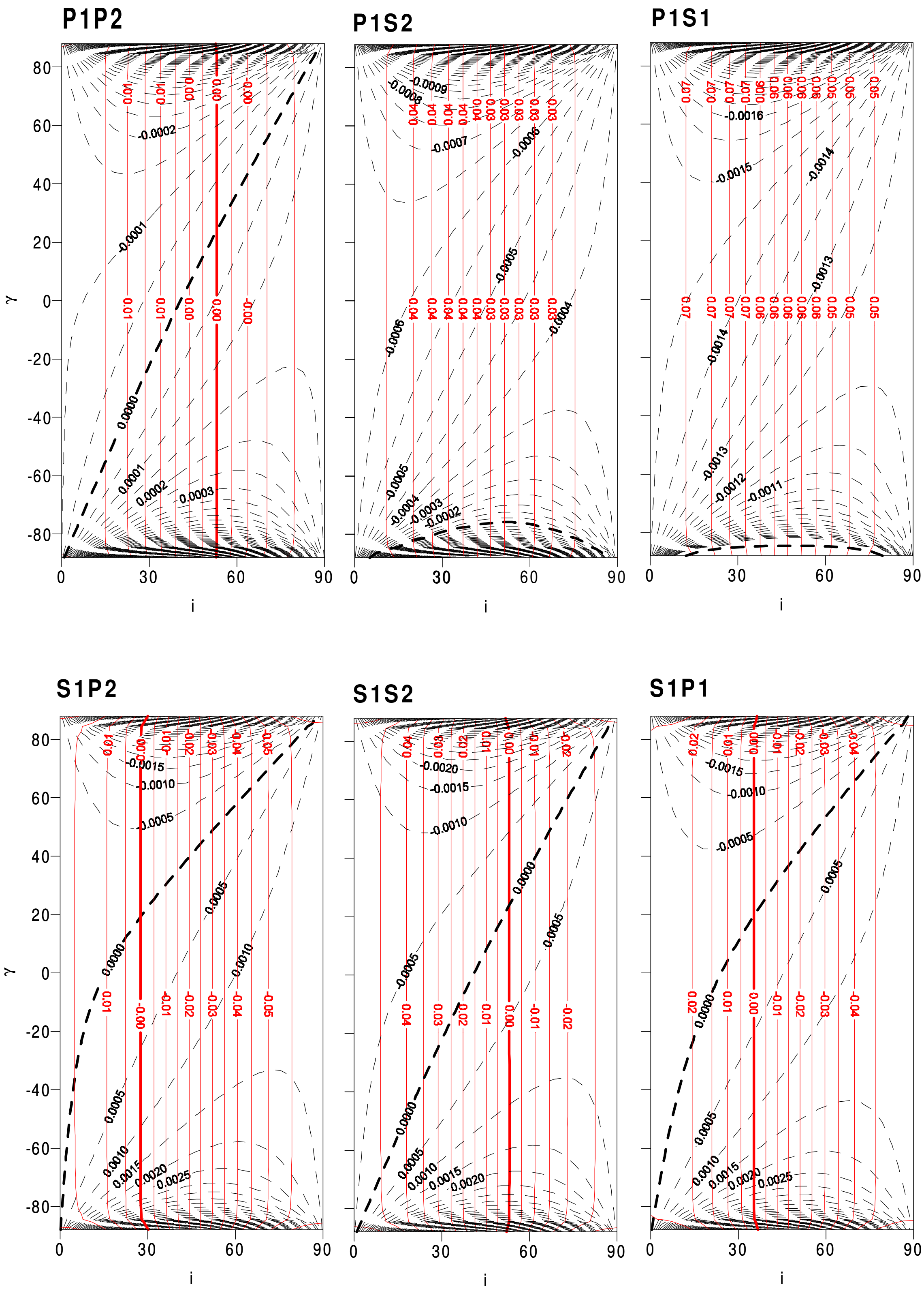

Figure 36: Model 2: σ^2-maps

post-critical regions may be different from those presented in Sections 6.2 and 6.3 if $\tilde{Q}/Q$ is inverted.

To see these differences, we shall consider **Model 3** as follows:

Model 3
CP1 = 6.4 km/s, CS1 = 3.698 km/s, RHO1 = 2.980 kg m^{-3}, QP1 = 150, QS1 = 75,
CP2 = 8.0 km/s, CS2 = 4.618 km/s, RHO2 = 3.300 kg m^{-3}, QP2 = 100, QS2 = 50.

Thus, the velocities and densities in Model 3 are the same as in Model 2, but the quality factors in the first halfspace are replaced by the quality factors in the second halfspace, and vice versa.

The σ^2-maps corresponding to Model 3 are displayed in Fig. 37. The angles i^R are influenced mainly by velocities, so that they are approximately the same as in Model 2; P1P2 ... $i^R = 53^o$, S1P2 ... $i^R = 27^o$, S1S2 ... $i^R = 53^o$, S1P1 ... $i^R = 35^o$. The behaviour of σ^2-maps for S1P1 and S1P2 square roots remain similar to those in Model 2, but the σ^2-maps of P1P2 and S1S2 square roots are changed radically. The reason is that $\tilde{Q}$ are greater than Q in Model 3, but $\tilde{Q}$ is less then Q in Model 2, for these two square roots. Note that the arguments of the square roots P1P2 and S1S2 behave anomalously only for $\gamma < -33^o$, whereas for Model 2 they behave anomalously for $\gamma < 20^o$. Thus, the phases of certain R/T coefficients in post-critical region will be opposite in Model 2 and Model 3 for a homogeneous incident wave ($\gamma = 0^o$), and even for an inhomogeneous incident wave with $\gamma = -30^o$.

We shall not present here a complete set of R/T coefficients as for Model 2, but only two simple and transparent examples:

a) The SH displacement R/T coefficients at a structural interface, see Fig. 38.

b) The pressure R/T coefficients on an interface between two liquid halfspaces, see Fig. 39.

As we can see in Figs. 38 and 39, the phases of R/T coefficients for non-dissipative and dissipative media are practically the same in this case, for all three γ under consideration: $\gamma = 0^o$ (homogeneous incident wave), $\gamma = 30^o$ and $\gamma = -30^o$.

6.5 Comparisons with other computations

Published papers on seismic plane waves in homogeneous dissipative media and on R/T coefficients on an interface between two homogeneous dissipative media are mostly theoretical, and give only analytical results.

Numerical computations of R/T coefficients and their discussion is not so common. The papers deal mainly with several selected R/T coefficients. Moreover, the numerical computations in published papers are related only to isotropic media and to the special case of coplanar **P**, **A** and **n**.

Krebes and Hron (1980) presented SH R/T coefficients for an inhomogeneous incident wave, with $\gamma = 0^o, \pm 20^o, \pm 40^o, \pm 60^o$ and $\pm 80^o$. Krebes (1983) discussed in detail two special cases: a) Incident homogeneous wave, with the same Q's for all waves, b) Incident

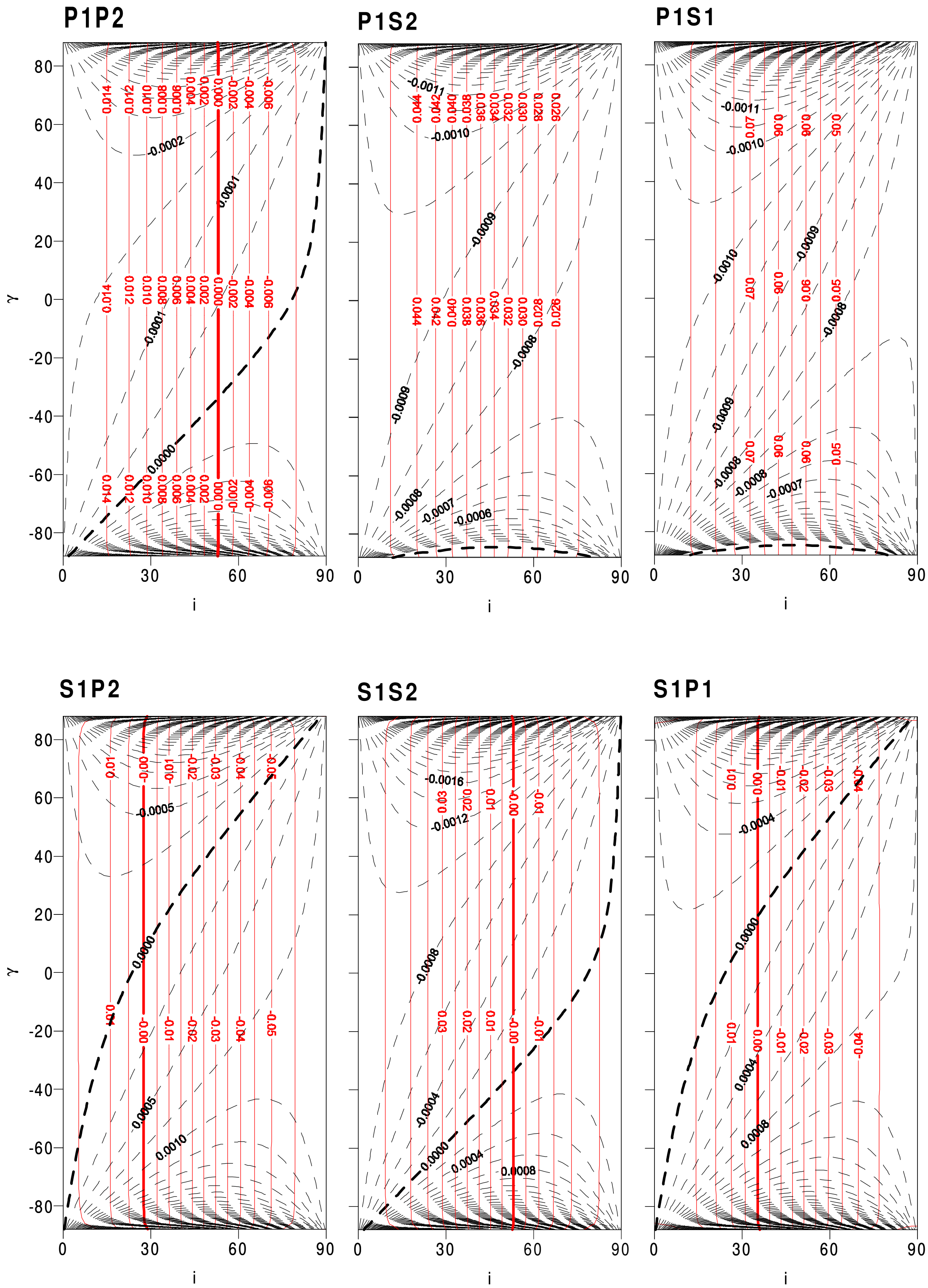

Figure 37: Model 3: σ^2-maps

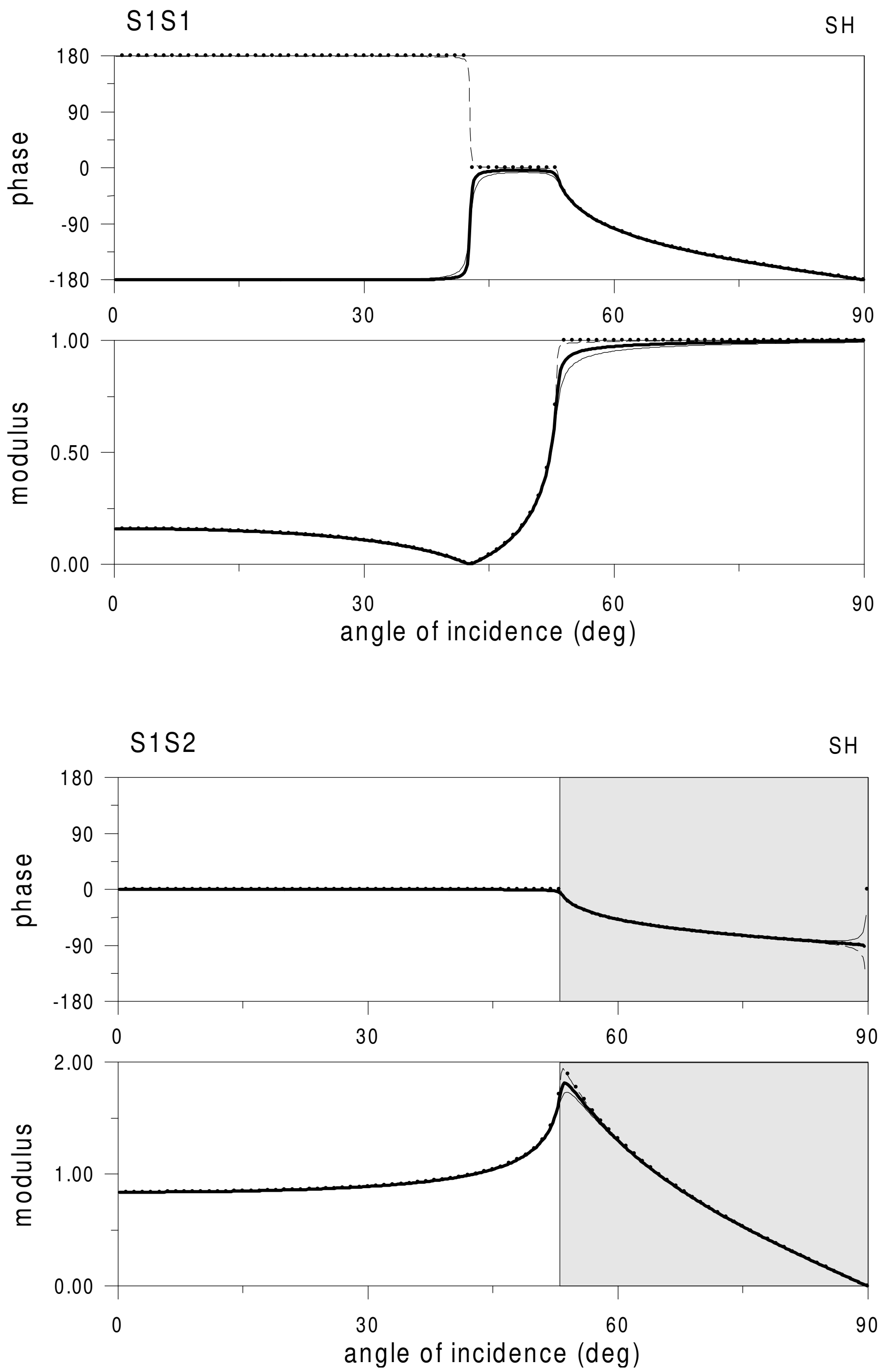

Figure 38: Model 3: Displacement SH R/T coefficients at the interface between two solid halfspaces. (Non-dissipative media: bold dotted line; dissipative media: bold continuous line for $\gamma = 0^o$, thin continuous line for $\gamma = 30^o$, thin dashed line for $\gamma = -30^o$.)

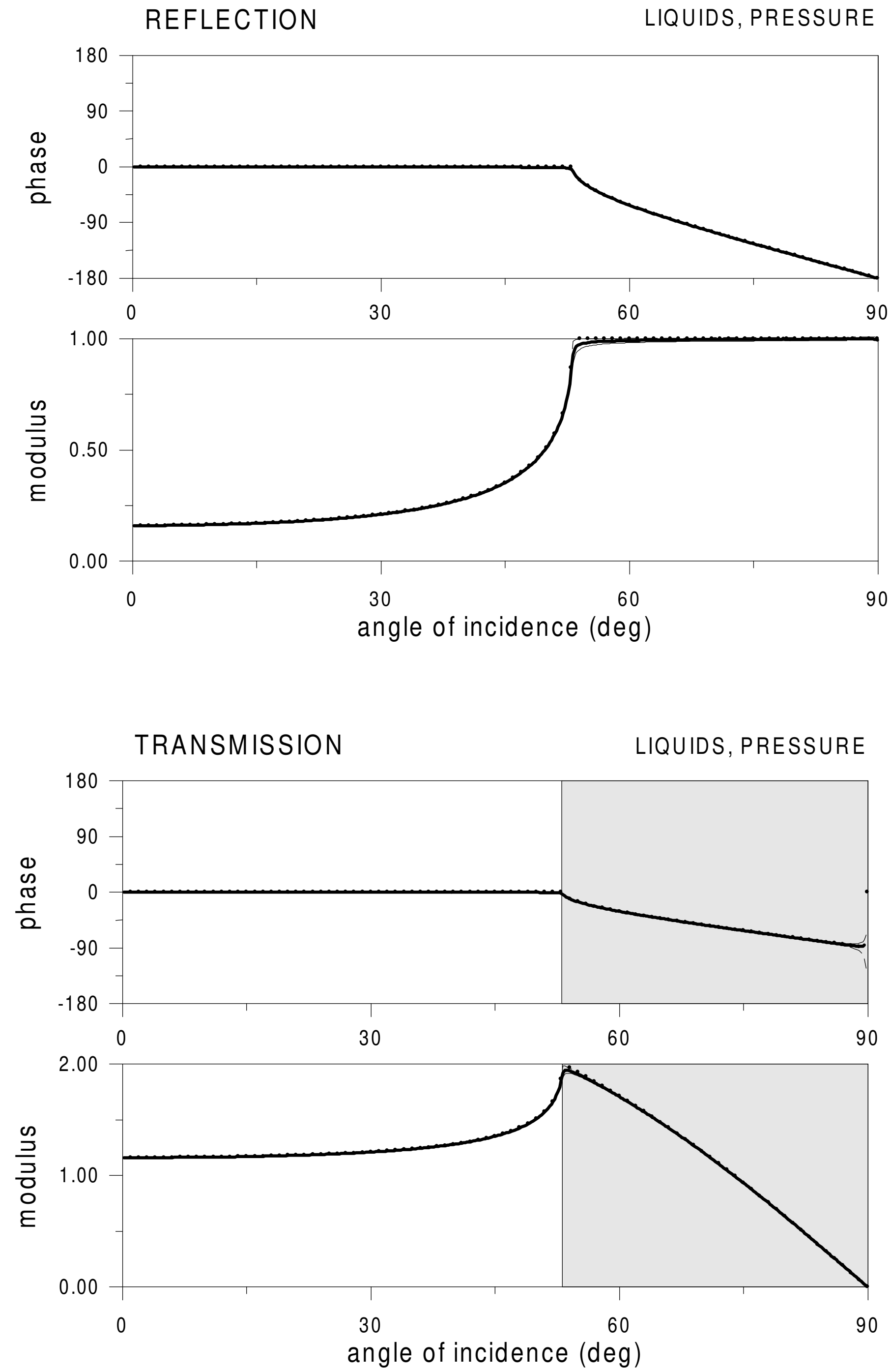

Figure 39: Model 3: Pressure R/T coefficients at the interface between two liquid halfspaces. (Non-dissipative media: bold dotted line; dissipative media: bold continuous line for $\gamma = 0^o$, thin continuous line for $\gamma = 30^o$, thin dashed line for $\gamma = -30^o$.)

wave with the attenuation angles $\gamma \to \pm 90^o$. He also gave a numerical example on SH R/T coefficients for $\gamma = 30^o, 60^o, 85^o$ and 89.99^o. A more detailed study can be found in Krebes (1984), related to SH and P1P1 reflection coefficients. See also Section 6.1, where the model proposed by Krebes was considered and all Krebes computations used as test examples.

Some numerical examples can be also found in Borcherdt, Glassmoyer and Wennerberg (1986), particularly for SH waves. The authors also present some comparisons with observations, with a very good fit.

Contrary to the previous references, Bourbiè and Gonzales-Serrano (1983) presented a more systematic study of various types of R/T coefficients (P1P1 at a liquid-solid interface, P1P1, P1S1, S1P1 and S1S1 at a solid-solid interface). They, however, consider an incident *homogeneous* plane wave only. Program COEF52 gives a perfect fit with all these computations. It should be noted that Bourbié and Gonzales-Serrano (1983) consider also models with a great jump in Q's across the interface, like QP1=∞, QS1=∞, QP2=33, QS2=20. In such cases, the differences between the R/T coefficients for dissipative and non-dissipative models are more pronounced than in Models 1 and 2, used here.

Nechtschein and Hron (1996, 1997) present graphs of P1P1, P1P2, P1S1 and S1S1 R/T coefficients for various models of interface. They compare these coefficients with some modified R/T coefficients, called by them the ART (asymptotic ray theory) R/T coefficients. We have performed the computations of standard R/T coefficients (not ART coefficients) with COEF52 for the same data as Nechtschein and Hron (1996, 1997). As they do not specify the attenuation angle γ of the incident plane wave, we took $\gamma = 0^o$ (homogeneous incident wave) in all computations. In general, the comparison is good. There is, however, one important difference. The moduli of P1P1 and S1S1 R/T coefficients of Nechtschein and Hron (1997) display some overshooting over unity in the critical region, for angles of incidence slightly exceeding i^R. In our computations, such an overshooting has not been observed.

Brokešová and Červený (1997) give a systematic study of all R/T coefficients at a structural interface, at the Earth's surface, and at an interface between two liquid halfspaces. They, however, consider only a real-valued ray parameter. This corresponds to an incident plane wave with the angle of incidence i equal to the attenuation angle γ. See Section 4.6 for explanation.

R/T coefficients on an interface between two dissipative media may be also extracted from other computations, performed by different methods. For example, Carcione (1993) presents a picture of moduli of four R/T coefficients (P1P1, P1P2, P1S1, P1S2) obtained from computations performed by a specific spectral method. He considers an interesting model, in which only the quality factors Q's jump across the interface, not the velocities and densities. The model is as follows:
CP1 = 3.249 km/s, CS1 = 2.235 km/s, QP1 = ∞, QS1 = ∞,
CP2 = 3.249 km/s, CS2 = 2.235 km/s, QP2 and QS2 are frequency dependent and are specified by a picture.

The Carcione's results of computations are presented in Fig. 40a. Only moduli are presented in Carcione (1993). We have repeated computations, considering a homogeneous incident wave. We have considered RHO1=RHO2=2.0 kg/m^3, and approximated QP2 and QS2 by values QP2=13.7, QS2=10.1, which fit approximately the frequency-

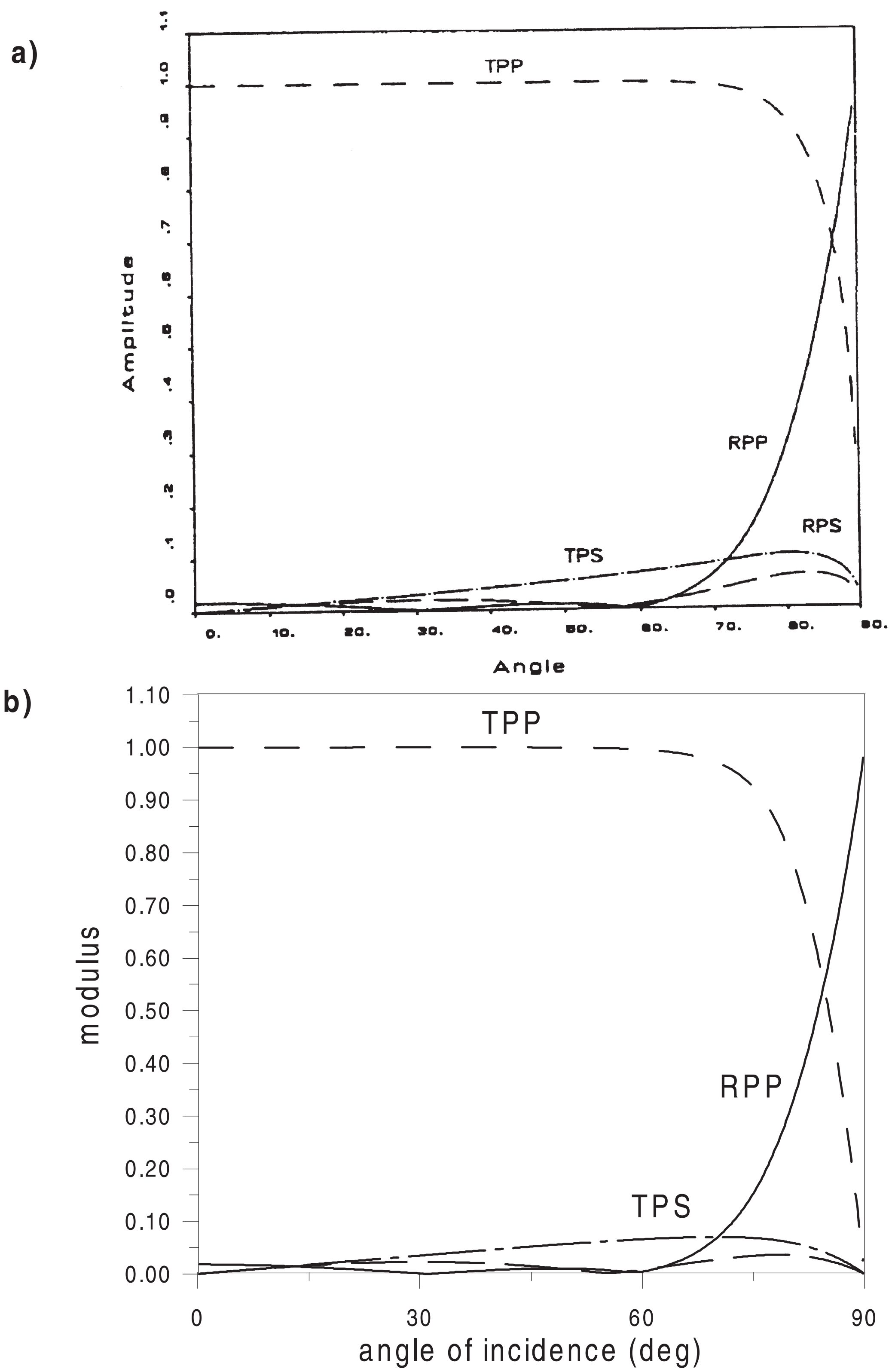

Figure 40: Comparison with R/T coefficients by Carcione (1993). Notation: RPP≡P1P1, RPS≡P1S1, TPP≡P1P2, TPS≡P1S2. Only moduli of R/T coefficients are displayed. Note that only the quality factors Q's jump across the interface, not the velocities. a) Carcione's results, b) results obtained using COEF52.

dependent QP2 and QS2 shown by Carcione, in the frequency range under consideration. See Fig. 40b. In general, the agreement is satisfactory.

7 Concluding remarks

The procedures proposed in this contribution may be used to study the inhomogeneous plane waves propagating in dissipative, isotropic and anisotropic, media. They can be also used to compute the R/T coefficients at a plane interface between two dissipative, isotropic or anisotropic, halfspaces. The attenuation angle γ of the inhomogeneous incident wave may be arbitrary.

The computer routine COEF52 described in this contribution is designed to compute all possible displacement R/T coefficients on a single structural interface between two isotropic halfspaces, pressure and particle velocity R/T coefficients on an interface between two liquids, displacement, pressure and particle velocity R/T coefficients and conversion coefficients on a free surface of an isotropic halfspace, and even all these coefficients on a transition isotropic layer. The constant-Q dispersion relation is considered. The only limitation of the routine COEF52 is the assumption that the attenuation vector $\mathbf{A}$ of the incident wave is situated in the plane of incidence, defined by a normal to the interface and by the propagation vector $\mathbf{P}$ of the incident wave. The attenuation angle γ of the incident wave, however, may be arbitrary. Thus, routine COEF52 is a generalization of the routine COEF51, described by Brokešová and Červený (1997), in which only a special case of γ (equal to the angle of incidence i) is considered.

Extensive numerical computations of "reference R/T coefficients" at a plane interface between two dissipative halfspaces have been performed. Under "reference R/T coefficients", we understand the R/T coefficients, computed for a reference frequency f_r for which the complex-valued elastic moduli are specified. It was shown by Brokešová and Červený (1997), that the reference R/T coefficients approximate well the frequency-dependent R/T coefficients in a broad range of frequencies close to the reference frequency f_r. The main attention has been devoted to the dependence of R/T coefficients on the attenuation angle γ of the incident wave. It should be emphasized that the attenuation angle γ of the incident wave is an additional input parameter related to the incident wave. It is quite independent on quality factors. The incident wave may be homogeneous (with $\gamma = 0^o$) even for strongly dissipative media (very low Q's), or strongly inhomogeneous (γ close to $\pm 90^o$) even for weakly dissipative media. For non-dissipative media, the incident wave may be also inhomogeneous, with $\gamma = 90^o$. The complete sets of all possible R/T coefficients for two different models are presented in Section 6. All figures also display the relevant R/T coefficients for non-dissipative media.

Let us first discuss the moduli of the R/T coefficients. It is shown that the moduli of the R/T coefficients for dissipative media are very close to the corresponding moduli of the R/T coefficients for non-dissipative media for small (sub-critical) angles of incidence. The conclusion is valid both for homogeneous incident waves ($\gamma = 0^o$) and for inhomogeneous incident waves, with γ not too close to $\pm 90^o$. The differences are greater for higher angles of incidence, particularly in critical and post-critical regions of angles of incidence, and for great jump of Q's across the interface. The differences are usually greater for γ negative, and increase with increasing $|\gamma|$, both for γ positive and negative. The differences can be also observed in the vicinity of Brewster angles. They are more pronounced mainly for the moduli of the S1S1 reflection coefficients. In general, the attenuation angle γ of the incident wave has a smoothing effect on R/T coefficients. This can be well observed mainly in critical regions of the angle of incidence. See, e.g., Figs. 8 and 9. However, for realistic Q's, for not too big jumps of Q's across the interface, and for γ not close to $\pm 90^o$ (say, $-50^o < \gamma < 50^o$), the differences between the moduli of R/T coefficients for dissipative and non-dissipative models are not too distinct, even in critical and post-critical regions.

An interesting effect can be observed in figures of phases of R/T coefficients in post-critical regions. For certain attenuation angle γ of the incident wave, the phases behave anomalously in the following sense: They are strongly different from the phases of R/T coefficients for non-dissipative media, even if the quality factors in dissipative media are very high ($Q \to \infty$). Mostly, the phases of R/T coefficients for dissipative and non-dissipative media have opposite signs in these cases. The explanation of these effects is not difficult. The direction of the attenuation vectors of generated waves in dissipative media is strictly determined by the model and by the properties of the incident wave. Thus, amplitudes of certain generated waves waves may either decrease or increase exponentially with increasing distance from interface. In non-dissipative media, only inhomogeneous plane waves with amplitudes decreasing with increasing distance from the interface are considered. This is impossible in dissipative media. See a more detailed discussion in Section 6.2, sub (6), and also in Richards (1984).

As mentioned above, the attenuation angle γ is an additional parameter in the reflection/transmission problem. The value of γ must be specified in input data, if we wish to calculate the R/T coefficients. It is fully independent of the model dissipative parameters (Q's), similarly as the angle of incidence. The question is how to choose γ of the incident wave. In ray computations for *weakly dissipative media*, usually only real rays for corresponding non-dissipative media have been used. To take into account the dissipative effects, only some dissipative filters along these real rays are computed. If the ray is incident at an interface, this approximation represents a *homogeneous incident wave* ($\gamma = 0^o$). The generated R/T waves are then again considered to be homogeneous. This, however, violates the Snell's law, as the generated waves are, in general, inhomogeneous ($\gamma \neq 0^o$) even if the incident incident wave is homogeneous ($\gamma = 0^o$). Thus, the approach which uses $\gamma = 0^o$ along the whole ray in a layered medium is not satisfactory.

Even if we consider correct Snell's law at the interfaces, the problem how to choose the attenuation angle at an initial point of the ray remains open. It should be emphasized that, for a given point source and receiver, the ray trajectory, travel time and amplitude depend on the choice of initial γ. Consequently, there is an infinite number of rays connecting the source and receiver, corresponding to different initial γ.

Hearn and Krebes (1990a,b) investigated this problem for 1-D layered dissipative model with an arbitrary situated source and receiver. The wave field can be then expressed exactly in terms of the Sommerfeld integral. For high-frequency waves, the integral can be evaluated by asymptotic methods, particularly by the saddle point method. The saddle point method then yields the initial γ, and, consequently, even γ along all ray elements in individual layers. The ray corresponding to the saddle point method yields the minimum travel time, and all other rays (with γ chosen differently) yield greater travel times. Thus, the ray found in this way satisfies the Fermat's principle of stationary time. Hearn and Krebes (1990a,b) call this ray the *stationary ray.* Note that even all other rays with different initial γ's, discussed above, satisfy the Snell's law at all interfaces. Consequently, it is not sufficient to require that the Snell's law at individual interfaces is satisfied to obtain the minimum travel time. The saddle point condition, yielding the stationary ray is, however, complex-valued, even for the source and the receiver situated in the real $\mathbf{x}$-space. This yields the concept of *complex rays.* The stationary rays are complex rays, i.e. the spatial coordinates of points along the stationary ray trajectory are complex numbers. See also Buchen (1971a,b), Richards (1984), Krebes and Slawinski (1991).

The theory of Hearn and Krebes (1990a,b) is applicable only to a 1-D structure, consisting of a sequence of flat horizontal homogeneous dissipative layers. A complete theory of complex seismic rays in laterally varying, isotropic or anisotropic, dissipative (anelastic) structures is given by Thomson (1997). The basic equations of the complex ray theory can be also deduced from our treatment. We shall consider the elastodynamic equation for unbounded anisotropic *inhomogeneous* dissipative medium with vanishing body forces,

$$(a_{ijkl}u_{k,l})_{,j} + \omega^2 u_i = 0, \tag{147}$$

analogous to (1). We shall look for high-frequency solutions of (147), using the ansatz solution (for fixed ω)

$$u_k(\mathbf{x},t) = U_k(\mathbf{x})\exp[-\mathrm{i}\omega(t - T(\mathbf{x}))]. \tag{148}$$

This is an alternative to (4) for inhomogeneous medium. It is assumed that U_k and T are smooth functions of coordinates $\mathbf{x}$. To determine U_k and T, we can proceed similarly as for non-dissipative media, see Červený (1997), Section 2.4. As a result, we arrive at the same eigenvalue problem as for plane waves, where $p_i = \partial T/\partial x_i$ and $g_i^{(m)}$ are smooth functions of coordinates. For example, the existence condition (36) for isotropic dissipative medium reads,

$$V_C^2 p_i p_i = 1, \quad \text{with} \quad p_i = \partial T/\partial x_i. \tag{149}$$

Here V_C, T and p_i are complex-valued. Equation (149) is called the *eikonal equation.* It represents a non-linear first-order partial differential equation for the complex-valued travel time T, with complex coefficients. The imaginary part of T describes the attenuation of waves. It is common to write the eikonal equation in the common form

$$\mathcal{H}(x_i, p_i) = 0, \quad \text{with} \quad p_i = \partial T/\partial x_i. \tag{150}$$

The function$\mathcal{H}(x_i, p_i)$ is called the Hamiltonian. Equation (150) may be used even for anisotropic media, where $\mathcal{H} = G_m - 1$; G_m being the eigenvalue of the Christoffel matrix.

There are two possibilities how to solve (150). First possibility is to work in the real $\mathbf{x}$-space. We can decompose (150) into real and imaginary parts and obtain two coupled non-linear partial differential equations of the first order for $\partial T^R/\partial x_i$ and $\partial T^I/\partial x_i$, with $T = T^R + \mathrm{i}T^I$. The next possibility is to work in the complex $\mathbf{x}$-space. Than it is possible to solve (150) in terms of characteristics. The complex ray tracing system is as follows:

$$\frac{\mathrm{d}x_i}{\mathrm{d}u} = \frac{\partial\mathcal{H}}{\partial p_i}, \quad \frac{\mathrm{d}p_i}{\mathrm{d}u} = -\frac{\partial\mathcal{H}}{\partial x_i}, \quad \frac{\mathrm{d}T}{\mathrm{d}u} = p_i\frac{\partial\mathcal{H}}{\partial p_i}. \tag{151}$$

This is fully analogous to the ray tracing system for non-dissipative media, see Červený (1997), Eq. (3.1.3). The basic difference, however, is that all quantities in (151) are complex-valued, including $x_i, p_i, u, T, \mathcal{H}$. Thus, the ray tracing is performed in a 12-dimensional phase space, with coordinates $x_i^R, x_i^I, p_i^R, p_i^I (i = 1, 2, 3)$. In an analogous way, it is also possible to derive the transport equation.

Thus, the rays in dissipative inhomogeneous media are complex-valued. For a very detailed and up-to-date treatment, see Thomson (1997), where also many other references are given. The theory of complex rays in dissipative inhomogeneous media is, in principle simple, and it is formally very close to the theory of real rays in non-dissipative media. There are, however, various problems which make the complex ray tracing in dissipative media more complicated. Let us name the problem of two point ray tracing (with both point source and receiver situated in the real **x**-space), the problems of multivalued travel-time branches and caustics, etc. All these problems are discussed in detail in Thomson (1997). Intuitively, we feel that the situation may be simpler for low-loss models (high Q's). Perhaps it would be possible to use perturbation methods, taking the dissipative model as a perturbation of a non-dissipative model. Then the non-perturbed ray (in non-dissipative medium) may be taken real-valued. Further research along this line would be useful.

Acknowledgements

The authors are greatly indebted to C. J. Thomson and L. Klimeš for the discussion of the subject. The research has been supported by the Consortium Project "Seismic Waves in Complex 3-D Structures".

References

Aki, K. and Richards, P.G. (1980). *Quantitative Seismology.* San Francisco: Freeman.

Borcherdt, R.D. (1973). Energy and plane waves in linear viscoelastic media. *J. Geophys. Res.* **78**, 2442 – 2533.

Borcherdt, R.D. (1977). Reflection and refraction of Type-II S waves in elastic and anelastic media. *Bull. seismol. Soc. Am.* **67**, 43 – 67.

Borcherdt, R.D. (1982). Reflection-refraction of general P- and Type-I S-waves in elastic and anelastic solids. *Geophys. J. R. astr. Soc.* **70**, 621 – 613.

Borcherdt, R.D. (1988). Volumetric strain in relation to particle displacements for body and surface waves in general viscoelastic half-space. *Geophys. J.* **93**, 215 – 228.

Borcherdt, R.D., Glassmoyer, G. and Wennerberg, L. (1986). Influence of welded boundaries in anelastic media on energy flow, and characteristics of P, S-I and S-II waves: Observational evidence for inhomogeneous body waves in low-loss solids. *J. Geophys. Res.* **91, B11**, 11503 – 11518.

Borcherdt, R.D. and Wennerberg, L. (1985). General P, Type-I S and Type-II S waves in anelastic solids: Inhomogeneous wave fields in low-loss solids. *Bull. seismol. Soc. Am.* **75**, 1729 – 1763.

Bourbiè, T. and Gonzales-Serrano, A. (1983). Synthetic seismograms in attenuating media. *Geophysics* **48**, 1575 – 1587.

Brokešová, J. and Červený, V. (1997). Reference reflection/transmission coefficients in dissipative media. Report No. 6. Consortium Project "Seismic Waves in Complex 3-D Structures", pp. 75 – 114. Department of Geophysics, Charles University, Prague.

Buchen, P.W. (1971a). Plane waves in linear viscoelastic media. *Geophys. J. R. astr. Soc.* **23**, 531 – 542.

Buchen, P.W. (1971b). Reflection, transmission and diffraction of SH-waves in linear viscoelastic solids. *Geophys. J. R. astr. Soc.* **25**, 97 – 113.

Carcione, J.M (1993). Seismic modeling in viscoelastic media. *Geophysics* **58**, 110 – 120.

Červený, V. (1997). *Seismic Ray Theory.* Report No. 5. Consortium Project "Seismic Waves in Complex 3-D Structures", Department of Geophysics, Charles University, Prague.

Chapman, C.H. (1994). Reflection/transmission coefficients reciprocities in anisotropic media. *Geophys. J. Int.*, **116**, 498 – 501.

Hearn, D.J. and Krebes, E.S. (1990a). On computing ray-synthetic seismograms for anelastic media using complex rays. *Geophysics* **55**, 422 – 432.

Hearn, D.J. and Krebes, E.S. (1990b). Complex rays applied to wave propagation in a viscoelastic medium. *Pure and Appl. Geophys.* **132**, 401 – 415.

Kennett, B.L.N. (1983). *Seismic wave propagation in stratified media.* Cambridge: Cambridge Univ. Press.

Krebes, E.S. (1983). The viscoelastic reflection/transmission problem: Two special cases. *Bull. seismol. Soc. Am.* **73**, 1673 – 1683.

Krebes, E.S. (1984). On the reflection and transmission of viscoelastic waves - Some numerical results. *Geophysics* **49**, 1374 – 1380.

Krebes, E.S. and Hron, F. (1980a). Ray-synthetic seismograms for SH waves in anelastic media. *Bull. seismol. Soc. Am.* **70**, 29 – 46.

Krebes, E.S. and Hron, F. (1980b). Synthetic seismograms for SH waves in a layered anelastic medium by asymptotic ray theory. *Bull. seismol. Soc. Am.* **70**, 2005 – 2020.

Krebes, E.S. and Slawinski, M.A. (1991). On raytracing in an elastic-anelastic medium. *Bull. seismol. Soc. Am.* **81**, 667 – 686.

Müller, G. (1985). The reflectivity method: a tutorial. *J. Geophys.* **58**, 153 – 174.

Nechtschein, S. and Hron, F. (1996). Reflection and transmission coefficients between two anelastic media using asymptotic ray theory. *Canad. J. Explor. Geophysics* **32**, 31 – 40.

Nechtschein, S. and Hron, F. (1997). Effects of anelasticity on reflection and transmission coefficients. *Geophys. Prospecting* **45**, 775 – 793.

Richards, P.G. (1984). On wavefront and interfaces in anelastic media. *Bull. seismol. Soc. Am.* **74**, 2157 – 2165.

Thomson, C.J. (1997). Complex rays and wave packets for decaying signals in inhomogeneous, anisotropic and anelastic media. *Studia Geoph. et Geod.* **41**, 345 – 381.

Thomson, C.J. (1998a). Notes on waves in layered media to accompany program Rmatrix. This volume.

Thomson, C.J. (1998b). Notes on Rmatrix, a program to find the seismic plane-wave response of a stack of anisotropic layers. This volume.

Thomson, C.J., Clarke, T. and Garmany, J. (1986). Observations on seismic wave equation and reflection coefficient symmetries in stratified media. *Geophys. J. R. astr. Soc.*, **86**, 675 – 686.

Wennerberg, L. (1985). Snell's law for viscoelastic materials. *Geophys. J. R. astr. Soc.* **81**, 13 – 18.